

PROCEEDINGS OF SPIE



SPIE—The International Society for Optical Engineering

Artificial Turbulence for Imaging and Wave Propagation

John D. Ginglewski
Mikhail A. Vorontsov
Chairs/Editors

20–21 July 1998
San Diego, California

Sponsored and Published by
SPIE—The International Society for Optical Engineering

DISTRIBUTION STATEMENT A
Approved for Public Release
Distribution Unlimited



Volume 3432

SPIE is an international technical society dedicated to advancing engineering and scientific applications of optical, photonic, imaging, electronic, and optoelectronic technologies.

19990315020

Development of the optically addressed spatial light modulators for dynamical holography applications using deformed helix ferroelectric liquid crystals

Leonid A. Beresnev, Thomas Weyrauch, Wolfgang Haase, Arkadii P. Onokhov^a,
Mikhail V. Isaev^a, Nataliya L. Ivanova^a, Elena A. Konshina^a, Nikolai A. Feoktistov^b,
Wolfgang Dultz^c, Aleksander N. Chaika^a, and Vladimir A. Berenberg^a

Institute of Physical Chemistry Darmstadt University of Technology, Petersenstr.20, 64287 Darmstadt, Germany;

^aAll-Russian S. I. Vavilov Research Center "GOI", Birzhevaya Liniya 12, St.Petersburg, 199034 Russia;

^bA.F. Ioffe Physical Engineering Institute, St.Petersburg, Russia;

^cDeutsche Telekom AG, Am Kavallieriesand 3, 64276 Darmstadt, Germany

ABSTRACT

The basic characteristics of the optically addressed spatial light modulators (OASLM's) are presented based on ferroelectric liquid crystal (FLC) as a light modulating media and amorphous hydrogenated silicon carbide a-SiC:H and dye-dopped polyimide films as photoconducting layers. The parameters of the constituent parts are described, among them: photoconductivity of photosensitive layers, data about newly developed light blocking layers, characteristics of the FLC materials, utilizing the deformed helix ferroelectric effect. The dynamics of the response in hundreds Hz region, the diffraction efficiency of 20% at spatial resolution better than 50lp/mm, and sensitivity in range of microWatt/cm² are obtained.

Keywords: Optically addressed spatial light modulators (OASLM's), amorphous silicon carbide photoconductors, polymer photoconductors, ferroelectric liquid crystals.

INTRODUCTION

Among the basic parameters of the recording materials for holographic applications is the diffraction efficiency, determined by the ratio of the intensity of light beam diffracted into the first order of diffraction to the intensity of the basic light beam. The silver photosensitive films have almost ideal value of the DE, but they require special treatment after recording the hologram and it is impossible to use them as the reversible media. The existing reversible materials e.g. photorefractive crystals, photothermoplastics and dye doped composite materials have very slow operation in range of parts of Hertz and their diffraction efficiency is much less than silver films. Last materials have very high spatial resolution of the order of 10³ lp/mm, but due to small sensitivity and slow operation they are not to be used for real time dynamical holography.

The optically addressed spatial light modulators¹ (OASLM's) composed of photoconductive film and liquid crystal layer, can realize the most serious requirements to the reversible recording media for dynamical holography. In the early OASLM developments the nematic liquid crystals were used as a light modulating media and they permitted to receive the operation rate in range of units of Hertz and the diffraction efficiency reached almost limit value 30% but for very small spatial resolution of the order 10 lp/mm. Last 10 years ferroelectric liquid crystals² attracted strong attention³ as a light modulating media owing to fast response in the range of microseconds.

For many applications e.g. real time holography⁴ or optical phase conjugation⁴ the high spatial resolution of OASLM should be accompanied with enhanced diffraction efficiency to have high enough conversion of read-out light into reconstructed image. To receive the diffraction efficiency of OASLM close to the theoretical limit 34% it is necessary to have the angle 90° between extreme positions of optical axis of FLC⁶. It means that FLC with the switchable molecular tilt angle 45° should be used. The diffraction efficiency of the known FLC based OASLM's^{4,5} doesn't exceed 10% due to the use of ferroelectric liquid crystals with the relatively small molecular tilt angle 22-30°.

In this paper we present the data about OASLM's utilizing FLC materials with large tilt angle 39-40°. The presence of helical structure with short pitch of helix less than 0.2μm gives us the possibility to realize the dynamical gray scale as well

as high sensitivity to the writing light intensity owing to the absence of threshold for electrooptical response of DHF effect⁷. The characteristics of the constituent parts of the developed OASLM's are described e.g. photoelectric properties of the used photoconductors: amorphous silicon carbide a-SiC:H as well as dye doped polyimide films. The parameters of newly developed light blocking layer on the basis of amorphous hydrogenated carbogen a-C:H are also discussed.

PHOTOCONDUCTING LAYERS

In this work we used the photoconductive films on the basis of amorphous hydrogenated silicon carbide a-SiC:H and polymer photoconductive layers on the basis of dye doped polyimides. The use of the silicon carbide films instead of widely applied for this purpose amorphous hydrogenated silicon a-Si:H⁸⁻¹⁰ has such advantages as: the possibility to vary the spectrum of photosensitivity as well as dark resistivity and optical transmission by means of variation of the carbon content in a-Si_{1-x}C_x:H film⁶⁻⁸. It is known that response time of the a-Si_{1-x}C_x:H layers is so fast as a-Si:H layers¹¹⁻¹³ and can be reduced to microseconds in case of p-i-n diode films. Owing to the higher dark resistivity these layers can realize higher spatial resolution owing to the decrease of lateral currents. The increase of content of carbogen leads to the shift of the absorption band to blue region of spectrum and to decrease of photosensitivity. But for many applications such photosensitivity is quite enough. Thus we have the compromise between some decrease of sensitivity and the pronounced increase of spatial resolution.

The preparation of a-SiC:H films by means of magnetron sputtering methods is described in^{14,15}. In case of photodiode pin structures composed from a-SiC:H the thickness of p-type layer was 150Å, the thickness of a-SiC:H layer with intrinsic conductivity was about 5000Å, of n-type layer - 300Å.

The another type of photoconducting layer used in our work is dye sensitized polyimide film with thickness about 1.5μm. The maximum of the photosensitivity of this film was in range 500-530nm¹⁶. The advantage of the polymer photoconductive layer is the very high spatial resolution, which can be obtained owing to very small dark conductivity^{16,17}, hence no significant lateral current occurs after writing exposure. Both used photoconductors were transparent for red light and it was possible to investigate the OASLM's in reflective and transmissive modes in visible range of spectrum.

LIGHT BLOCKING LAYER

For majority of applications of the OASLM's it is necessary to decouple the write and read out light beams. If the read out light does penetrate into the photoconducting layer the strong deterioration of sensitivity, contrast and spatial resolution takes place. Usually the dielectric or metal pixelized mirrors deposited onto photoconductor allow it to reduce the influence of the read out beam, but in a small value about 10² times. The strong increase of the decoupling between write and read out beams is accomplished by means of embedding the additional light absorbing layer. The requirements to their properties are relatively strong due to that it should have the good absorbance of the read out light and the high resistivity at very small thickness. In our work the "optically black" carbon films were developed¹⁸ to fulfil the numerous requirements to light blocking layer.

The discussed layer consists of amorphous hydrogenated carbogen a-C:H and it was fabricated by the chemical vapor deposition of hydrocarbon precursor, composed from the mixture of acetylene C₂H₂ with argon Ar, or pure acetylene, using the d.c. glow discharge^{19,20}. In Fig's. 1 and 2 the volt-current characteristics of the developed a-C:H films are presented,

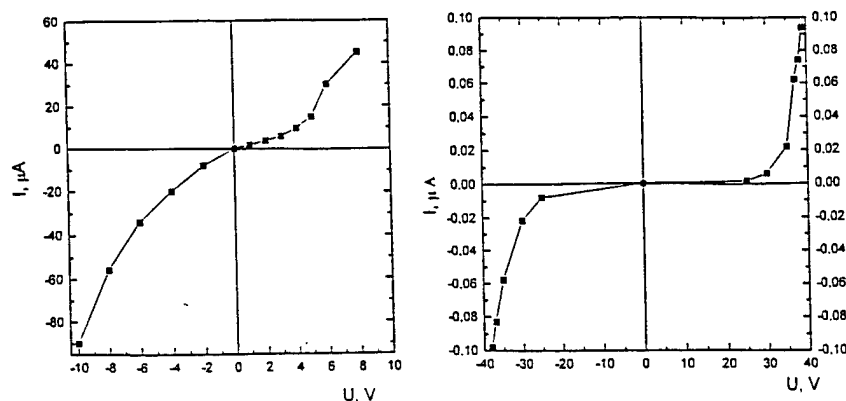
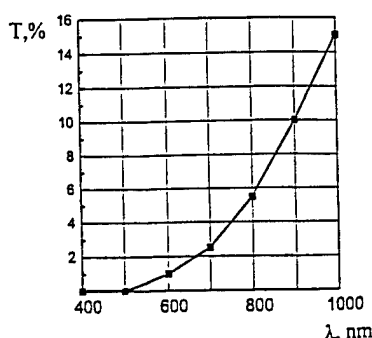


Fig.1. The voltage-current characteristic U(I) for the structure ITO+a-C:H+metal. a-C:H layer prepared from mixture acetylene + argon.

Fig.2. The same as in Fig.1, but a-C:H layer prepared from pure acetylene.

showing the variety of the possible resistivities of the developed blocking layers from 10^8 to 10^{12} Ohm.cm, if the carbon film was prepared from mixture of acetylen with argon, or from pure acetylen, resp.



In Fig. 3 the spectrum of the optical transmission is shown for carbon film a-C:H with the thickness of the order of 1 μm. It is seen the very small transmission of film for whole visible spectrum and even for red light with wavelength 632 nm the transmission doesn't exceed 1%, that is essentially better than characteristics of known carbon films, developed for instance for contrast enhancement layers for liquid crystal displays²¹.

Fig. 3. The spectral dependence of the transmission of the a-C:H layer with thickness 1 μm

The application of the described carbon a-C:H film as a blocking layer has the additional advantage in case of use the amorphous silicon carbide a-SiC:H film as a photoconducting layer owing to the possibility to unify the procedure of the preparation of both layers in one technological circle, taking into account the use of acetylene as a constituent fracture of gas mixture with silane SiH₄ for preparation of the a-SiC:H film.

preparation of both layers in one technological circle, taking into account the use of acetylene as a constituent fracture of gas mixture with silane SiH₄ for preparation of the a-SiC:H film.

MIRRORS

The dielectric mirrors or aluminium pixelized films were used in case of preparation of OASLM's operating in reflecting mode. The dielectric mirrors were based on interchanging layers of SiO₂ and TiO₂ or SiO₂ and Si. The size of Al pixels was varied from 50 μm to 5 μm, and the gap between pixels from 5 μm to 1 μm, respectively.

PHOTOELECTRIC CHARACTERISTICS OF THE PHOTOCOndUCTING FILMS TOGETHER WITH BLOCKING AND REFLECTING LAYERS

These measurements allowed us to make the preliminary selection of photolayers with high dark resistivity and high photoelectric sensitivity. In Fig. 4 the sketch of measurements is presented, where the mercury (Hg) drop was used as an electrode, contacting with the multi-layer structure, involving the photoconducting film. The another electrode was ITO layer, deposited onto glass substrate.

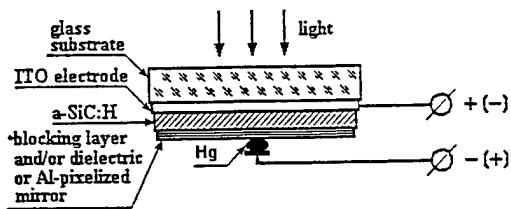


Fig. 4. The sketch of measurements of the voltage current characteristics of the thin-film structures, involving photoconducting, light-blocking and reflecting layers.

The area of contact of Hg drop with testing surface of structure ITO/photolayer/light blocker/mirror was about 10^{-3} cm² and determined under microscope.

In Fig's 5-8 the d. c. voltage-current measurements are presented for some samples of a-Si:H and a-SiC:H layers in intrinsic and p-i-n configurations. As it seen, for intensity 1 mW/cm² of white light, the change of conductivity reaches 10^3 times,

samples 577 with intrinsic conductivity, Fig. 5, and 10^4 times for p-i-n structures, samples 566 without mirror, Fig. 6, and sample 566 with Al pixelized mirror, Fig. 7.

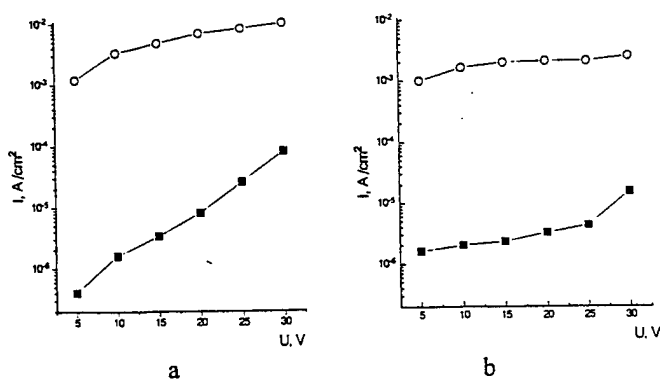


Fig. 5. The current-voltage dependencies of the photoconductive film a-SiC:H (intrinsic conductivity) in dark (■) and light (o) conditions, white light 300 μW/cm², sample 577. a) positive voltage on Hg, b) negative voltage on Hg.

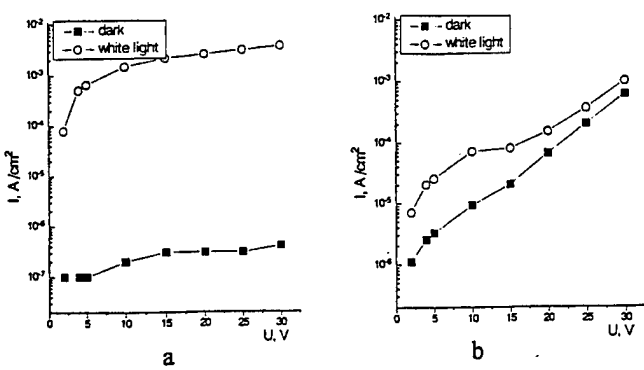


Fig. 6. The current-voltage dependencies of the photoconductive film a-SiC:H (p-i-n diode structure) in dark (■) and light (○) conditions, white light $300 \mu\text{W}/\text{cm}^2$, sample 566. a) positive voltage on Hg, b) negative voltage on Hg.

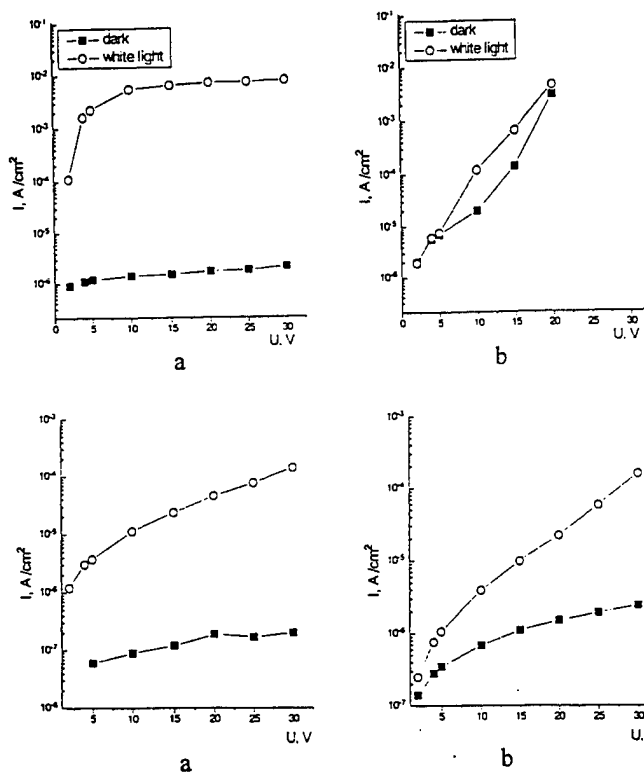


Fig. 7. The current-voltage dependencies of the photoconductive film a-SiC:H (p-i-n diode structure) with pixelized Al mirror in dark (■) and light (○) conditions, white light $300 \mu\text{W}/\text{cm}^2$, sample 566. a) positive voltage on Hg, b) negative voltage on Hg.

Polymeric photoconductive film 277 showed also the large change of conductivity 10^3 times, Fig. 8.

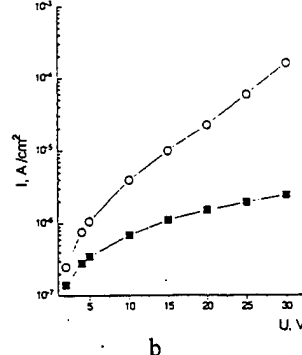


Fig. 8. The current-voltage dependencies of the photoconductive polymer film on the basis of dye-sensitized polyimide, in dark (■) and light (○) conditions, white light $300 \mu\text{W}/\text{cm}^2$, sample 277. a) positive voltage on Hg, b) negative voltage on Hg.

The presence of blocking layer decreased the effective value of photoconductivity, Fig. 9, sample 568 with structure a-SiC:H/a-C:H/Al-mirror. But in some cases the relatively good d. c. photoconductive properties of structure took place even with the dielectric mirror, sample 451, Fig. 10.

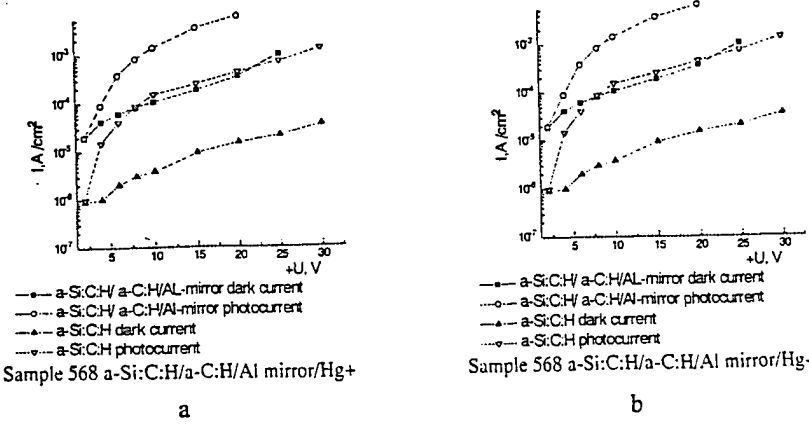


Fig. 9. The current-voltage dependencies of the photoconductive film a-SiC:H (intrinsic conductivity) with light blocking a-C:H layer and Al-pixelized mirror, in dark (■) and light (○) conditions. White light $300 \mu\text{W}/\text{cm}^2$, sample 568. a) positive voltage on Hg, b) negative voltage on Hg.

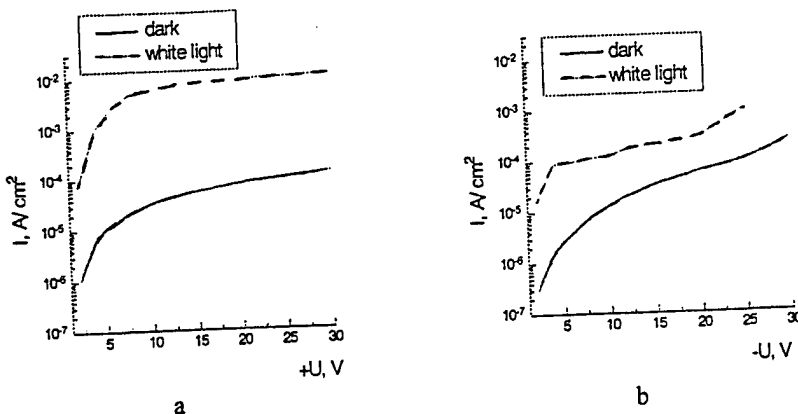


Fig.10. The current-voltage dependencies of the photoconductive film a-SiC:H (p-i-n diode structure) with dielectric mirror in dark (■) and light (○) conditions, white light $300\mu\text{W}/\text{cm}^2$, sample 451. a) positive voltage on Hg, b) negative voltage on Hg. Dielectric mirror is composed from 5 interchanging layers Si-SiO₂-Si...

DEFORMED HELIX FERROELECTRIC MATERIALS.

The deformed helix ferroelectric (DHF) effect is considered as the lowest voltage effect in liquid crystals²². The absence of any threshold voltage allowed us to receive the very high sensitivity of OASLM's utilizing the DHF effect⁷. Additional advantages of this effect useful for design of OASLM's are the intrinsic gray scale and relatively fast response which can be of the order of $100\mu\text{s}$ ²². In Table 1 the basic parameters of the developed DHF materials are presented. For design of OASLM's with enhanced diffraction efficiency we used mixtures with high tilt angle in range $39\text{--}40^\circ$. The response times of these materials in DHF mode were less than 1ms, pitch of helix p_0 was of the order $0.2\mu\text{m}$.

Table 1. Parameters of DHF FLC materials.

Parameter	FLC material	FLC-464	FLC-471	FLC-474
Interval of SmC* phase		+5...+62°C	+2...+62.5°C	-5...+52°C
Tilt angle (25°C)		40°	39.5°	31°
Spontaneous polarization, nC/cm ² (25°C)		120	115	190
Pitch of helix, μm (25°C)		0.18	0.19	0.26
Response time, μs (25°C)		500	500	250

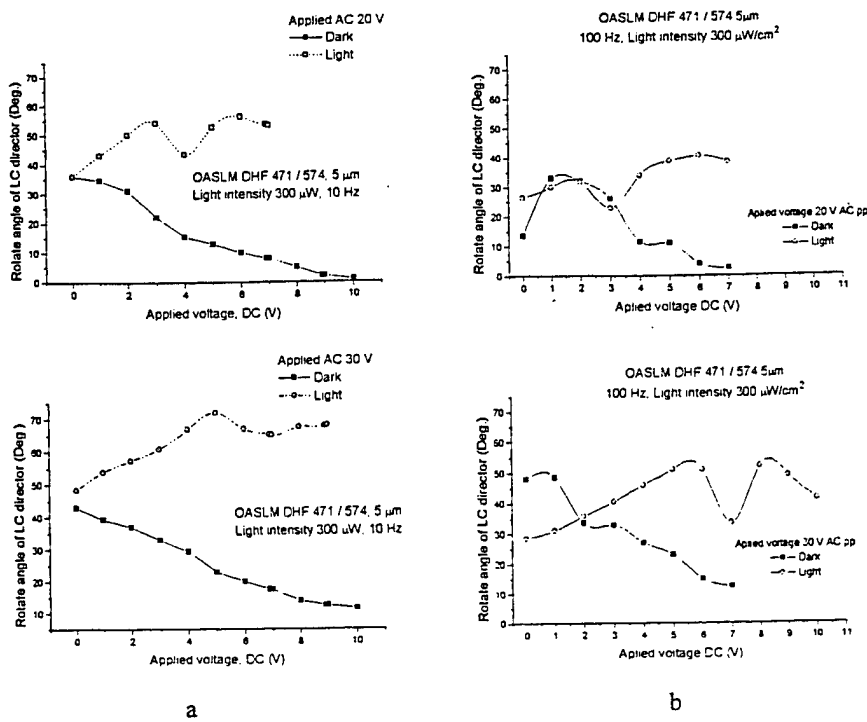
THE TESTING OF THE OASLMS'S

For characterization of photo-optical response of the developed OASLM's we have measured at first the switchable angle of optical axis of FLC layer at switching the polarity of a.c. voltage (meander) in darkness and under illumination with blue light pulses with intensity $300\mu\text{W}/\text{cm}^2$. Set-up was used, based on two-path microscope, supplied with video-camera, frame grabber with computer and video recorder for writing and reading out in different wavelength spectra, in transmissive and reflective modes. The light induced difference of the value of switchable tilt angle was used as a primary characteristic for evaluation of possible limit of diffraction efficiency. The switchable tilt angle was determined from two extreme positions of the cell, corresponding to opposite polarities of applied square-wave voltage, found by means of minimization of the response oscillosogram²³.

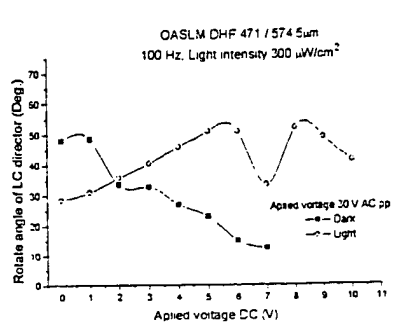
It is found, that at appropriate choice of amplitude of a.c. voltage and d.c. offset the light induced difference between two extreme positions of optical axis of FLC layer reaches $50\text{--}56^\circ$, Fig's 11,12, sample 471/574-5μm and 471/574-12μm, resp., curves for a.c. 30Vpp, d.c.offset 10V, 10Hz.

Owing to the large difference of "rotate angle" between illuminated and dark states (e.g. 56°) at frequencies of the order of tens Hz the large phase difference can be obtained, (e.g. 112°) between neighbour (odd and even) stripes of phase diffraction grating written in OASLM. Hence, the high diffraction efficiency η can be obtained in case of cell thickness d satisfying to the condition "half of lambda"²⁴:

$$\eta = [2/\pi \sin(2\Theta)]^2 \quad (1)$$



a



b

Fig.11. The total angle of switching of optical axis of FLC layer at change of polarity of applied voltage in darkness (closed symbols) and under illumination with light intensity 300 μW/cm² (open symbols). a-SiC:H (i), layer Nr.574; FLC-471, d=5 μm. a) 10Hz, b) 100Hz. Transmissive OASLM. Light pulses follow during the negative polarity of meander voltage applied to photoconductor.

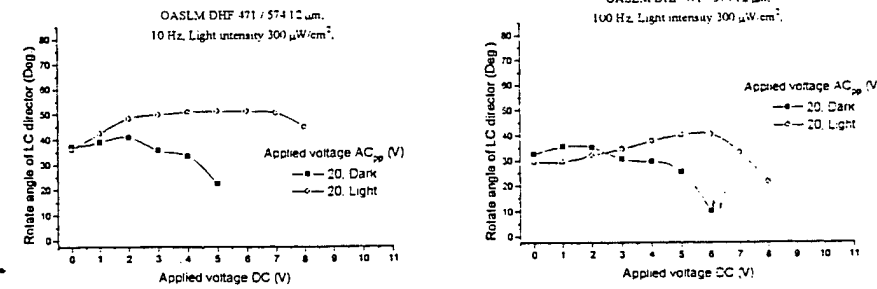
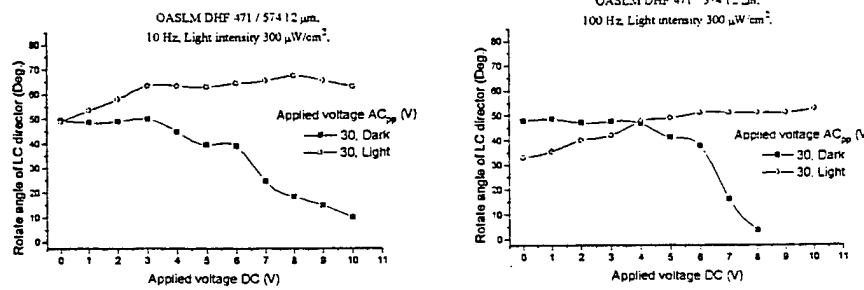
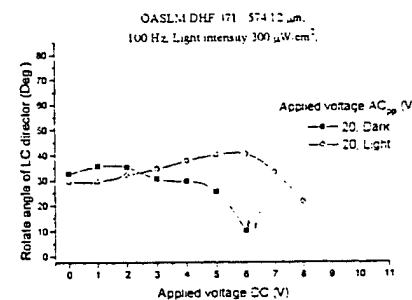
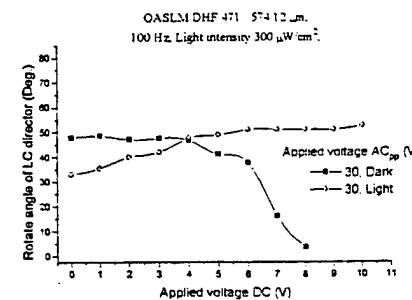


Fig.12. The same as in Fig.11, but FLC layer thickness 12 μm.



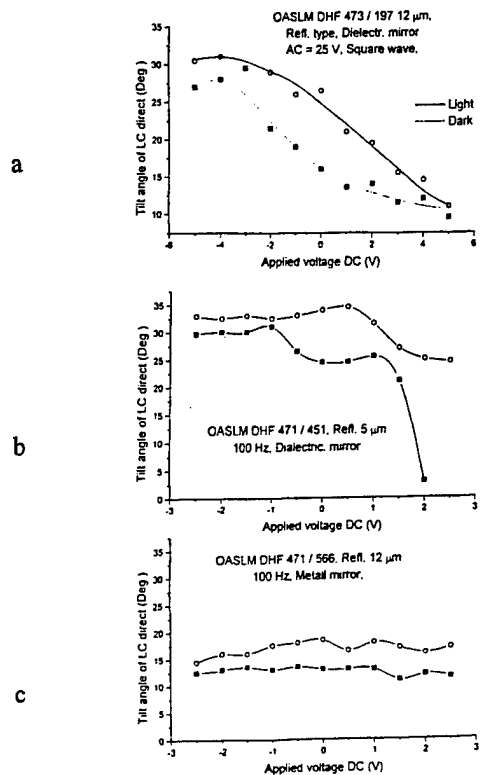
a



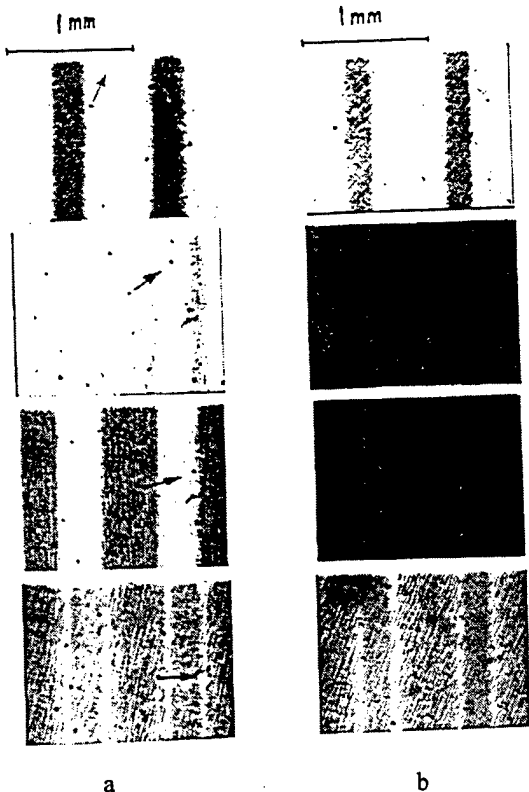
b

In our case $\Theta = 28^\circ$ and $\eta_{\max} = 27.8\%$. These values are not so far from ideal case $\Theta = 45^\circ$, $\eta_{\max} = 40.5\%$. Due to complicated profile of effective refractive index close to sinusoidal behavior in the phase diffraction grating and periodical deviations of phase retardation from condition "half of lambda" in helical structure we should expect smaller value η than 27.8%.

For all investigated OASLM's in transmissive mode the spatial resolution was better than 66 lp/mm on the level of the modulation transfer function 50%, measured with target projection technique²⁵.



Fig's 14, 15 demonstrate the operation of OASLM's of reflective type.



Three OASLM's were prepared of reflective type and it was the significantly smaller light induced difference of the switchable angle 10-15° in comparison with the described OASLM's of transmissive type, Fig.13. We suppose that thickness of FLC layer in these devices as well as driving voltage conditions were far from the optimum values in scope of complicity of the multi-layer structure, consisting of interchanging semi-conductive and dielectric layers.

Fig.13. The total angle of switching of optical axis of FLC layer at change of polarity of applied voltage in darkness (closed symbols) and under illumination with light intensity 1mW/cm^2 (open symbols). Photoconductor : a-SiC:H p-i-n diode film or intrinsic conductivity (i) films, FLC-471. 100 Hz, continuous light illumination.

- (a) layer 197(I), thickness of FLC layer 12 μm ; dielectric mirror 12 interchanging layers $\text{TiO}_2-\text{SiO}_2-\text{TiO}_2-\dots$
- (b) layer 451, thickness of FLC layer 5 μm ; dielectric mirror 5 interchanging layers $\text{Si}-\text{SiO}_2-\text{Si}-\dots$
- (c) layer 566, thickness of FLC layer 12 μm , metal Al pixelized mirror.

Fig.14. Operation of OASLM of reflective type. Continuous light illumination. Two stripes with width about 200 μm separated with gap 600 μm are projected onto photoconductive layer. Photoconductor 451, a-SiC:H (p-i-n). FLC-473, d=12 μm . Thin dielectric mirror, 5 layers $\text{Si}-\text{SiO}_2-\text{Si}-\dots$ Meander voltage $\pm 3.75\text{V}$, d.c. offset -0.25V . White light 1mW/cm^2 . (a) 100Hz, (b) 500Hz. From up to bottom: rotation of cell clockwise.

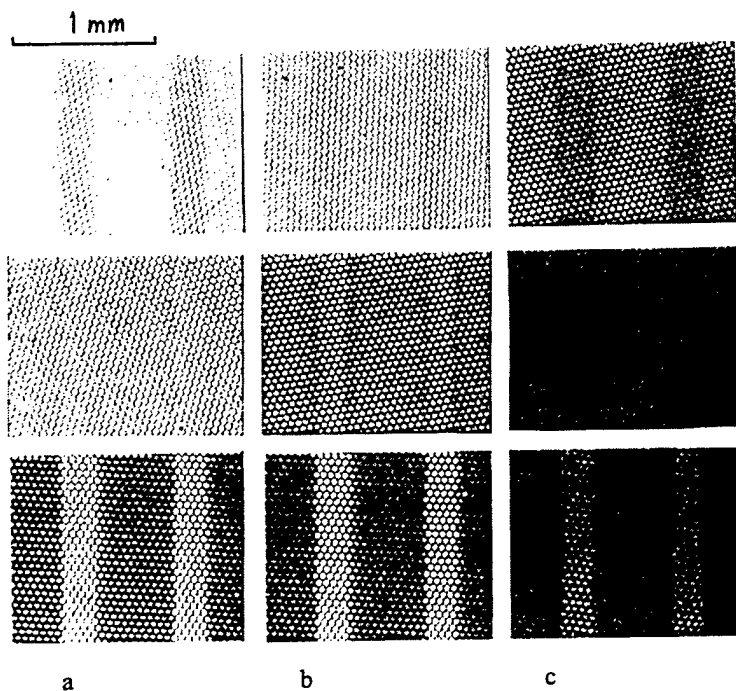


Fig.15. The same as in Fig.14, but metal Al pixelized mirror. Pixel size 50 μ m. Photoconductor a-SiC:H layer 566, FLC-471, d=12 μ m Meander voltage ± 3.75 V, d.c. offset -0.25V. White light 1mW/cm². (a) 100Hz, (b) 500Hz, (c) 1kHz. From up to bottom: rotation of cell clockwise.

In case of thick dielectric mirror, composed from 12 interchanging layers TiO_2 - SiO_2 - TiO_2 -..., the operation of OASLM was similar to presented in Fig.14, but bluring of the recorded image with the decrease of resolution to 5 lp/mm was observed with characteristic time of the order of 20 ms. Nevertheless the fast moving pictures could be recorded with the resolution better than 10 lp/mm. The contrast of reflective type OASLM's was of the order of 5:1 estimated for visible range of spectrum, which probably is related with mentioned above non-optimized thicknesses of FLC layer and driving conditions.

The operation of the OASLM's of reflective type containing the light blocking layer a-C:H and Al pixelized mirror was similar to presented in Fig.15.

KINETICS OF THE OASLM RESPONSE

In Fig. 16 the kinetics of the optical response is presented for OASLM, illuminated with blue light pulses which followed during the half of period of square-wave voltage with negative polarity relative to photoconductor.

It is seen the gray scale capability of the DHF based OASLM as well as high threshold sensitivity of the device, better than $5 \cdot 10^{-7}$ W/cm². The response time of the order of 1-2ms permit us to have the operation rate in range of about 200Hz.

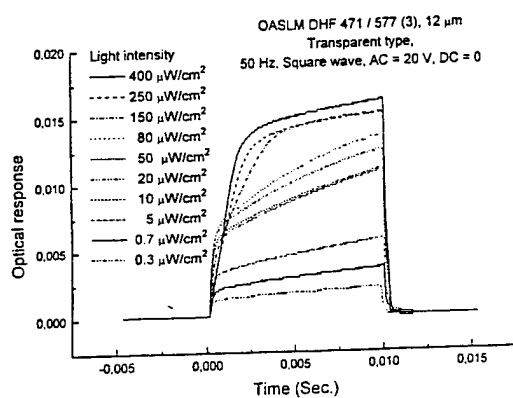


Fig.16. Kinetics of optical response of OASLM at different intensities of light pulses, synchronized with negative polarity of square wave voltage relative to photosensor. Photoconductor a-SiC:H layer 577, intrinsic conductivity, liquid crystal FLC-471, thickness of FLC layer 12 μ m. Pick-to-pick amplitude 20V, 50Hz, bias field $V_b=0$.

THE DIFFRACTION EFFICIENCY OF THE DEVELOPED OASLM's.

In Fig. 17 the sketch of set-up is shown, which allowed us, at first, to measure the diffraction efficiency (DE) of the OASLM's, at second, to demonstrate the ability of the described OASLM's to realize the holographic correction of aberrations of lenses in telescope systems²⁶.

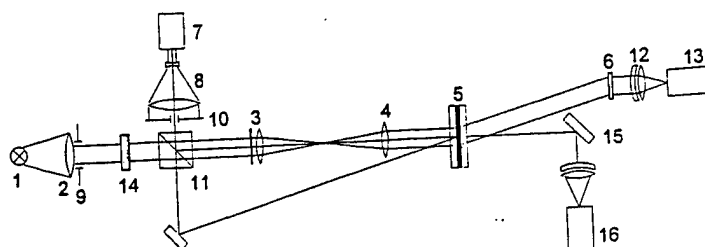


Fig. 17. Experimental set-up for measurement of diffraction efficiency and quality of image correction using OASLM (5). (13, 16) - CCD video cameras, (6)-phase diffraction grating 95 lp/mm, (7)-pulse laser, wavelength $\lambda=0.53\mu\text{m}$, pulse duration 20-30ns.

For measurements of value and response time of diffraction efficiency the HeNe laser with wavelength $\lambda=0.63\mu\text{m}$ or light emitting diode, $\lambda=0.82\mu\text{m}$, were used. The signal was recorded by means of photo-diode placed instead of CCD camera (13) and analyzed using the oscilloscope. Energy of writing beam was measured by means of photoelectric sensor. Spatial frequency of written hologram can be varied by means of change of angle between signal and reference laser beams in wide range up to 100 lp/mm. The diffraction efficiency η was measured at change of electrical voltage conditions (pick-to-pick amplitude V_{pp} , bias field V_b , time delay τ between change of polarity of square-wave voltage and writing laser pulse, also the dependence of DE from read-out light polarization was measured.

We have found the minor dependence of DE on polarization orientation relative to vector of written grating, where the maximum DE corresponded to coincidence of grating vector and normal to smectic layers. It is related with the property of the phase diffraction grating, composed from interchanging deviations of the optical axes, where the period of diffraction is determined by the length of the repeating unit²⁷. It follows from the symmetrical splitting of the any polarization into two polarizations, which interfere after passing through the assembly of uni-axial optical plates with interchanging signs of the deviation of the slow optical axes²⁷. Namely ferroelectric liquid crystal is the single electrooptical media which can simply realize such kind of controlled diffraction grating²⁸.

In Fig.18 the diffraction efficiency is presented for OASLM, based on photoconductive polymer and in Fig.19 the same for OASLM, utilizing the silicon carbide based photoconductor. In case of a-SiC:H photosensor three OASLM's were

investigated with the same photoconductive layer Nr. 577 (intrinsic conductivity), and with FLC-471 layer of variable thickness, 2 μm , 5 μm and 12 μm , resp.

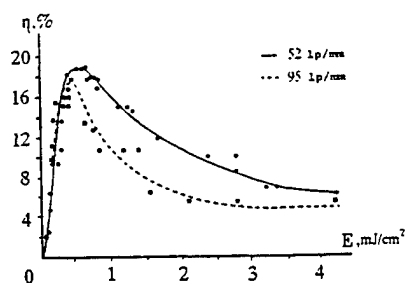


Fig. 18. Dependence of the diffraction efficiency η on energy density E of writing laser pulse (duration about 25ns) for phase gratings with two space frequencies, 52lp/mm and 95lp/mm. Duration of voltage pulse 1s, repetition 0.1Hz. OASLM with photoconductive polymer Nr.277.

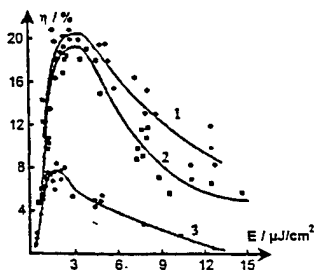


Fig.19. Dependence of the diffraction efficiency on the energy of writing light pulses (25ns, 532nm) for a-SiC:H based OASLM's. Photoconducting layer a-SiC:H, Nr.577 (intrinsic conductivity). Curve 1 for FLC layer thickness 12 μm , curves 2 and 3 for FLC layer thickness 5 μm . Spatial resolution of gratings 52 lp/mm (curves 1 and 2), and 100lp/mm (curve 3)

In our papers^{26,29} the detailed driving conditions are described for measurements of the diffraction efficiencies of these OASLM's. It follows from data, presented in Fig's 18 and 19, the very high diffraction efficiency of OASLM's based on both kinds of photosensors, reaching 20% for spatial resolution better than 50 lp/mm. It is two times higher than that obtained in papers^{4,5} where the binary OASLM's are investigated with SSFLC material, having smaller switchable molecular tilt angle of the order of 22-30°. The significant decrease (2.5 times) of DE at increase of spatial frequency from 52 to 100lp/mm, Fig.19, is connected with higher dark conductivity of a-SiC:H layer in comparison with polymer photosensor.

The devices differ strongly in values of pulse energy, providing the maximum diffraction efficiency: 600-800μJ/cm² for polymer version and 3-5μJ/cm² or silicon carbide version, resp. The operation rate of the first is restricted with frequencies 0.1-1Hz, whereas silicon carbide devices are able to operate till hundreds of Hertz. The advantage of polymer based OASLM is the very high spatial resolution which can reach probably many hundreds with the reduced diffraction efficiency. We have found that for a-SiC:H based OASLM the repetition rate of the writing laser pulses can be 6-8Hz with conservation of maximum diffraction efficiency on the level 20%. At higher frequency, e.g 100Hz, the diffraction efficiency was not less than 5-6%, but in this case the light pulses with duration 50mc, intensity 200-500μW/cm² and wavelength 0.63μm were used for writing the holograms with spatial frequency 85lp/mm.

In the paper²⁶ we have presented the successful application of the OASLM's based on a-SiC:H as well as dye-doped polymer in combination with the described DHF materials for holographic correction of telescope aberrations.

CONCLUSIONS

We presented the data about basic characteristics of the optically addressed spatial light modulators, utilizing the deformed helix ferroelectric liquid crystal materials with large tilt angle as a light modulating media and amorphous hydrogenated silicon carbide a-SiC:H and dye-sensitized polymer films as a photoconducting layers.

In transmissive OASLM's the spatial resolution is of the order of 100lp/mm at the level of MTF (modulation transfer function) 50%. The threshold sensitivity of OASLM's, using a-SiC:H (i) films and DHF materials is of the order of 10⁻⁷ μW/cm². For a-SiC:H films in p-i-n configuration the threshold sensitivity can be of the order of 10⁻⁸ W/cm².

The response time of OASLM's, using a-SiC:H (i) films and DHF materials with large tilt angle 39° - 40° are of the order of 1-2ms. In case of p-i-n structures and DHF materials with smaller tilt angle 31° the response time is of the order of 200μs.

The use of the deformed helix ferroelectric liquid crystals with large tilt angle allows us to receive the high diffraction efficiency 20% in OASLM's, utilizing both considered photo-layers, that is about 60% of theoretical limit for phase diffraction gratings with sinusoidal profile. The OASLM's based on amorphous silicon carbide allow us to design the holographic correctors of images in optical systems with operation rate in range of hundreds Hz. The photoconductive polymer allows us to design the dynamical holography devices with very high spatial resolution and with real time operation.

ACKNOWLEDGEMENTS

The work was done in frames of Volkswagen Stiftung Project I/72011 and I/72818, The support by Deutsche Telekom (L.A.B.), Contract 4160/75028, and partly by European Research Office, Contract N68171-97-M-5781 are gratefully acknowledged.

L.A.Beresnev's current address is the Army Research Laboratory, 2800 Powder Mill Road, Adelphi MD, 20783 USA

REFERENCES

1. J. Grinberg, A. Jacobson, W. Bleha, L. Miller, L. Fraas, D. Boswell, and G. Myer, *Opt. Eng.*, **14**, pp.217-225, 1975.
2. R. B. Meyer, L. Liebert, L. Strzelecki and P. Keller, "Ferroelectric liquid crystals", *Journal de Phys.-Lett.*, **36**, L69-L71, 1975.
3. G. Moddel, "Ferroelectric liquid crystal spatial light modulators", "Spatial Light Modulation Technology", ed. by U. Efron, Dekker, New York, pp. 287-359, 1994.
4. S. Fukushima, T. Kurokawa, and M. Ohno, "Real-time hologram construction and reconstruction using a high-resolution spatial light modulator", *Appl. Phys. Lett.*, **58**, pp. 787-789, 1991.
5. K. M. Johnson, C. C. Mao, G. Moddel, M. A. Handschy, and K. Arnett, "High-speed, low-power optical phase conjugation using a hybrid amorphous silicon/ferroelectric-liquid-crystal device", *Optics Letters*, **15** (20), pp.1114-1116, 1990.

6. M. T. Gruneisen, and J. M. Wilkes, "Compensated Imaging by Real-Time Holography with Optically Addressed Spatial Light Modulators", *OSA Trends in Optics and Photonics Series 1997*, Presented at the Topical Meeting on Spatial Light Modulators, Lake Tahoe, NV, March 17-19, 1997, Paper STuB5.
7. L. A. Beresnev, L. M. Blinov, D. I. Dergachev, A. I. Zhindulis, I. S. Klimenko, S. I. Paeda, and A. A. Sergeev, "Photosensitive structure consisting of a ferroelectric liquid crystal and a photoconductor", *Sov. Tech. Phys. Lett.*, **14** (3), pp. 117-118, 1988.
8. G. Moddel, K. M. Johnson, W. Li, R. A. Rice, L. A. Pagano-Stauffer, and M. A. Handschy, "High speed binary optically addressed spatial light modulators", *Appl. Phys. Lett.*, **55** (6), pp. 537-539, 1989.
9. L. Abdulhalim, G. Moddel, K. M. Johnson, "High-speed analog spatial light modulator using a hydrogenated amorphous silicon photosensor and an electroclinic liquid crystal", *Appl. Phys. Lett.*, **55** (16), pp. 1603-1605, 1989.
10. P. R. Barbier, G. Moddel, "Hydrogenated amorphous silicon photo-diodes for optical addressing of spatial light modulators", *Applied Optics*, **31** (20), pp. 3898-3907, 1992.
11. K. Akiyama, A. Takimoto, and H. Ogawa, "Photoaddressed spatial light modulator using transmissive and highly photosensitive amorphous-silicon carbide film", *Applied Optics*, **32** (32), pp. 6493-6500, 1993.
12. N. A. Feoktistov, and L. E. Morozova, *J. Tech. Phys.-Lett. (Russ.)*, **20** (5), pp. 12-16, 1994.
13. N. L. Ivanova, N. A. Feoktistov, A. N. Chaika, A. P. Onokhov, and A. B. Pevtsov, "The spatial light modulator with photosensitive layer of hydrogenated amorphous silicon carbide", *Mol. Cryst. Liq. Cryst.*, **282**, pp. 315-322, 1996.
14. A. V. Zherzdev, V. G. Karpov, A. B. Pevtsov, A. G. Pilatov, and N. A. Feoktistov, "Electroluminescence emitted by *p-i-n* structures made of $\alpha\text{-Si}_{1-x}\text{C}_x\text{:H}$ ", *Sov. Phys. Semicond.*, **26** (4), pp. 421-423, 1992.
15. N. L. Ivanova, L. E. Morozova, A. P. Onokhov, A. B. Pevtsov, and N. A. Feoktistov, *J. Tech. Phys.-Lett. (in Russ.)*, **22** (4), pp. 7-11, 1996.
16. V. Mylnikov, "Liquid crystal light valves with organic polymeric photoconductors", *Mol. Cryst. Liq. Cryst.*, **152**, pp. 597-607, 1987.
17. V. S. Mylnikov, M. A. Grosnov, N. A. Vasilenko, B. V. Kotov, L. N. Soms, *J. Tech. Phys.-Lett. (in Russ.)*, **11** (1), pp. 749-753, 1985.
18. E. A. Konshina, A. P. Onokhov, N. A. Feoktistov, W. Dultz, L. A. Beresnev, and W. Haase, "Investigation of optical and photoelectric properties of $\alpha\text{-Si:C:H} / \alpha\text{-C:H}$ structures", to be published.
19. A. V. Balakov, E. A. Konshina, "Methods of fabrication and properties of diamont-like carbon films", *Sov. J. Opt. Technol.*, **49** (9), pp. 591-599, 1982.
20. A. Bubezzer, B. Dischler, G. Brandt, P. Koidl, "Optical properties of hydrogenated hard carbon thin films", *Thin Solid Films*, **91**, pp. 81-87, 1982; D. R. McKenzie, R. C. McPhedran, N. Savvides, "Analysis of films prepared by plasma polymerization of acetylene in a d. c. magnetron", *Thin Solid Films*, **108**, pp. 247-256, 1983.
21. B. Singh, S. McClelland, F. Tams, B. Halon, O. Mesker, D. Furst, "Use of black diamond-like carbon films as a contrast enhancement layer for liquid-crystal displays", *Appl. Phys. Lett.*, **57** (22), pp. 2288-2290, 1990.
22. L. A. Beresnev, V. G. Chigrinov, D. I. Dergachev, E. P. Pozhidaev, J. Fuenfschilling, and M. Schadt, "Deformed helix ferroelectric liquid crystal display: a new electrooptical mode in ferroelectric chiral C liquid crystals", *Liquid Crystals*, **5** (4), pp. 1171-1177, 1989.
23. V. A. Baikalov, L. A. Beresnev, and L. M. Blinov, "Measures of the molecular tilt angle and optical anisotropy in ferroelectric liquid crystals", *Mol. Cryst. Liq. Cryst.*, **127**, pp. 397-406, 1985.
24. A. P. Onokhov, V. A. Berenberg, A. N. Chaika, N. L. Ivanova, M. V. Isaev, N. A. Feoktistov, L. A. Beresnev, W. Dultz, and W. Haase, "Novel liquid crystal spatial light modulators for adaptive optics and image processing", *Proceedings of SPIE*, Vol. 3388, Presented to SPIE's 12th Annual Int. Symp. on Aerospace/Defense Sensing, Simulation, and Controls "AeroSense'98", Advanced Technical Program, p.52.
25. L. A. Beresnev, A. P. Onokhov, W. Dultz, and W. Haase, "Local optical limiting devices based on photoaddressed spatial light modulators, using ferroelectric liquid crystals", *Mol. Cryst. Liq. Cryst.*, **304**, pp. 285-293, 1997.
26. V. A. Berenberg, L. A. Beresnev, W. Haase, A. A. Leshchev, A. P. Onokhov, L. N. Soms, M. V. Vasil'ev, and V. Yu. Venediktov, "Polychromatic correction for aberrations in the lenses of telescopic systems using liquid crystal optically addressed spatial light modulators", *Proceedings of SPIE*, Vol. 3388, Presented to SPIE's 12th Annual Int. Symp. on Aerospace/Defense Sensing, Simulation, and Controls "AeroSense'98", Advanced Technical Program, p.52.
27. M. J. O'Callagan, M. A. Handschy, "Diffractive ferroelectric liquid-crystal shutters for unpolarized light", *Optics Letters*, **16** (10), pp. 770-772, 1991; *United States Patent*, Number 5,181,665, January 26, 1993.

28. L. A. Beresnev, J. Hossfeld W. Dultz, A. P. Onokhov, and W. Haase, "Demonstration st-up for fast switchable diffraction of laser light using the computer controlled diffraction grating based on ferroelectric liquid crystal", *Mat. Res. Soc. Proc.*, 413, pp. 363-370, 1996.
29. L. A. Beresnev, W. Haase, A. P. Onokhov, W. Dultz, M. V. Isaev, N. A. Feoktistov, N. L. Ivanova, E. A. Konshina, A. N. Chaika, and V. A. Berenberg, "Deformed helix ferroelectric liquid crystals with large tilt angle in optically addressed spatial light modulators for dynamical holography applications", submitted to *Mat. Res. Soc. Proc.*, presented to MRS Fall Meeting, December 1-4, 1997, Boston, USA.

Copies of papers, presented for publication

2. V. A. Berenberg, A. A. Leshchev, M. V. Vasil'ev, V. Yu. Venediktov, A. P. Onokhov, and L. A. Beresnev,
“Dynamic Correction for Distortion in Imaging Optical Systems using Liquid Crystal SLMs”,

Proceedings of SPIE, Vol. 3432, pp. 110-119, presented to SPIE Meeting, San Diego, 19-24 July 98, USA,
session on “Dynamic measurement, control, and correction approaches for severely aberrated large optics”

Dynamic Correction for Distortions in Imaging Optical Systems using Liquid Crystal SLMs

V.A.Berenberg, A.A.Leshchev, M.V.Vasil'ev, V.Yu.Venediktov, A.P.Onokhov

Institute for Laser Physics, SC "Vavilov State Optical Institute"
199034, Birzhevaya, 12, St.-Petersburg, Russia

L.A.Beresnev

Technical University, Darmstadt, Germany

ABSTRACTS

Given are the results of experimental study on the quasi real time holographic correction for the lens distortions in the passive observational telescope in the visible range of spectrum, using the liquid crystal optically addressed spatial light modulator.

Keywords: dynamic hologram, holographic corrector, liquid crystal spatial light modulator, passive imaging telescope.

1. INTRODUCTION

The method of holographic correction for distortions, imposed by the primary mirror (lens) of the telescope, was first proposed and realized in the experiment in ^{1,2}. The holographic corrector was recorded by the coherent radiation, and its chromatism (grating disperse) was corrected for by use of the auxiliary diffraction grating, providing thus the possibility of imaging in the comparatively wide spectral range. These works, as well as much later investigations in USA³⁻⁵ were realized with the use of static holographic media, providing thus correction only for the static distortions.

The principle of the holographic correction for the telescope lens distortions is illustrated by the Fig.1. Let the telescope is comprised by the distorted lens 1 and the eye-piece 2. This system is imaging the remote self-luminous object 4 in the registration plane 3. In the case of the high optical quality of the elements 2 and 3 the system resolution is determined by the properties of the lens 1. One can compensate for the lens distortions by the holographic corrector 5, mounted in the plane to which the eye-piece 2 images the pupil of the lens 1^{1,2}. The hologram is recorded by the coherent radiation as the interference pattern of the plain reference wave and the object wave, emitted by the point source, mounted in the plane of the object 4.

The light wave from this point source which has passed through the distorted lens bears the information on its distortions. This information is encoded in the hologram. On the stage of the hologram reconstruction the radiation, emitted by the point source and distorted on its path through the telescope will diffract on the hologram into the plain wave, coinciding with the reference wave, used for the hologram recording. Any luminous object can be treated as a set of the point sources. Hence the radiation from the object, distorted by the telescope, will diffract to the set of plain waves. These waves will reconstruct in the plane 3 the non-distorted image of the object notwithstanding the arbitrary distortions of the telescope lens 1.

The non-monochrome radiation from the object would be expanded by the hologram to the spectrum. This chromatism is to be corrected by the auxiliary static diffraction grating whose spatial frequency is equal to the spatial carrier of the holographic corrector.

2. THE CHOICE FOR THE CORRECTING ELEMENT

One can use the nonlinear optical phase conjugation for the dynamic correction for the primary lens (mirror) distortions⁶. In particular, in^{7,8} it was realized with the use of the stimulated Brillouin scattering. In this case, however, the imaged object is either to emit the coherent radiation or to be illuminated by such a radiation.

The highest efficiency among the nonlinear-optical media for holograms recording, providing dynamic correction for distortions in the wide spectral range, is revealed by the liquid crystal spatial light modulators (LC SLM)⁹ and by the photorefractive crystals¹⁰. For example, in¹¹, the use of LC SLM made it possible to correct for distortions in the spectral band with the width 10 nm, separated from the hologram recording wavelength in 90 nm. In the experiment¹⁷ similar schematics was realized with the use of the auxiliary static holographic grating, compensating for the dynamic hologram chromatism. In¹² the correction for the distortions of the optical elements was realized with the use of the photorefractive crystals BSO and NBS with the hologram record at the wavelength 514 nm. The holograms were reconstructed by the Ar-ion laser radiation at several discrete wavelength in the range of 476..514 nm.

Not that for the correction for distortions, imposed by the lens into the image of the distant and spatially-incoherent radiation it is sensible to use the thin holograms. The use of the volume (thick) holograms will result in extra limitations due to their angular and spectral selectivity¹², resulting in most cases in the impossibility to realize the most important advantage of this class of holograms - the high diffraction efficiency. So, to our opinion, the LC SLM medium is more prospective from the point of view of dynamic correction than the photorefractive media. The comparison of the combination of such a basic parameters, as the sensitivity, response time, reversibility, resolution and depth of phase modulation, realized in these two media, also puts the LC SLM ahead.

This paper is devoted to the experimental results on thermal object imaging in the wide spectral range by the model telescope with the dynamic holographic correction for its primary lens and auxiliary correction for the hologram chromatism. The dynamic hologram was recorded in LC SLM, using the polymer photoconductor^{13,14} or the photoconductor on the base of silicon carbide¹⁸⁻²¹. The S-effect was used for the holograms record in SLM with the nematic LC, and in the case of ferroelectric LC we have used the DHF-effect^{22,23}. The holograms were recorded in pulsed mode^{15,16}.

Variation of the voltage pulse, feeding the SLM, duration and of its synchronization with respect to the light pulse provides the control of the temporal delay from the hologram recording to the moment of its highest diffraction efficiency. In our experiments we could vary this delay from 100 msec to several dozen seconds.

The diffraction efficiency of the realized holographic correctors equaled 20-25%. The holograms, recorded in FLC SLM, revealed very weak dependence of their diffraction efficiency on the polarization of reconstructing radiation. So in the case of imaging of test-object, illuminated by the incoherent (thermal) radiation, the effective efficiency was two times higher.

3. EXPERIMENTAL SETUP

The experimental setup is shown in the Fig.2. The thermal source at the infinity was simulated by the standard test object 1, illuminated by the light of the tungsten lamp. The imaged test-object was mounted in the focal plane of the auxiliary lens 2. The absolute angular dimension of the object was equal 0.02 radian. This object was imaged by the lens telescope, comprised by the primary lens 3 to be corrected and the eye-piece 4. Two identical achromatic lenses with the focal length of 230 mm were used as the elements 3 and 4. The corrector unit comprised the LC SLM 5, the transparent phase (holographic) diffraction grating 6 for the dynamic hologram chromatism compensation and the scheme for the corrector recording.

The hologram-corrector was recorded by the pulsed radiation of second harmonics (0.54 μm) of Nd:YAP laser 7 as the interference pattern of the plain reference wave and the object wave, transmitted via the telescope. The telescope 8 (10⁵) improved the spatial homogeneity of the recording beams. The useful clear aperture of the SLM was determined by the apertures 9 and 10 and equaled 15 mm. Beam split cube 11 (transparency 50 %) separated the recording beams and, in a time, combined the radiation from the imaged object 1 and the probe beam of laser radiation.

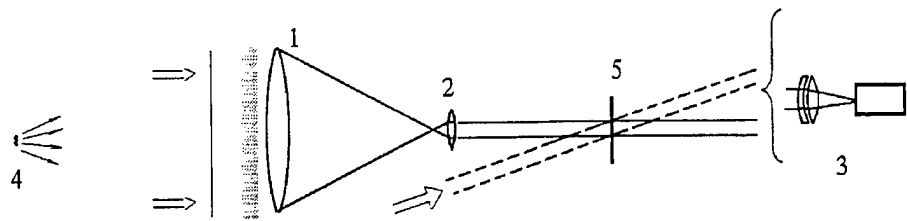


Fig.1. Principle scheme of holographic correction for telescope lens distortion

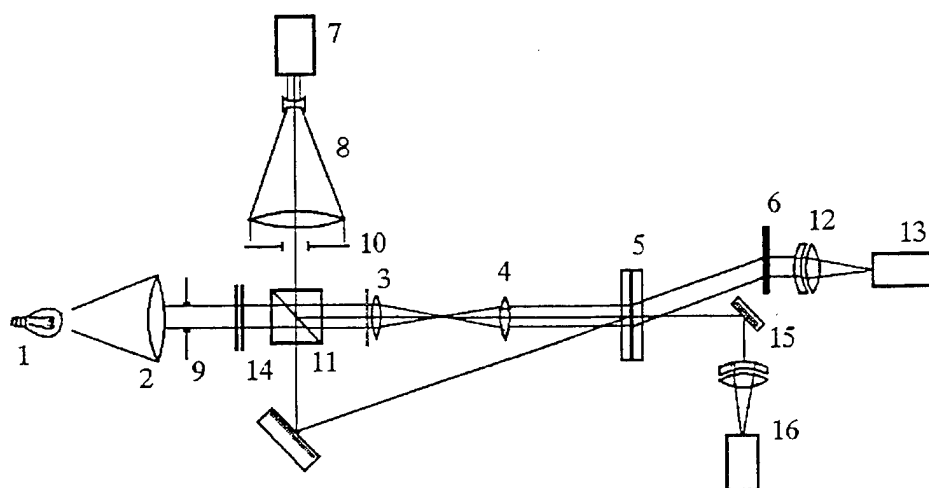


Fig.2. Experimental setup

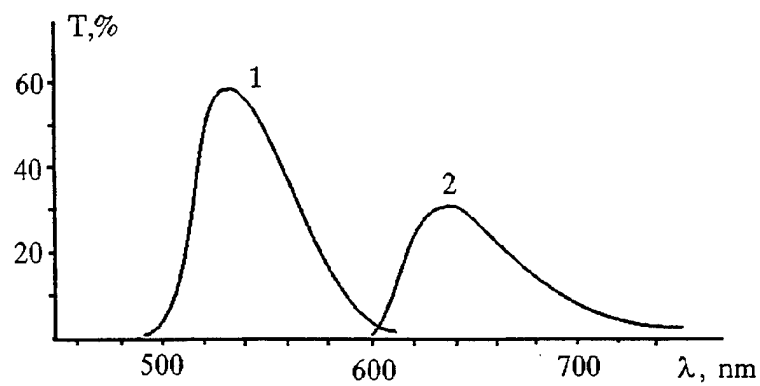


Fig.3. Spectral dependence of the colored filters transparency:
 1 — colored filters GS-18 + Szs-22 (KC-18 + C3C-22);
 2 — colored filters KS-10 + Szs-23 (KC-10+C3C-23)

The eye-piece 4 imaged the pupil of the lens 3 in the plane of the corrector 5. The spatial carrier frequency of the dynamic hologram was equal to the spatial frequency of the grating 6 and was equal 95 mm^{-1} . Such a value was chosen as the trade-off value, providing both spatial separation of the object images in different diffraction orders and sufficiently high diffraction efficiency.

The radiation from the thermal source, diffracted from the grating 6, was caught by the lens 12 and focused to the CCD-matrix 13. The spectral range, used for the object imaging, was varied by the colored filters 14. We have used the filters made of standard colored glasses (the spectral characteristics of the filters transparency are shown in the Fig.3), and filters made of standard colored glasses (the spectral characteristics of the filters transparency are shown in the Fig.3), and the band interference filter with the width of the transparency band 10 nm centered at $0.53 \mu\text{m}$. The zero order diffraction on element 5 radiation from the thermal object was caught by the plain mirror 15 and used for control non-corrected image of the object, registered by the system 16.

4. EXPERIMENTAL RESULTS

The various distorters were mounted in the signal beam. Small-scale distortions of the lens were simulated with the use of glass plates etched in hydrofluoric acid. For an example, in the Fig.4 the interferogram is shown of the "strongest" distorter of this kind, providing beam divergence of ~ 0.006 radian (FWHM). The Fresnel bi-prism was used for simulation of the local wedge-like distortions, which in practice can be caused, for example, by the mutual tilt of the primary mirror segments; the angular misalignment of "images" in our case was ~ 0.01 radian. We have used the tungsten wire of lamp, the sharp edge and the standard test object as the objects of imaging. The latter two kinds of test-objects provided the application of standard methods of the quantitative evaluation of the correction fidelity and its dependence on the spectral range of imaging radiation.

The following results were obtained with the NLC SLM.

We have measured the frequency-contrast characteristics of the optical system under correction with the imitation of the small-scale scattering distorter with the angular divergence of ~ 0.006 radian. It was measured for the green range of spectrum (see filter transparency - curve 1 in the Fig.3), for the red range of spectrum (curve 2 in the Fig.3) and for the "white" light of tungsten lamp. In the Fig.5 the results are shown of this characteristic measuring as $K = \{I_{\max} - I_{\min}\} / \{I_{\max} + I_{\min}\}$. One can see from the Fig.5, that in the case of imaging in the green range of spectrum (the width of spectral range $\sim 50 \text{ nm}$), whose maximum approximately coincides with the wavelength of laser radiation used for the hologram recording, the system performance is close to the diffraction limited. The use of "white" light also provides rather good quality of image. Significant deterioration of the image is observed only while imaging in red spectral band whose maximum is shifted in $\sim 100 \text{ nm}$ with respect to the recording wavelength. In the Fig.6-10 are shown the photographs of the standard test object, which confirm the above said. In the case of the wedge-like distortions the shift of imaging spectrum to the red range or use of "white" light the image was "expanded" in the "wedge" direction.

Additional information on the correction fidelity was got from the analysis of the photographs of the sharp edge (Fig.11,12). One can see that in the case of spectral band shift with respect to the recording wavelength, and of the strong distortions of the probe beam, the wings in the edge spread function (ESF) are observed. These wings are responsible for the decrease of the complicated image contrast, and they are resulted from non-sufficient correction for the chromatism of the probe beam. One can also see from these photographs that the point spread function (PSF) consists of two components: the narrow core, resulting of nearly diffraction limited performance of the OS, and of the wings, caused by the non-sufficient chromatic correction for the optical distortions. According to evaluations, in the absence of the distortions in the probe beam the image core contains $\sim 65 \%$ of total energy for reading out both in the green and in the red spectral ranges (Fig.11). Distortions of the probe beam by the etched plate with the distortions rate of 0.006 rad result, in the green range, in preservation of the core energy, while in the red range of spectrum it is reduced down to $\sim 35\%$ (Fig.12).

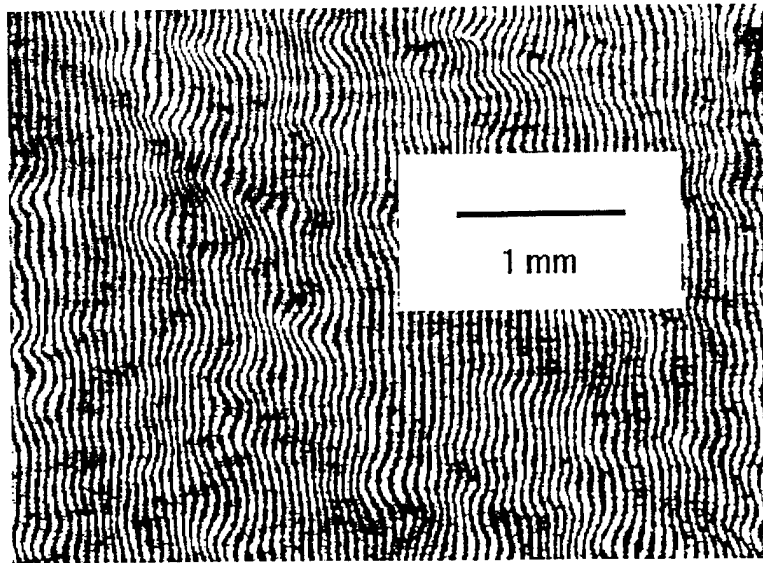


Fig.4. The part of interferogram of the distorting plate, providing beam divergence of 0.006 radian.

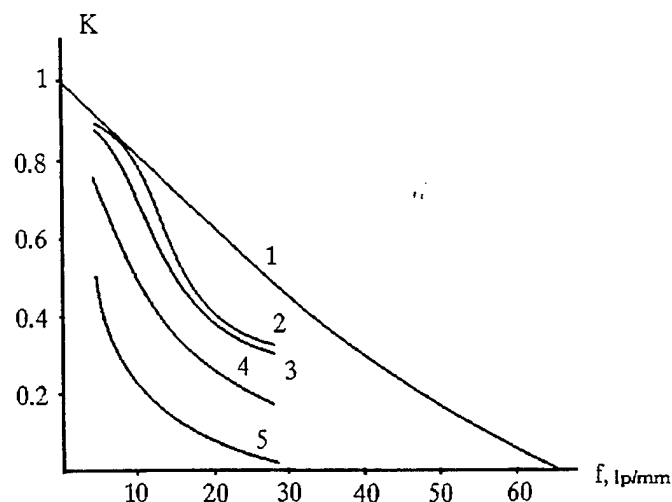


Fig.5. Frequency-contrast characteristics of the optical system under correction in the absence (curves 1, 2) and in the presence (curves 3, 4, 5) of small-scale distortions. Curve 1 - the ideal lens, curve 2 - optical system used in our experiment, 3 - correction in the green range of spectrum, 4 - correction in the "white" and 5 - light correction in the red range of spectrum.

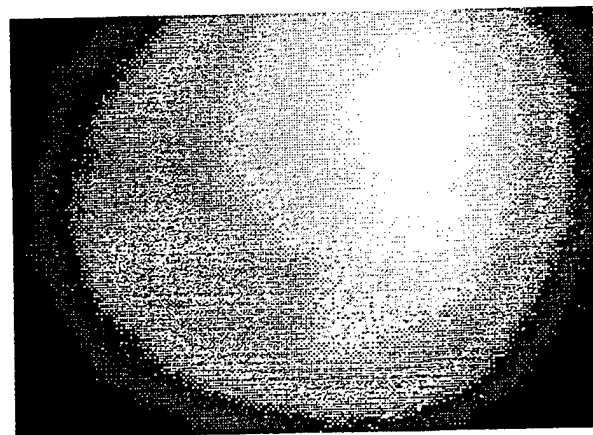


Fig.6. Image of standard test-object without correction for lens distortions.

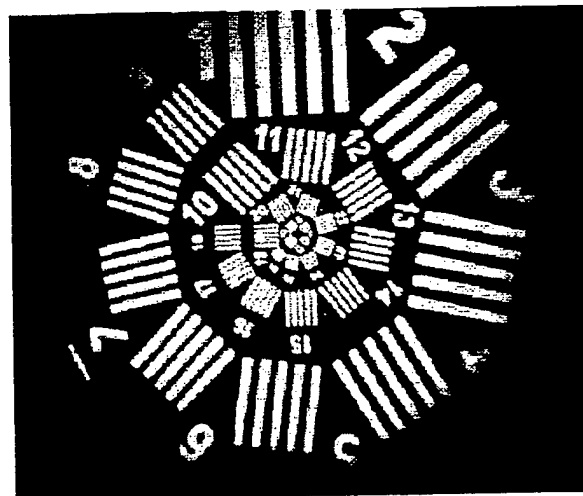


Fig.7. Image of test object in green light with correction for distortions.

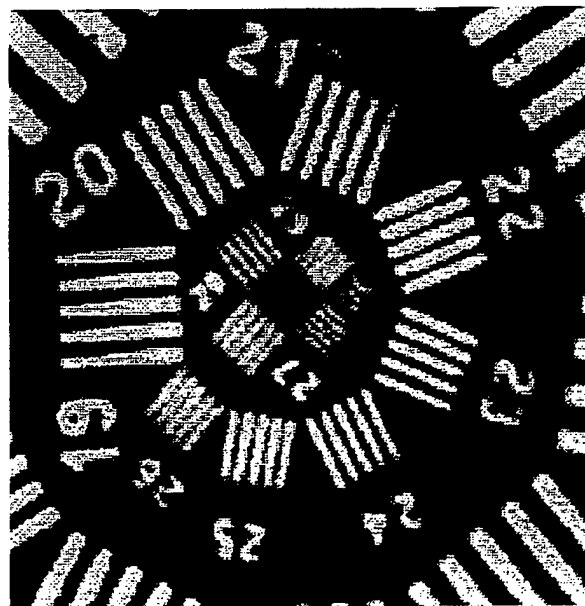


Fig.8. Central zone of standard test object image in green light with the correction for distortions.

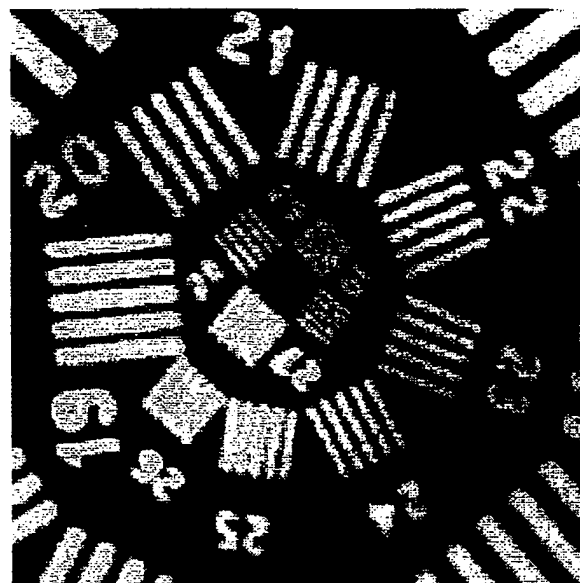


Fig.9. Central zone of standard test object image in “white” light with the correction for distortions.

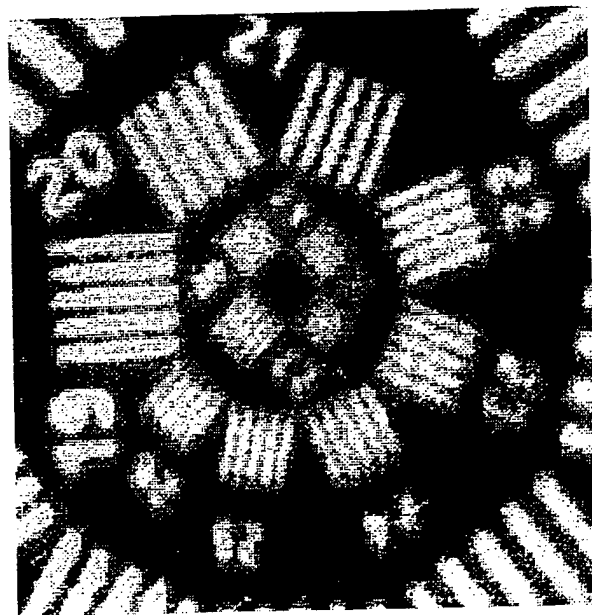


Fig.10. Central zone of standard test object image in red light with the correction for distortions.

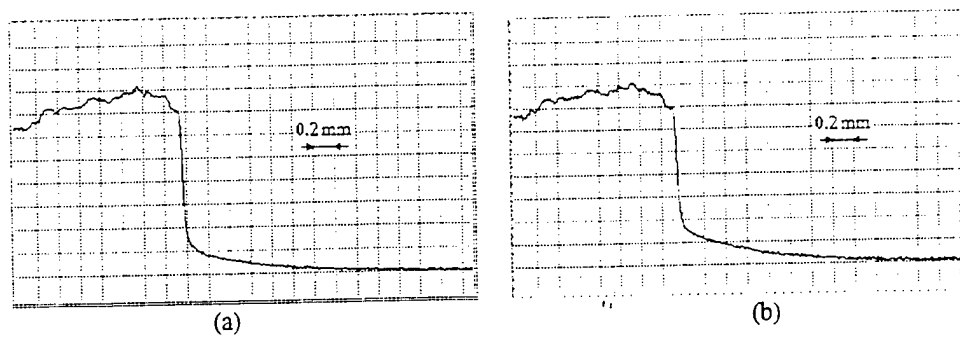


Fig.11. Reconstructed image of the sharp edge without distortions,
read out in green (a) and red (b) spectral bands (see Fig.3.).

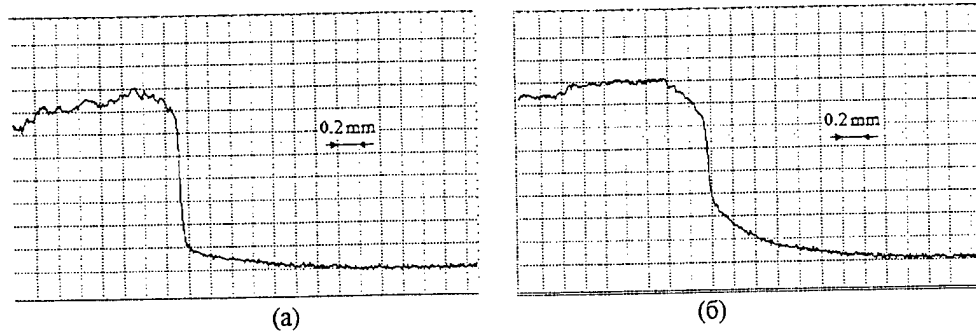


Fig.12. Reconstructed image of the sharp edge with distorter 0.006 rad.
read out in green (a) and red (b) spectral bands.

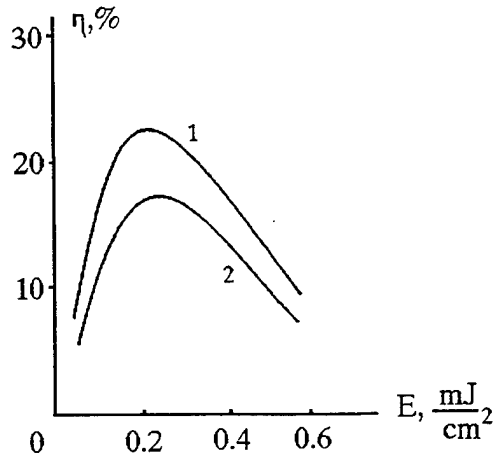


Fig. 13. Peak values of DE vs. radiation energy fluency without distorter (1)
and with the distorter 0.006 radian (2).

It was found out that the influence of the small-scale distortions onto the absolute value of the hologram-correctors DE reveals itself for the etched glass distorters providing random divergence of more than 0.004-0.005 radian. These values are approximately in an order of magnitude smaller than the angular separation of neighboring orders of diffraction. Corresponding results, obtained by reading out by He-Ne laser radiation, are shown in the Fig. 13.

In course of the experiments we have also tried the image correction with the use of SLM based on the ferroelectric LC. Visual correction ability was not worse than in the case of nematic LC application. Image brightness, however, was much higher: in this case the radiation from thermal object is used much better, for the FLC SLM performance is almost polarization independent.

5. CONCLUSION

In the reported experiment the source of coherent radiation, used for the corrector record, was mounted in the plane of the object (or, generally speaking, optically conjugate plane). In practice of imaging of the remote object it is impossible. In the so called bypass optical schemes⁷ the source of the radiation, used for reading out of the primary lens (mirror) distortions can be mounted nearby this lens or mirror, say, in the latter center of curvature. In this case the distortions are compensated (corrected) not completely, but down to some residual error. However, depending on the telescope design the surplus can be some dozen or hundred times^{7,8}.

Hence the results of the reported experiment promise the successful use of the optically addressed LC SLM as the dynamic holographic media for the record of the holographic correctors to be used in the passive bypass imaging telescopes.

REFERENCES

1. Denisuk Yu.N., Soskin S.I. Holographic correction of deformational aberrations of the primary mirror of the telescope. Opt. Spektrosk., 1971, Vol. 31, No. 6, p. 991-997, (in Russian).
2. Denisuk Yu.N., Soskin S.I. Holographic correction of deformational aberrations of the primary mirror of the telescope. Opt. Spektrosk., 1972, Vol. 33, No. 5, p. 994-996, (in Russian).
3. Munch J., Wuerker R. Holographic technique for correcting aberrations in a telescope//Appl. Opt. - 1989. - Vol. 28, No. 7. - P. 1312-1317.
4. Munch J., Wuerker R., Heflinger L. Wideband holographic correction of an aberrated telescope objective//Appl. Opt. - 1990. - Vol. 29, No. 16. - P. 2440-2445.
5. Andersen G., Munch J., Veitch P. "Holographic correction of large telescope primaries by proximal, off-axis beacons// Appl. Opt. -1996-V.35, No.4 P. 603-608.
6. Zel'dovich B.Ya., Pilipetsky N.F., Shkunov V.V. Phase conjugation. - Moscow, 1985, 240 p. (in Russian).
7. Leshchev A.A., Pasmanik G.A., Sidorovich V.G., Vasil'ev M.V., Venediktov V.Yu.. Compensation for distortions in the imaging systems, using phase conjugation technique. Izvestiya Akademii Nauk SSSR, v.55, 2, p.260-266, 1991. (In Russian).
8. Leshchev A. A., Sidorovich V. G., Vasil'ev M. V., Venedictov V.Yu., Pasmanik G.A. Nonreciprocal optical systems with phase-conjugating mirrors - a new class of optical imaging systems. International Journal of Nonlinear Optical Physics. - 1994. - Vol. 3, No. 1. - p. 89-100.
9. Vasil'ev A.A.. Casasent D., Kompanets I.N., Parfenov A.V. Spatial light modulators. Moscow, Radio i Svyaz. 1987. 320 p. (in Russian)
10. Petrov M.P., Stepanov S.I.. Khomenko A.V. Photorefractive crystals in coherent optics. St.-Petersburg. Nauka. 1992. 320 p. (in Russian)
11. Kramer M. A., Wetterer C. J., Martinez Ty. One-way imaging through an aberrator with spatially incoherent light by using an optically addressed spatial light modulator// Appl. Opt. - 1991. - Vol. 30, No. 23. - P. 3319-3323.
12. Dimakov S.A., Klimentiev S.I., Sventsitskaya N.A., Sherstobitov V.E. Compensation for optical elements distortions by means of dynamic holography in "white light". Opt. Spektr., 1996, Vol.80. No 4, p. 699-704 (in Russian).
13. Groznov M.A., Myl'nikov V.S., Soms L.N., Tarasov A.A. Liquid crystal spatial light modulator with the resolution of more than 1000 lines per mm. Zh. Tekh. Fiz. 1987, Vol . 57. No. 10. p. 2041-2042, (in Russian).
14. Myl'nikov V.S. Liquid crystal spatial light modulators with the organic polymer photoconductor. Optical Journal. 1993, #7, p.41-45 (in Russian).
15. Kamanina N.V., Soms L.N., Tarasov A.A. Holographic correction for distortions using the liquid crystal phase light modulators. Opt. Spektrosk., 1990. Vol. 68. No. 3, p. 691-693 (in Russian).
16. Berenberg V.A., Kamanina N.V., Soms L.N. Holographic correction for distortions using the liquid crystal phase light modulators under different frequencies of recording and reconstructing radiation. Izv. Akad. Nauk SSSR. Ser. Fiz.. 1991. Vol. 55. No. 2. p. 236-238, (in Russian).
17. Berenberg V.A., Vasil'ev M.V., Venediktov V.Yu., Leshchev A.A., Soms L.N. Journal of Optical Technology, Vol.64, No.9, p.73-74, 1997.
18. Ahiyama K., Takimoto A., Ogawa H. Jpn.J.Appl. Phys., 1993, Part 1, Vol. 32, p. 590.
19. Feoktistov N.A., Morozova L.E. Pisma v ZhTF, 1994, Vol.20, No.5, p.12-16, (in Russian).
20. Ahiyama K., Takimoto A., Ogawa H. Appl.Opt., 1993, Vol.32, No.32, p. 6493-6500.
21. Ivanova N.L., Morozova L.E., Onokhov A.P., Pevtsov A.B., Feoktistov N.A. Pisma v ZhTF, 1996, Vol.22, No.4, p.7-11, (in Russian).
22. Beresnev L.A., Blinov L.M., Dergachev D.I., Loseva M.V., Chernova N.I. Pisma v ZhTF, 1988. Vol. 14, No. 3, p. 260-263. (in Russian).
23. Abdulhalim I., Moddel G. Mol. Cryst. Liq. Cryst., 1991, Vol.200, p.79-101.

Copies of papers, presented for publication

3. A. P. Onokhov, V. A. Berenberg, A. N. Chaika, N. L. Ivanova, M. V. Isaev, N. A. Feoktistov,
L. A. Beresnev, and W. Haase,
“Novel liquid crystal spatial light modulators for adaptive optics and image processing”

Proceedings of SPIE, Vol. 3388, presented to SPIE's 12 Annual Int. Symp. “AeroSense”, section
“Advances in Optical Information Processing VIII”, 13-17 April 1998, Orlando, Florida USA, Advanced
Technical Program, p.52.

Novel liquid crystal spatial light modulators for adaptive optics and image processing

Arkadii P. Onokhov^a, Vladimir A. Berenberg^a, Aleksander N. Chaika^a,
Natalia L. Ivanova^a, Mikhail V. Isaev^a, Nikolai A. Feoktistov^b, Leonid A. Beresnev^c,
Wolfgang Dultz^d and Wolfgang Haase^a

^aAll-Russian Research Center Vavilov State Optical Institute, St. Petersburg, Russia

^bIoffe Physical Engineering Institute, St. Petersburg Russia; ^cDarmstadt University of Technology, Darmstadt, Germany, Research Center Darmstadt-Deutsche Telekom AG, Darmstadt, Germany

ABSTRACT

The subject of the study were spatial light modulators (SLM), comprised by polymer photoconductor (PC) or a-Si_{1-x}:C_x:H photoconductor, and ferroelectric liquid crystal (LC). The polymer PC provides the highest available diffraction efficiency (DE) among all layers when the spatial frequency of the hologram exceeds ~100lp/mm. At the same time the parameters of the a-Si_{1-x}:C_x:H PC layer can be varied across the wide range and thus the proper tradeoff between the spatial resolution and reversibility can be chosen.

Keywords: liquid crystals, spatial light modulators, photoconductive layers.

1. INTRODUCTION

The diffraction efficiency of the holograms, recorded in the OA LC SLM using the organic polymer PC and nematic^{1,2} in the range of spatial frequencies of more than 100 lp/mm, can be as high as 20-35%^{2,3}. Such high diffraction efficiency is available because of the low mobility of charge carriers in the polymer PC¹. Low mobility, at the same time, results in rather low reversibility of such SLM - just several Hz or even less. Some improvement of the situation can be achieved by the recording schematic improvement, namely, by recording of sequential dynamical holograms in various zones of large SLM; note, that polymer PC is rather cheap and large size elements are easily available. In^{4,5} there was shown the possibility to use the SLM of such kind for the correction for the distortions in the monochrome radiation.

2. SLM WITH POLYMER PC AND FERROELECTRIC LC.

The SLM's, tested in our experiments, were realized as the sandwich structure, whose layers were positioned between two glass substrates (diameter 35 mm). The element cut is shown in the Fig.1. The thickness of the polyimide PC layer was ~ 1.2-1.4 μm. Optical quality of the element across the zone of 15 mm width was not worse than λ/4.

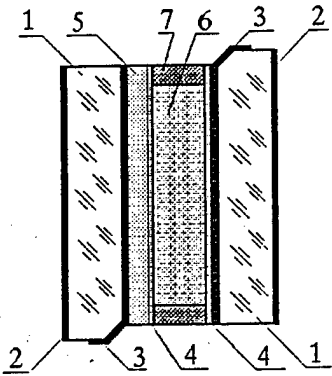


Fig.1. SLM design: 1 - glass substrata, 2 - AR coating, 3 - transparent electrode, 4 - alignment layer, 5 - PC layer, 6 - LC layer, 7 - spacer.

One specimen of SLM with ferroelectric LC was fabricated for these studies. The LC compound consisted of non-chiral smectic C LC with chiral admixtures. Spontaneous polarization of FLC equaled $150..200 \text{ nC/cm}^2$, its helicon step was $0.2 \mu\text{m}$ and the tilt angle of the director θ_0 in smectic layer was 40 degrees. The thickness of FLC layer d was $5 \mu\text{m}$. The value of d was significantly much more than helicon step; hence the refraction index modulation was obtained via the effect of the Deformed Helix Ferroelectric, DHF-effect^{6,7}. The DHF-effect was chosen due its advantages^{6,9} in comparison with the other possible effect in FLC, viz. Clark-Lagerwall effect⁸. This effect is less sensitive to the FLC layer thickness variation nearby its optimal value. The effective birefringence for DHF-effect is ~ 1.5 times smaller than that for Clark-Lagerwall effect. Long time optical storage is possible for the voltage values nearby the de-twist voltage. The storage time depends on viscosity and elasticity coefficients, on the helicon step, and also of the specific method of electrodes surface processing. This time can be varied from several dozen milliseconds to several dozen seconds. DHF-effect also provides the natural gray scale. FLC can be aligned by the means applicable to the nematic crystals. It was obtained that, in the case of Clark-Lagerwall effect, the maximal value of DE does not depend on the polarization of the reading out radiation and can be described by the relationship:

$$\eta_{\max} = [2/\pi \sin(2\theta_0) \sin(\Gamma/2)]^2$$

Here Γ is the phase retardation in FLC at the wavelength of reading radiation. Further increase of the tilt angle θ_0 in comparison with the realized 40° is hardly practically reasonable. It is obvious that in the case of DHF-effect the phase retardation can be also described by the same formula. However, the dependence of the phase retardation Γ vs. FLC layer thickness d and vs. optical anisotropy of LC for DHF-effect is more complicated than for Clark-Lagerwall effect. One can see from the formula that the maximal value of DE is realized when $\sin^2(\Gamma/2) = 1$.

The standart setup, was used for measuring of DE absolute value and its temporal behavior using the He-Ne laser radiation. SLM was controlled by the combination of CW voltage with the sequence of rectangular shaped voltage pulses. The pulses of positive polarity with the amplitude V_{pp} and controlled duration were superposed onto the negative bias V_b . In the course of our experiments we have varied the polarization of reading radiation, grating vector orientation with respect to the smectic layers normal, the recording energy fluency E, the value of peak-to-peak amplitude of controlling voltage V_{pp} , the bias V_b , the duration of the rectangular shaped pulses, and the delay of the recording radiation pulse with respect to the forward front of the rectangular shaped pulse. The results were as follows:

DE value only slightly depends on the reading-out light polarization orientation with respect to the grating vector. The value of DE is maximal when the grating vector is parallel to the direction normal to the smectic layers. The tilt of the grating vector results in the graduate reduce of DE, reaching its minimum when the said vector and normal are orthogonal to each other. Seemingly, this dependence results from the flex-electric polarization of FLC, which, in turn, is caused first of all by variation of the polar angle of LC molecules with respect to smectic layers, induced by the electric field^{6,10}.

DE absolute value and temporal behavior to a large extent depend on relationship between V_{pp} and V_b and on their absolute value, on the recording energy fluency E and on recording pulse delay τ_0 . The simplest dependence is that on τ_0 value. This delay increase up to some 10-20 ms results in shortening of the response pulse forward front. Further increase of the delay τ_0 practically does not cause any variation in DE value and behavior. For any recording energy fluency E the maximal DE was observed when V_{pp} was equal 40-50 V. At the same time for each specific value of E there exists some value of bias V_b , providing maximal peak value of DE. For some values of V_b there was realized the effect of optical memory. The above said is illustrated by the curves, shown in the Fig.2-6, registered when the grating with the spatial frequency 95 lp/mm was recorded. The Fig.2-5 represent the transformation of DE response temporal behavior with variation of the bias V_b for fixed $V_{pp} = 40$ V. The duration of rectangular voltage pulses was 3 seconds, their repetition rate 0.1 Hz and $\tau_0 = 2$ ms. Modification of the response temporal behavior when the delay time was increased up to 1 second is illustrated by the Fig.6. The optical memory regime corresponds to Fig.5,6 – the diffraction response lasts until the driving voltage V_{pp} exists.

It was determined that, in comparison with the SLM using NLC, those with FLC provide higher reversibility of diffraction grating record without DE decrease. For the record repetition rate of 1 Hz the each sequential recorded grating did not reveal any residual noise from the preceding grating (Fig.7). The residual light modulation, which can be seen at the oscillograms, is caused first of all by radiation scattering on domains, induced by the voltage polarity switching. The possibility to renew the gratings with the repetition rate of 1 Hz is illustrated by the Fig.8. Response amplitude variation from pulse to pulse is correlated with the recording pulses energy variation. The presence of spontaneous polarization in FLC is, probably, responsible for dumping of the processes of the slow relaxation of the charge relief in polyimide. The intense internal fields in FLC layer may cause, after the switching, an additional driving voltage applied to PC thus helping the washing out the charge relief⁶.

We have measured the peak values of DE of gratings with arbitrary spatial frequency. For the spatial frequency of 52 lp/mm the peak value of DE equaled 17-19%, and for 95 lp/mm - 16-18%. The comparatively "low" value of DE is resulted, most probably, from non-optimal FLC layer thickness. Note the very small reduce of DE value while increase of spatial frequency of the grating from ~ 50 to ~ 100 lp/mm. In the Fig.20 are shown the dependencies of the peak DE values vs. recording energy fluency for two values of spatial frequency. These dependencies were recorded for $V_{pp} = 40$ V. The bias V_b was chosen so as to provide the highest possible value of DE. For the spatial frequency of 52 lp/mm the optimal voltage was $V_b = 23$ V, while for 95 lp/mm - $V_b = 21$ V. Voltage pulse duration was equal 1s, pulse repetition rate - 0.1Hz and $\tau_0 = 2$ ms.

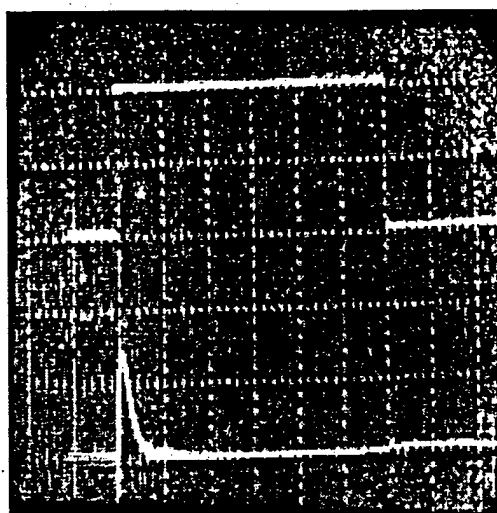


Fig.2. Temporal behavior of DE (lower curve) for $V_b = 13$ V;
upper curve - feeding voltage pulse, single unit = 0.5 sec.

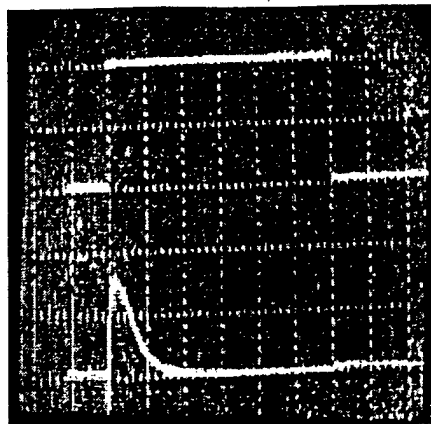


Fig.3. Temporal behavior of DE (lower curve) for $V_b = 16$ V;
upper curve - feeding voltage pulse, single unit = 0.5 sec

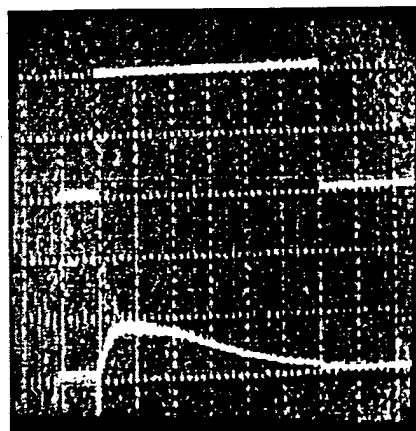


Fig.4. Temporal behavior of DE (lower curve) for $V_b = 24$ V;
upper curve - feeding voltage pulse, single unit = 0.5sec.

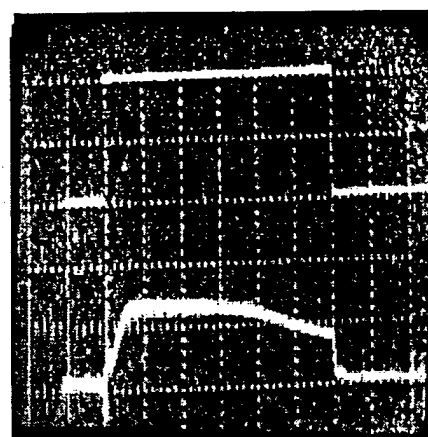


Fig.5. Temporal behavior of DE (lower curve) for $V_b = 25$ V;
upper curve - feeding voltage pulse, single unit = 0.5 sec.

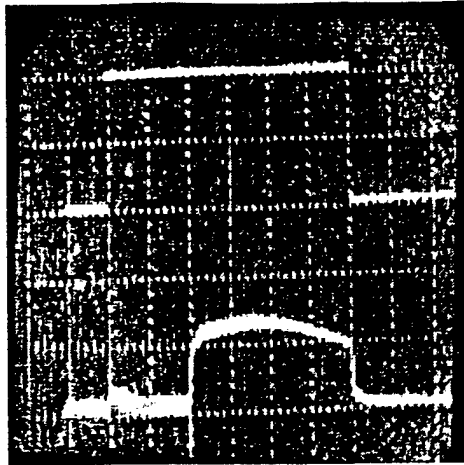


Fig.6. Temporal behaviour of DE (lower curve) for $V_b = 25$ V and recording pulse delay in 1 second;
upper curve - feeding voltage pulse, single unit = 0.5 sec.

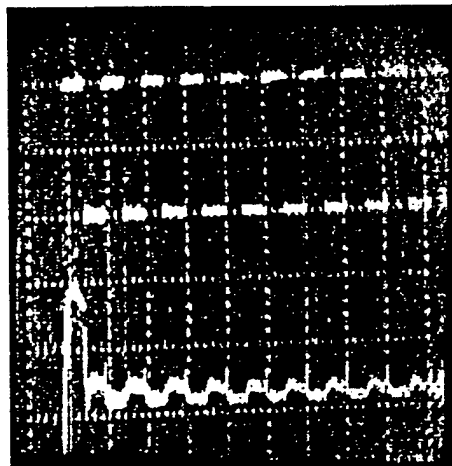


Fig.7. SLM response to single recording pulse (lower curve);
upper curve - feeding voltage pulses, single unit = 1 sec.

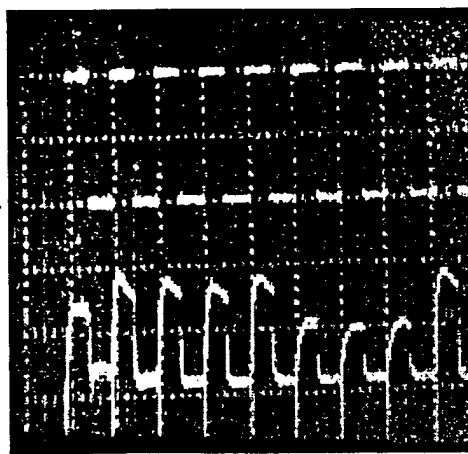


Fig.8. SLM response to repetitively (1 Hz) recorded grating (lower curve);
upper curve - feeding voltage pulses, single unit = 1 sec.

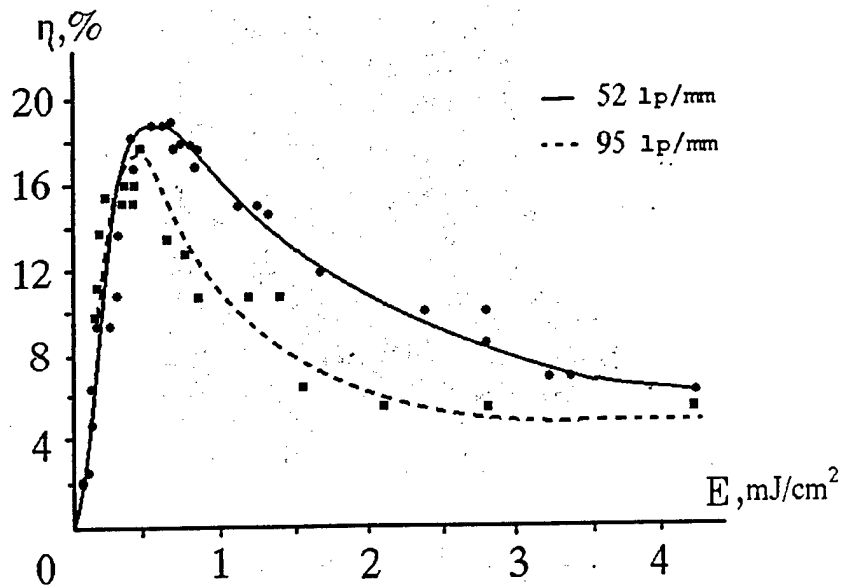


Fig.9. DE dependence vs. recording radiation energy fluency for gratings with various spatial frequency

3. DIFFRACTION EFFICIENCY OF SLM WITH a-Si:C:H PC

Until now the best response time in OA LC SLM was realized with the use of PC, made of the amorphous hydrated silicon (a-Si:H) and p-i-n structures on this base ¹¹⁻¹³. However, the comparatively high dark conductivity of this medium puts under the question realization of high DE values, close to the extreme possible (30-40%), for the spatial frequencies of 50-100 lp/mm. In addition, transparency of a-Si:H PC in the visible range of spectrum is low, resulting thus in radiation energy losses in the transparent SLM elements.

The use of elements with $\text{a-Si}_{1-x}\text{C}_x\text{H}$ PC ¹⁴ makes it possible to improve spatial resolution of SLM, preserving yet high reversibility. According the results of our studies the variation of Si and C content in composition provides variation of the dark conductivity, spectral and optical properties of a-Si:C:H layers across the wide range ^{15,16}. It can be seen from the curves in the Fig.10-12.

The layers of the material were obtained by means of radio frequency dissociation of silane in the multichamber setup. The carbon concentration has been varied by means of control of flows of the methane-containing and silane-containing gaseous mixtures. One can see from the presented curves that the carbon content increase results in reduce of conductivity and refraction index of a-Si:C:H layers. The zones' gap in layer is thus increased, resulting in the reduce of the absorption in red spectral range. Of course, the reduce of dark conductivity results in smaller light sensitivity with that of a-Si:H PC layer; however, its absolute value is yet rather high. In ^{17,18} there was shown the possibility to make up the p-i-n structure of a-Si:C:H , which is necessary for the SLM element realization. In ¹⁷ the SLM with FLC and such PC layer was realized. Its resolution was 70 lp/mm with the reversibility of 1.5 kHz. The SLM of such a kind with NLC layer, realized in ¹⁸, revealed the resolution of 50 lp/mm with the reversibility of 50 Hz.

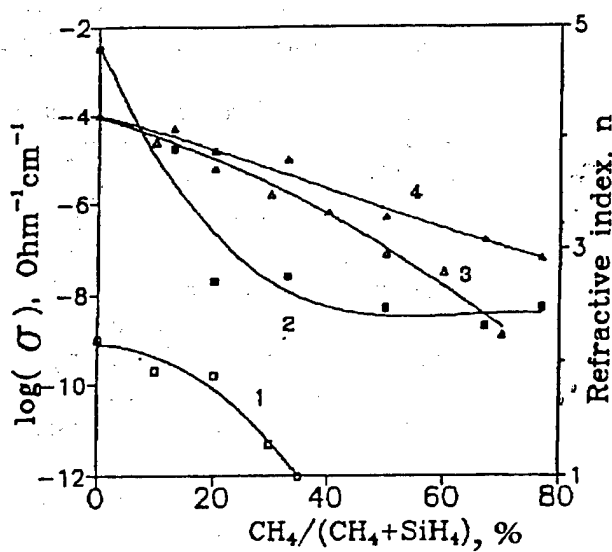


Fig.10. Conductivity (curves 1,2) and refraction index (curves 3,4) of $\alpha\text{-Si}_{1-x}\text{C}_x\text{:H}$ film vs. C content; 1, 3 - undoped film, 2, 4 - phosphorus doped film.

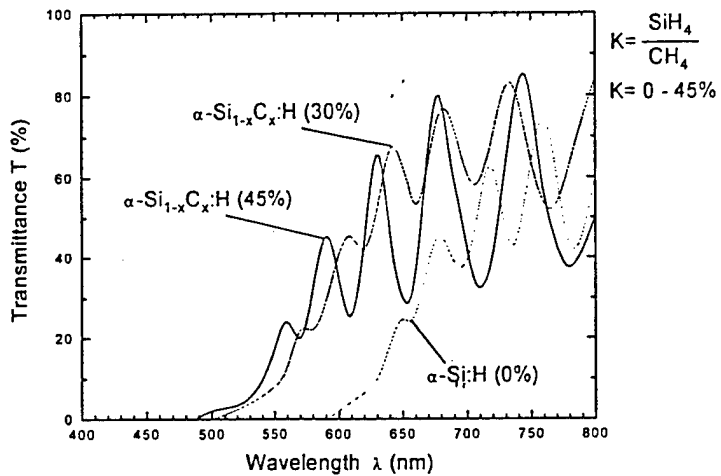


Fig.11. Spectral transparency of $\alpha\text{-Si}_{1-x}\text{C}_x\text{:H}$ layer with the thickness of 1.2 μm .

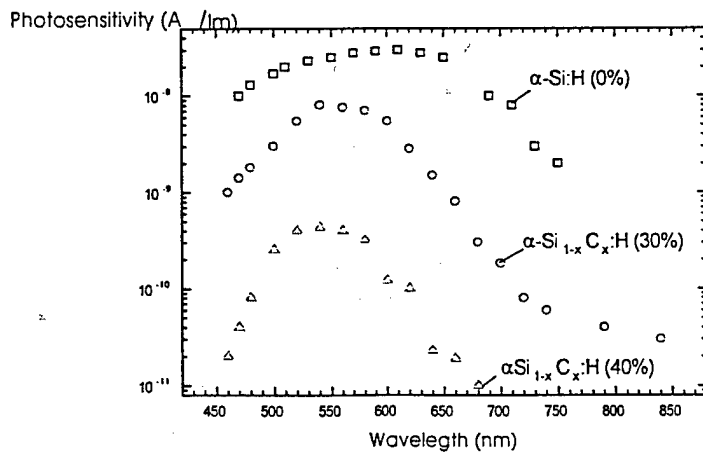


Fig.12. Spectral dependence of photo current of $\alpha\text{-Si}_{1-x}\text{C}_x\text{:H}$ films.

We have fabricated for these studies three specimens of SLM with the FLC layer thickness 2 μm (SLM 1), 5 μm (SLM 2) and 12 μm (SLM 3). Spontaneous polarization of FLC equaled 150..200 nC/cm², its helicon step was 0.2 μm and the tilt angle of the director θ_0 in smectic layer was 40 degrees. The refraction index modulation was obtained via DHF-effect.

The SLM was fed by the superposed CW bias and sequence of rectangular voltage pulses. DE absolute value and its temporal behavior were measured in two modes of grating recording. In the first one the gratings were recorded by the pulsed (20-30 ns) radiation at 0.54 μm . In the second mode we have used the pulses of radiation with the wavelength 0.63 μm with the duration 50 ms and repetition rate 100 Hz. These pulses were cut off the CW emission of He-Ne laser, and reached the modulator synchronously with voltage pulses. The light pulses had the fronts 1 ms, light contrast ratio was not less than 1:20000.

In the course of our experiments we have varied the polarization of reading radiation, grating vector orientation with respect to the normal to the smectic layers, the recording energy fluency E, the bias V_b , the amplitude of controlling voltage pulses V_{pp} and the duration of the rectangular shaped pulses and the delay of the recording radiation pulse with respect to the forward front of the rectangular shaped pulse.

In the case of grating record with the use of the short light pulses the character of DE absolute value and temporal behavior dependence on the listed parameters was rather similar to that in the case of SLM with polymer PC and FLC. Of course, the values of V_{pp} and V_b voltages, providing the maximal DE were another, as well as that of the grating reversibility without DE decrease. In the Fig.13 are shown the dependencies of DE vs. E, recorded for SLM 2 and SLM 3 for $V_{pp} = 60 \text{ V}$ and $V_b = 45.5 \text{ V}$ (SLM 2) and $V_b = 48.5 \text{ V}$ (SLM 3). The positive polarity of pulses was applied to FLC layer. The said bias values V_b provided realization of the optical memory mode (see Fig.5 and 6). Voltage pulse duration equaled 2 seconds, their repetition rate - 0.25 Hz and $\tau_0 = 5 \text{ ms}$. The gratings were read out by the non-polarized emission of the light emitting diode at 0.82 μm . The grating vector was perpendicular to smectic layers.

Significant DE drop with the spatial frequency increase from 50 to 100 lp/mm indicates the necessity to work over the reduce of the PC dark conductivity. Note, however, that in this case the gratings' reversibility is to reduce. The discussed SLMs provided the reversibility of gratings record without the peak DE value drop for the repetition rates up to 6-8 Hz.

Higher reversibility of grating record was observed in the quasi-CW mode of SLM use. In the Fig.14 and Fig.16 are shown the dependencies of DE vs. recording radiation intensity fluency and vs. amplitude of pulses V_{pp} while recording the gratings with spatial frequency 85 lp/mm and the recording pulses repetition rate 100 Hz.

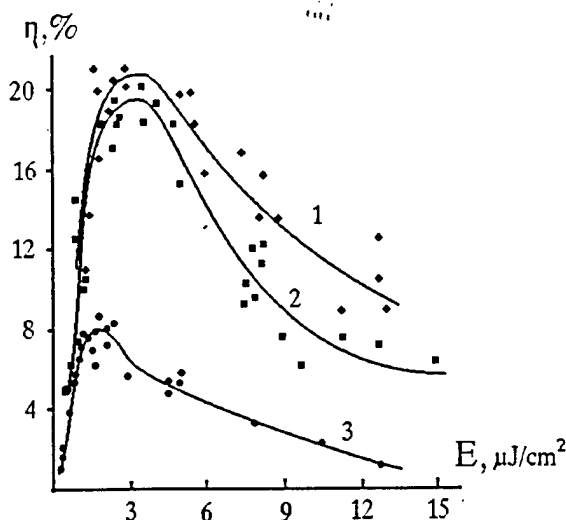


Fig.13 DE dependence on the recording radiation energy fluency for SLM 3 (curve 1) and SLM 2 (curves 2, 3); spatial frequency of grating 52 lp/mm (1, 2) and 100 lp/mm (3).

The dependencies in Fig.14 were taken for $V_{pp} = 39$ V and $V_b = 29$ V. The curves 1 and 2 illustrate the DE dependence on the voltage pulses polarity. The curve 1 corresponds to the case when positive pulse polarity was applied to LC layer and curve 2 - to PC layer. The dependencies in the Fig.15 were taken with the fixed recording radiation intensity fluency of $280 \mu\text{W}/\text{cm}^2$. For each voltage V_{pp} the bias value V_b was chosen so as to realize the maximal DE. The curves 2 and 3 correspond to the cases when positive pulses were applied either to LC (curve 2) or PC (curve 3). Note that the dependence $V_b(V_{pp})$ is practically linear and practically does not depend on the FLC layer thickness and on the polarity of pulses V_{pp}

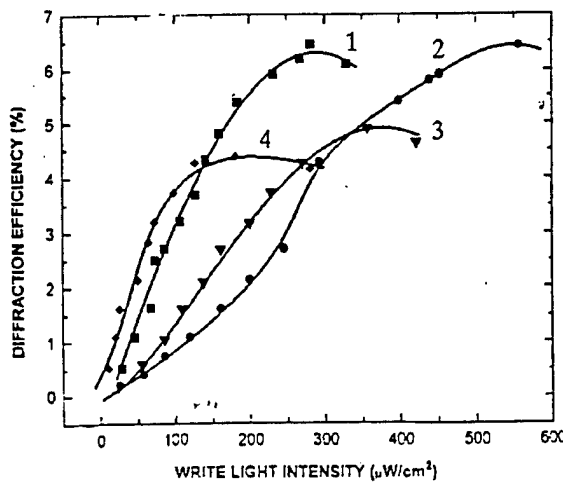


Fig.14. DE dependence on recording radiation intensity fluency for SLM with the FLC layer liquid of 2 μm (1, 2), 5 μm (3) and 12 μm (4).

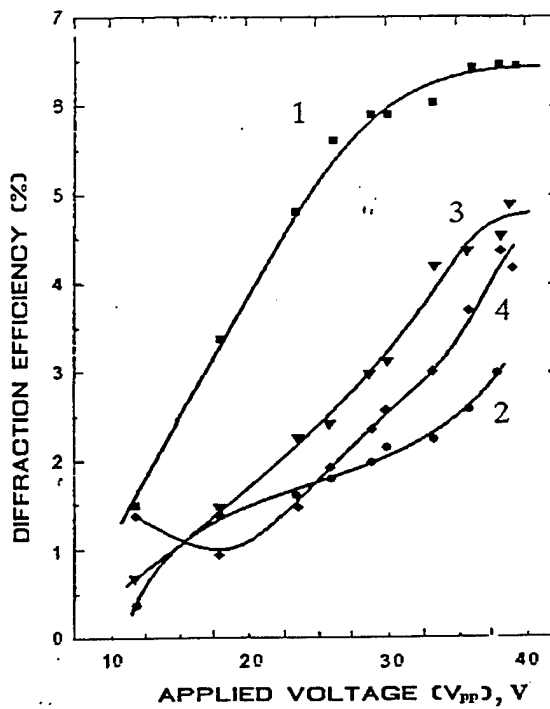


Fig.15. DE dependence on feeding pulses voltage for SLM with the FLC layer liquid of 2 μm (1), 5 μm (2, 3) and 12 μm (4).

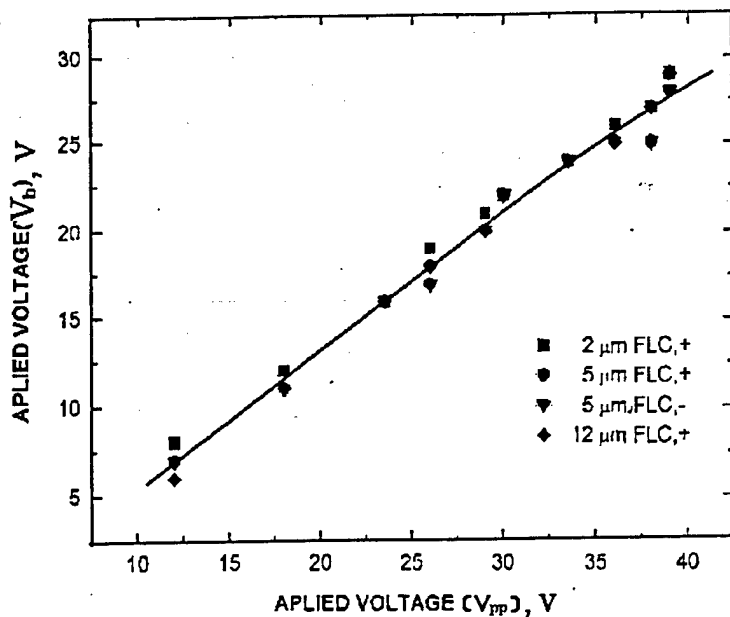


Fig.16 Mutual dependence of feeding voltages V_b vs. V_{pp} .

One can see from the given results that in quasi-CW (repetition rate 100 Hz) mode of gratings record the DE absolute value is much higher than one could expect on the base of the data on grating record by short pulses with the repetition period longer than the character time of transient processes. Most probably, this is the indication of some difference in the mechanism of the charge relief formation in two discussed modes of record.

4. CONCLUSION

On the base of the studies performed, we have shown that the diffraction efficiency of SLM with FLC is almost independent to the polarization of the reading-out radiation. This is very important from the point of view of the discussed application of the device in the imaging optical systems. The reversibility and response time of such devices are determined by the properties of photoconductor.

The organic polymer photoconductors are interesting from the point of view of SLM design for the gratings with high (> 100 lp/mm) spatial frequency and high diffraction efficiency. The reversibility of gratings record in FLC SLM with polymer PC is limited by several Hz. Higher reversibility can be obtained by use of optical schematics of holograms recording (e.g. moving of record zone over the surface of a large SLM).

To our opinion, the photoconductor $\alpha\text{-Si}_{1-x}\text{C}_x\text{:H}$ is more promising than the widely used now $\alpha\text{-Si:H}$. Carbon content variation provides tuning of the dark conductivity of the layer, its sensitivity and spectral transparency across the wide range. So one can determine the proper trade-off between the spatial resolution and reversibility and to choose the PC sensitivity, corresponding to the problem under solution. In the reported work we have used this kind of $\alpha\text{-Si}_{1-x}\text{C}_x\text{:H}$ PC of our own fabrication and with the definite carbon concentration, DE was realized about 20% and 6-8% for the gratings with the spatial frequency of 52 and 85-100 lp/mm correspondingly; reversibility of these elements was ~ 100 Hz. This result can definitely be improved by further optimization of carbon content and LC layer thickness and also by use of p-i-n structures; the possibility of such structures realization on the base of $\alpha\text{-Si}_{1-x}\text{C}_x\text{:H}$ layers was shown in several papers, including ours.

5. REFERENCES

1. V.S.Mylnikov, Photoconductivity of polymers, L.Khimiya, 1990, 240 p., (in Russian).
2. V.S.Mylnikov, Optik.Zn., 1993, No7, p.41-45, (in Russian).
3. M.A.Groznov, V.S.Mylnikov, L.N.Soms, A.A.Tarasov, Zh.Tekh.Fiz., 1987, Vol .57, No.10, p.2041-042, (in Russian).
- 4 .N.V.Kamanina, L.N.Soms, A.A.Tarasov, Opt.Spektrosk., 1990, V.68, No.3, p.691-693, (in Russian).
5. V.A.Berenberg, N.V.Kamanina, L.N.Soms, Izv.Akad.Nauk SSSR, Ser.Fiz., 1991, Vol.55, No.2, p.236-238, (in Russian).
6. G.S.Chilaya, V.G.Chigrinov. Uspehi Fizicheskikh Nauk, 1993, Vol.163, No.10, p.1-28 (in Russian).
7. I.Abdulhalim, G.Moddel. Mol. Cryst. Liq. Cryst., 1991, Vol.200, p.79-101.
8. N.A.Clark, S.T.Lagerwall. Appl. Phys. Lett. 1980, Vol. 36, No. 11, p.899-901.
9. M.F.Grebenkin, A.V.Ivashenko. Liquid crystal materials. Moscow, Khimiya, 1989, 288 p. (in Russian).
- 10 .V.G.Chigrinov, V.A.Baykalov, E.P.Pozhidaev, L.M.Blinov, L.A.Beresnev, A.I.Allagulov. Zhurnal Eksperimentalnoi i Teoreticheskoi Fiziki, 1985, Vol.88, No.6, p.2015-2024.(in Russian).
11. G.Moddel, K.M.Johnson, W.Li, R.A.Rice, L.A.Pagano-Stauffer, M.A. Handschy. Appl. Phys. Lett., 1989, Vol. 55, No. 6, p. 537-539.
12. I.Abdulhalim, G.Moddel, K.M.Johnson. Appl. Phys. Lett., 1989, Vol.55, No.16. p.1603-1605.
13. P.R.Barbier, G.Moddel. Appl.Opt., 1992, Vol.31, No 20, p. 3898-3907.
14. K.Ahiyama, A.Takimoto, A.Ogivara, H.Ogawa. Jpn.J.Appl. Phys., 1993, Part 1, Vol. 32. p. 590.
15. N.A.Feoktistov, L.E.Morozova. Pisma v ZhTF, 1994, Vol.20, No.5, p.12-16, (in Russian).
16. N.L.Ivanova, N.A.Feoktistov, A.N.Chaika, A.P.Onokhov, A.B.Pevtsov. Mol. Cryst. Liq. Cryst.. 1996. Vol. 282, p. 315-322.
17. K.Ahiyama, A.Takimoto, H.Ogawa. Appl.Opt., 1993, Vol.32, No.32, p. 6493-6500.
18. N.L.Ivanova, L.E.Morozova, A.P.Onokhov, A.B.Pevtsov, N.A.Feoktistov. Pisma v ZhTF, 1996. Vol.22. No.4, p.7-11, (in Russian).

Copies of papers, presented for publication

4. V. A. Berenberg, M. V. Vasiliev, V. Yu. Venediktov, A. A. Leshchev, L. N. Soms, A. P. Onokhov, L. A. Beresnev, and W. Haase,
“Polychromatic correction for aberrations in the lenses of telescopic systems using liquid-crystal optically addressed spatial light modulators”,

Proceedings of SPIE, Vol. 3388, presented to SPIE's 12 Annual Int. Symp. “AeroSense”, section “Advances in Optical Information Processing VIII”, 13-17 April 1998, Orlando, Florida USA, Advanced Technical Program, p.52..

Polychromatic correction for aberration in the lenses of telescopic systems using liquid crystal optically addressed spatial light modulator

V.A.Berenberg^a, L.A.Beresnev^b, W.Haase^b, A.A.Leshchev^a,
A.P.Onokhov^a, L.N.Soms^a, M.V.Vasil'ev^a, V.Yu.Venediktov^a

^aInstitute for Laser Physics, SC "Vavilov State Optical Institute"
199034, Birzhevaya, 12, St.-Petersburg, Russia

^bTechnische Hochschule, Darmstadt, Germany

ABSTRACTS

Given are the results of experimental study on the quasi real time holographic correction for the lens distortions in the passive observational telescope in the visible range of spectrum, using the liquid crystal optically addressed spatial light modulator.

Keywords: dynamic hologram, holographic corrector, liquid crystal spatial light modulator, passive imaging telescope.

1. INTRODUCTION

The method of holographic correction for distortions, imposed by the primary mirror (lens) of the telescope, was first proposed and realized in the experiment in ^{1,2}. The holographic corrector was recorded by the coherent radiation, and its chromatism (grating disperse) was corrected for by use of the auxiliary diffraction grating, providing thus the possibility of imaging in the comparatively wide spectral range. These works, as well as much later investigations in USA ³⁻⁵ were realized with the use of static holographic media, providing thus correction only for the static distortions.

The principle of the holographic correction for the telescope lens distortions is illustrated by the Fig.1. Let the telescope is comprised by the distorted lens 1 and the eye-piece 2. This system is imaging the remote self-luminous object 4 in the registration plane 3. In the case of the high optical quality of the elements 2 and 3 the system resolution is determined by the properties of the lens 1. One can compensate for the lens distortions by the holographic corrector 5, mounted in the plane to which the eye-piece 2 images the pupil of the lens 1^{1,2}. The hologram is recorded by the coherent radiation as the interference pattern of the plain reference wave and the object wave, emitted by the point source, mounted in the plane of the object 4.

The light wave from this point source which has passed through the distorted lens bears the information on its distortions. This information is encoded in the hologram. On the stage of the hologram reconstruction the radiation, emitted by the point source and distorted on its path through the telescope will diffract on the hologram into the plain wave, coinciding with the reference wave, used for the hologram recording. Any luminous object can be treated as a set of the point sources. Hence the radiation from the object, distorted by the telescope, will diffract to the set of plain waves. These waves will reconstruct in the plane 3 the non-distorted image of the object notwithstanding the arbitrary distortions of the telescope lens 1.

The non-monochrome radiation from the object would be expanded by the hologram to the spectrum. This chromatism is to be corrected by the auxiliary static diffraction grating whose spatial frequency is equal to the spatial carrier of the holographic corrector.

2. THE CHOICE FOR THE CORRECTING ELEMENT

One can use the nonlinear optical phase conjugation for the dynamic correction for the primary lens (mirror) distortions⁶. In particular, in ^{7,8} it was realized with the use of the stimulated Brillouin scattering. In this case, however, the imaged object is either to emit the coherent radiation or to be illuminated by such a radiation.

The highest efficiency among the nonlinear-optical media for holograms recording, providing dynamic correction for distortions in the wide spectral range, is revealed by the liquid crystal spatial light modulators (LC SLM)⁹ and by the photorefractive crystals¹⁰. For example, in ¹¹, the use of LC SLM made it possible to correct for distortions in the spectral band with the width 10 nm, separated from the hologram recording wavelength in 90 nm. In the experiment¹⁷ similar schematics was realized with the use of the auxiliary static holographic grating, compensating for the dynamic hologram chromatism. In ¹² the correction for the distortions of the optical elements was realized with the use of the photorefractive crystals BSO and NBS with the hologram record at the wavelength 514 nm. The holograms were reconstructed by the Ar-ion laser radiation at several discrete wavelength in the range of 476..514 nm.

Not that for the correction for distortions, imposed by the lens into the image of the distant and spatially-incoherent radiation it is sensible to use the thin holograms. The use of the volume (thick) holograms will result in extra limitations due to their angular and spectral selectivity¹², resulting in most cases in the impossibility to realize the most important advantage of this class of holograms - the high diffraction efficiency. So, to our opinion, the LC SLM medium is more prospective from the point of view of dynamic correction than the photorefractive media. The comparison of the combination of such a basic parameters, as the sensitivity, response time, reversibility, resolution and depth of phase modulation, realized in these two media, also puts the LC SLM ahead.

This paper is devoted to the experimental results on thermal object imaging in the wide spectral range by the model telescope with the dynamic holographic correction for its primary lens and auxiliary correction for the hologram chromatism. The dynamic hologram was recorded in LC SLM, using the polymer photoconductor^{13,14} or the photoconductor on the base of silicon carbide¹⁸⁻²¹. The S-effect was used for the holograms record in SLM with the nematic LC, and in the case of ferroelectric LC we have used the DHF-effect^{22,23}. The holograms were recorded in pulsed mode^{15,16}.

Variation of the voltage pulse, feeding the SLM, duration and of its synchronization with respect to the light pulse provides the control of the temporal delay from the hologram recording to the moment of its highest diffraction efficiency. In our experiments we could vary this delay from 100 msec to several dozen seconds.

The diffraction efficiency of the realized holographic correctors equaled 20-25%. The holograms, recorded in FLC SLM, revealed very weak dependence of their diffraction efficiency on the polarization of reconstructing radiation. So in the case of imaging of test-object, illuminated by the incoherent (thermal) radiation, the effective efficiency was two times higher.

3. EXPERIMENTAL SETUP

The experimental setup is shown in the Fig.2. The thermal source at the infinity was simulated by the standard test object 1, illuminated by the light of the tungsten lamp. The imaged test-object was mounted in the focal plane of the auxiliary lens 2. The absolute angular dimension of the object was equal 0.02 radian. This object was imaged by the lens telescope, comprised by the primary lens 3 to be corrected and the eye-piece 4. Two identical achromatic lenses with the focal length of 230 mm were used as the elements 3 and 4. The corrector unit comprised the LC SLM 5, the transparent phase (holographic) diffraction grating 6 for the dynamic hologram chromatism compensation and the scheme for the corrector recording.

The hologram-corrector was recorded by the pulsed radiation of second harmonics (0.54 μ m) of Nd:YAP laser 7 as the interference pattern of the plain reference wave and the object wave, transmitted via the telescope. The telescope 8 (10^x) improved the spatial homogeneity of the recording beams. The useful clear aperture of the SLM was determined by the apertures 9 and 10 and equaled 15 mm. Beam split cube 11 (transparency 50 %) separated the recording beams and, in a time, combined the radiation from the imaged object 1 and the probe beam of laser radiation.

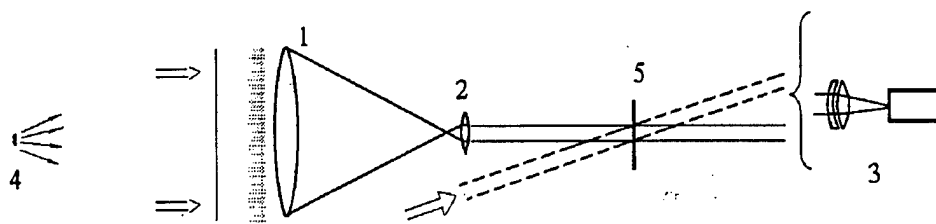


Fig.1. Principle scheme of holographic correction for telescope lens distortion

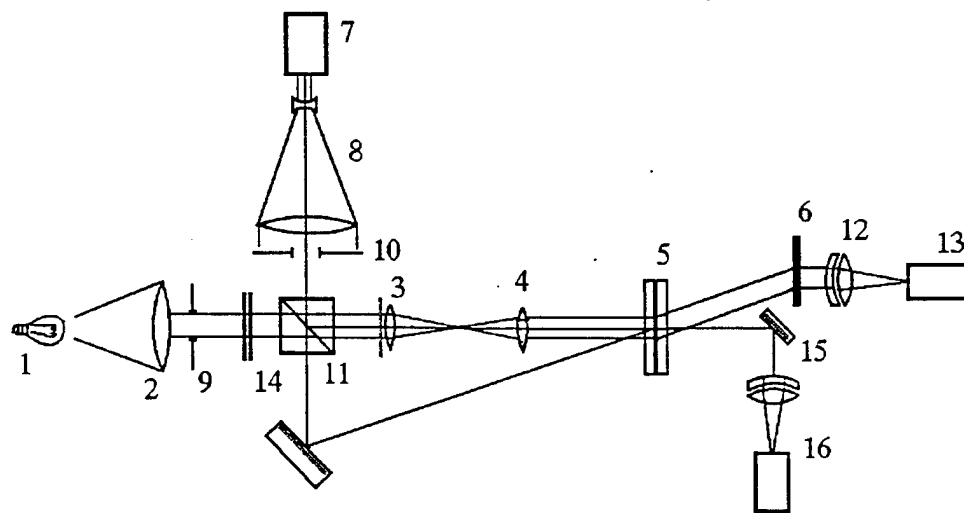


Fig.2. Experimental setup

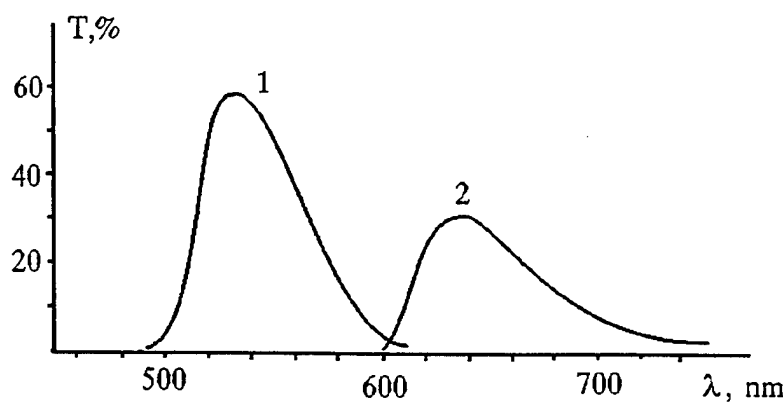


Fig.3. Spectral dependence of the colored filters transparency:

- 1 — colored filters GS-18 + SZS-22 (OKC-18 + C3C-22);
- 2 — colored filters KS-10 + SZS-23(KC-10+C3C-23)

The eye-piece 4 imaged the pupil of the lens 3 in the plane of the corrector 5. The spatial carrier frequency of the dynamic hologram was equal to the spatial frequency of the grating 6 and was equal 95 mm^{-1} . Such a value was chosen as the trade-off value, providing both spatial separation of the object images in different diffraction orders and sufficiently high diffraction efficiency.

The radiation from the thermal source, diffracted from the grating 6, was caught by the lens 12 and focused to the CCD-matrix 13. The spectral range, used for the object imaging, was varied by the colored filters 14. We have used the filters made of standard colored glasses (the spectral characteristics of the filters transparency are shown in the Fig.3), and the band interference filter with the width of the transparency band 10 nm centered at $0.53 \mu\text{m}$. The zero order diffraction on element 5 radiation from the thermal object was caught by the plain mirror 15 and used for control non-corrected image of the object, registered by the system 16.

4. EXPERIMENTAL RESULTS

The various distorters were mounted in the signal beam. Small-scale distortions of the lens were simulated with the use of glass plates etched in hydrofluoric acid. For an example, in the Fig.4 the interferogram is shown of the "strongest" distorter of this kind, providing beam divergence of ~ 0.006 radian (FWHM). The Fresnel bi-prism was used for simulation of the local wedge-like distortions, which in practice can be caused, for example, by the mutual tilt of the primary mirror segments; the angular misalignment of "images" in our case was ~ 0.01 radian. We have used the tungsten wire of lamp, the sharp edge and the standard test object as the objects of imaging. The latter two kinds of test-objects provided the application of standard methods of the quantitative evaluation of the correction fidelity and its dependence on the spectral range of imaging radiation.

The following results were obtained with the NLC SLM.

We have measured the frequency-contrast characteristics of the optical system under correction with the imitation of the small-scale scattering distorter with the angular divergence of ~ 0.006 radian. It was measured for the green range of spectrum (see filter transparency - curve 1 in the Fig.3), for the red range of spectrum (curve 2 in the Fig.3) and for the "white" light of tungsten lamp. In the Fig.5 the results are shown of this characteristic measuring as $K = \{I_{\max} - I_{\min}\} / \{I_{\max} + I_{\min}\}$. One can see from the Fig.5, that in the case of imaging in the green range of spectrum (the width of spectral range ~ 50 nm), whose maximum approximately coincides with the wavelength of laser radiation used for the hologram recording, the system performance is close to the diffraction limited. The use of "white" light also provides rather good quality of image. Significant deterioration of the image is observed only while imaging in red spectral band whose maximum is shifted in ~ 100 nm with respect to the recording wavelength. In the Fig.6-10 are shown the photographs of the standard test object, which confirm the above said. In the case of the wedge-like distortions the shift of imaging spectrum to the red range or use of "white" light the image was "expanded" in the "wedge" direction.

Additional information on the correction fidelity was got from the analysis of the photographs of the sharp edge (Fig.11,12). One can see that in the case of spectral band shift with respect to the recording wavelength, and of the strong distortions of the probe beam, the wings in the edge spread function (ESF) are observed. These wings are responsible for the decrease of the complicated image contrast, and they are resulted from non-sufficient correction for the chromatism distortions. One can also see from these photographs that the point spread function (PSF) consists of two components: the narrow core, resulting of nearly diffraction limited performance of the OS, and of the wings, caused by the non-sufficient chromatic correction for the optical distortions. According to evaluations, in the absence of the distortions in the probe beam the image core contains $\sim 65\%$ of total energy for reading out both in the green and in the red spectral ranges (Fig.11). Distortions of the probe beam by the etched plate with the distortions rate of 0.006 rad result, in the green range, in preservation of the core energy, while in the red range of spectrum it is reduced down to $\sim 35\%$ (Fig.12).

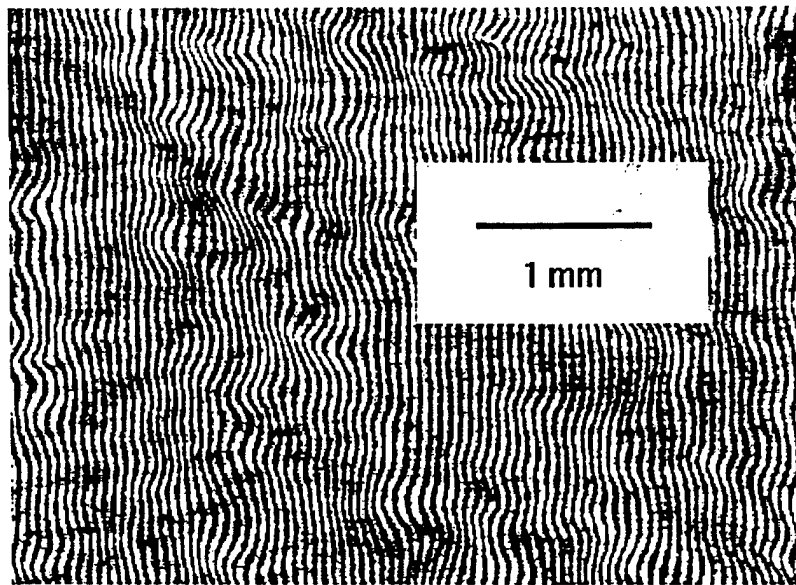


Fig.4. The part of interferogram of the distorting plate, providing beam divergence of 0.006 radian.

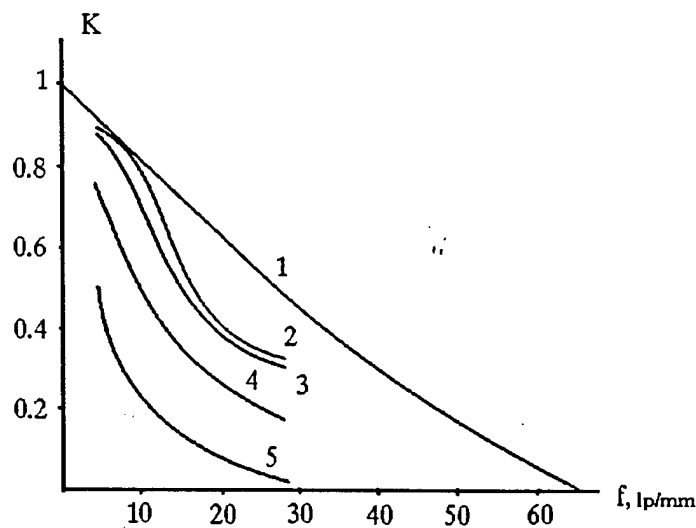


Fig.5. Frequency-contrast characteristics of the optical system under correction in the absence (curves 1, 2) and in the presence (curves 3, 4, 5) of small-scale distortions. Curve 1 - the ideal lens, curve 2 - optical system used in our experiment. 3 - correction in the green range of spectrum, 4 - correction in the "white" and 5 - light correction in the red range of spectrum.

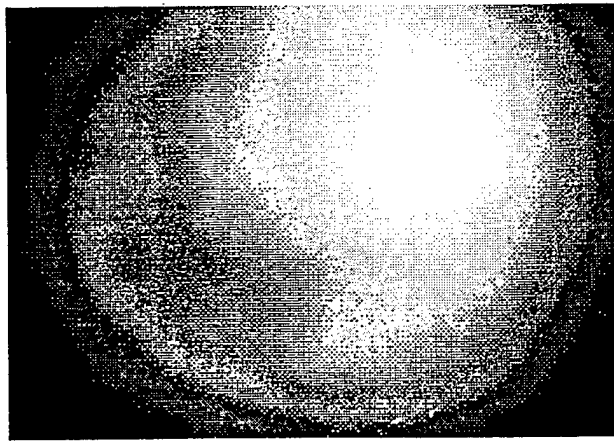


Fig.6. Image of standard test-object without correction for lens distortions.

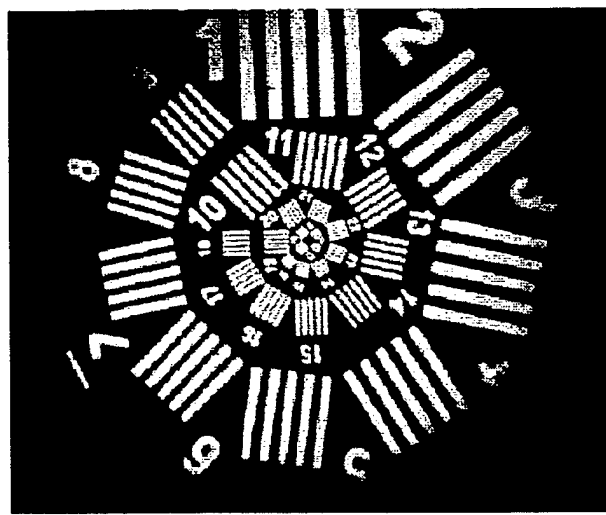


Fig.7. Image of test object in green light with correction for distortions.

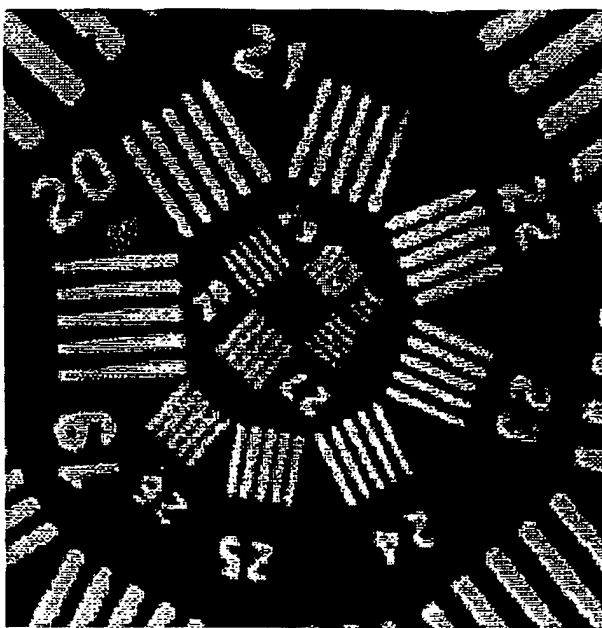


Fig.8. Central zone of standard test object image in green light with the correction for distortions.

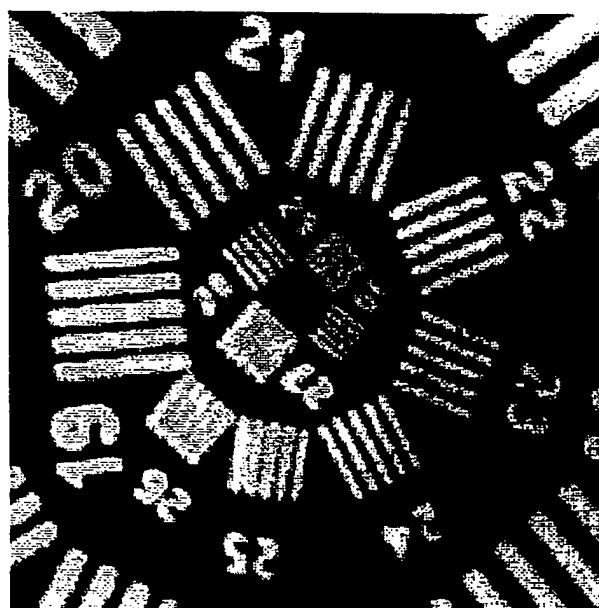


Fig.9. Central zone of standard test object image in “white” light with the correction for distortions.

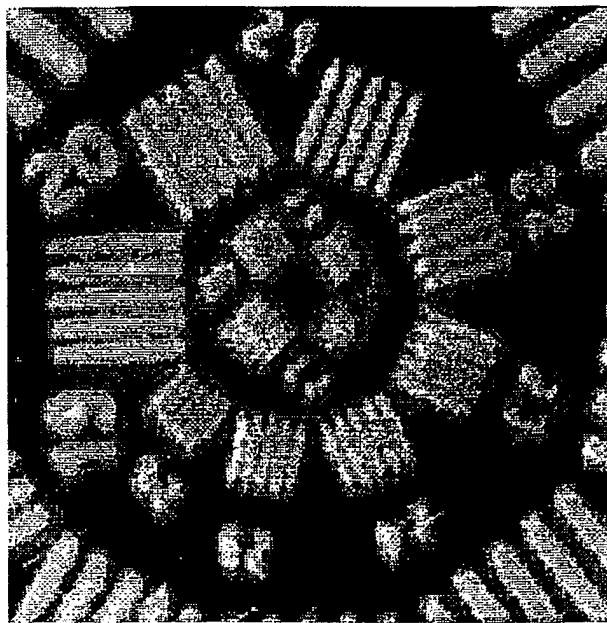


Fig.10. Central zone of standard test object image in red light with the correction for distortions.

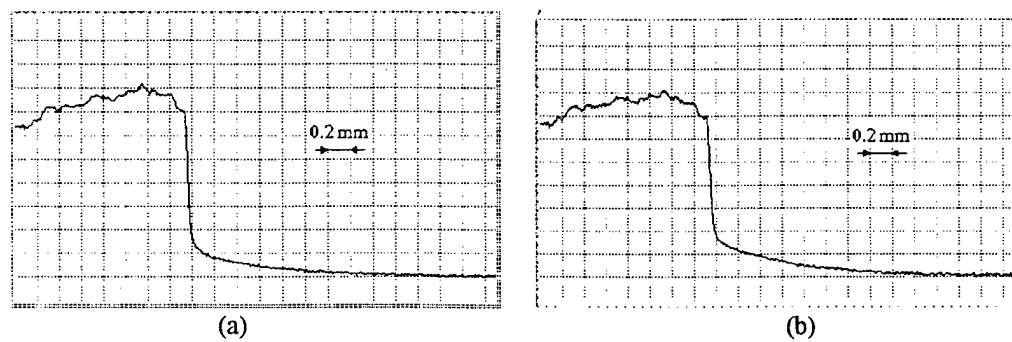


Fig.11. Reconstructed image of the sharp edge without distortions,
read out in green (a) and red (b) spectral bands (see Fig.3.).

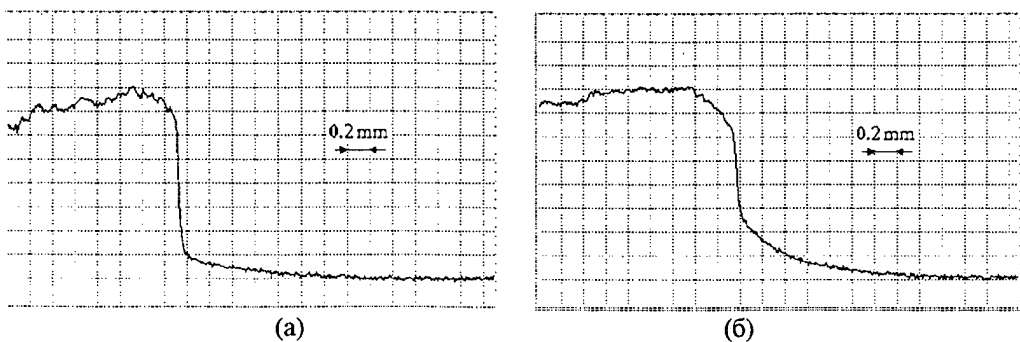


Fig.12. Reconstructed image of the sharp edge with distorter 0.006 rad,
read out in green (a) and red (b) spectral bands.

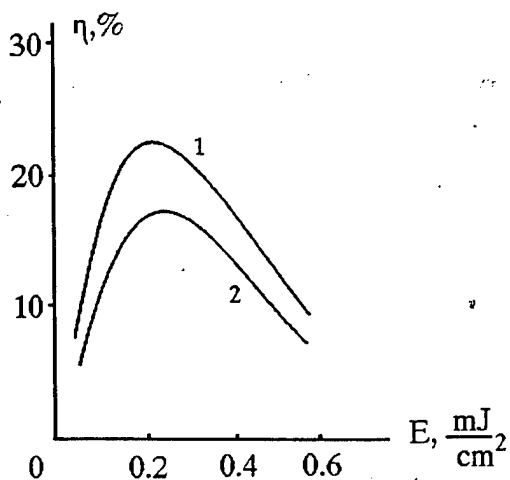


Fig.13. Peak values of DE vs. radiation energy fluency without distorter (1)
and with the distorter 0.006 radian (2).

It was found out that the influence of the small-scale distortions onto the absolute value of the hologram-correctors DE reveals itself for the etched glass distorters providing random divergence of more than 0.004-0.005 radian. These values are approximately in an order of magnitude smaller than the angular separation of neighboring orders of diffraction. Corresponding results, obtained by reading out by He-Ne laser radiation, are shown in the Fig.13.

In course of the experiments we have also tried the image correction with the use of SLM, based on the ferroelectric LC. Visual correction ability was not worse than in the case of nematic LC application. Image brightness, however, was much higher: in this case the radiation from thermal object is used much better, for the FLC SLM performance is almost polarization independent.

5. CONCLUSION

In the reported experiment the source of coherent radiation, used for the corrector record, was mounted in the plane of the object (or, generally speaking, optically conjugate plane). In practice of imaging of the remote object it is impossible. In the so called bypass optical schemes the source of the radiation, used for reading out of the primary lens (mirror) distortions can be mounted nearby this lens or mirror, say, in the latter center of curvature. In this case the distortions are compensated (corrected) not completely, but down to some residual error. However, depending on the telescope design the surplus can be some dozen or hundred times^{7,8}.

Hence the results of the reported experiment promise the successful use of the optically addressed LCoSLM as the dynamic holographic media for the record of the holographic correctors to be used in the passive bypass imaging telescopes.

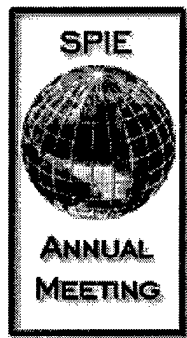
REFERENCES

1. Denisuk Yu.N., Soskin S.I. Holographic correction of deformational aberrations of the primary mirror of the telescope. Opt. Spektrosk., 1971, Vol. 31. No. 6, p. 991-997, (in Russian).
2. Denisuk Yu.N., Soskin S.I. Holographic correction of deformational aberrations of the primary mirror of the telescope. Opt. Spektrosk., 1972, Vol. 33, No. 5, p. 994-996, (in Russian).
3. Munch J., Wuerker R. Holographic technique for correcting aberrations in a telescope//Appl. Opt. - 1989. - Vol. 28. No. 7. - P. 1312-1317.
4. Munch J., Wuerker R., Hefflinger L. Wideband holographic correction of an aberrated telescope objective//Appl. Opt. - 1990. - Vol. 29, No. 16. - P. 2440-2445.
5. Andersen G., Munch J., Veitch P. "Holographic correction of large telescope primaries by proximal, off-axis beacons// Appl. Opt. - 1996-V.35, No.4 P. 603-608.
6. Zel'dovich B.Ya., Pilipetsky N.F., Shkunov V.V. Phase conjugation. - Moscow, 1985, 240 p. (in Russian).
7. Leshchev A.A., Pasmanik G.A., Sidorovich V.G., Vasil'ev M.V., Venediktov V.Yu.. Compensation for distortions in the imaging systems, using phase conjugation technique. Izvestiya Akademii Nauk SSSR, v.55, 2, p.260-266, 1991. (In Russian).
8. Leshchev A. A., Sidorovich V. G., Vasil'ev M. V., Venedictov V.Yu., Pasmanik G.A. Nonreciprocal optical systems with phase-conjugating mirrors - a new class of optical imaging systems. International Journal of Nonlinear Optical Physics. - 1994. - Vol. 3, No. 1. - p. 89-100.
9. Vasil'ev A.A., Casasent D., Kompanets I.N., Parfenov A.V. Spatial light modulators. Moscow, Radio i Svyaz. 1987. 320 p. (in Russian)
10. Petrov M.P., Stepanov S.I., Khomenko A.V. Photorefractive crystals in coherent optics. St.-Petersburg. Nauka. 1992. 320 p. (in Russian)
11. Kramer M. A., Wetterer C. J., Martinez Ty. One-way imaging through an aberrator with spatially incoherent light by using an optically addressed spatial light modulator// Appl. Opt. - 1991. - Vol. 30, No. 23. - P. 3319-3323.
12. Dimakov S.A., Klimentiev S.I., Sventsitskaya N.A., Sherstobitov V.E. Compensation for optical elements distortions by means of dynamic holography in "white light". Opt. Spektr., 1996, Vol.80. No 4, p. 699-704 (in Russian).
13. Groznov M.A., Myl'nikov V.S., Soms L.N., Tarasov A.A. Liquid crystal spatial light modulator with the resolution of more than 1000 lines per mm. Zh. Tekh. Fiz.. 1987, Vol . 57. No. 10. p. 2041-2042, (in Russian).
14. Myl'nikov V.S. Liquid crystal spatial light modulators with the organic polymer photoconductor. Optical Journal. 1993, #7, p.41-45 (in Russian).
15. Kamanina N.V., Soms L.N., Tarasov A.A. Holographic correction for distortions using the liquid crystal phase light modulators. Opt. Spektrosk., 1990. Vol. 68. No. 3, p. 691-693 (in Russian).
16. Berenberg V.A., Kamanina N.V., Soms L.N. Holographic correction for distortions using the liquid crystal phase light modulators under different frequencies of recording and reconstructing radiation. Izv. Akad. Nauk SSSR, Ser. Fiz.. 1991. Vol. 55. No. 2. p. 236-238, (in Russian).
17. Berenberg V.A., Vasil'ev M.V., Venediktov V.Yu., Leshchev A.A., Soms L.N. Journal of Optical Technology, Vol.64. No.9. p.73-74, 1997.
18. Ahiyama K., Takimoto A., Ogivara A., Ogawa H. Jpn.J.Appl. Phys.. 1993, Part 1, Vol. 32, p. 590.
19. Feoktistov N.A., Morozova L.E. Pisma v ZhTF. 1994. Vol.20, No.5, p.12-16. (in Russian).
20. Ahiyama K., Takimoto A., Ogawa H. Appl.Opt.. 1993. Vol.32, No.32, p. 6493-6500.
21. Ivanova N.L., Morozova L.E., Onokhov A.P., Pevtsov A.B., Feoktistov N.A. Pisma v ZhTF. 1996, Vol.22. No.4. p. 7-11, (in Russian).
22. Beresnev L.A., Blinov L.M., Dergachev D.I., Loseva M.V., Chernova N.I. Pisma v ZhTF. 1988. Vol. 14. No. 3. p. 260-263. (in Russian).
23. Abdulhalim I., Moddel G. Mol. Cryst. Liq. Cryst.. 1991. Vol.200, p.79-101.

Copies of papers, presented for publication

5. L. A. Beresnev, W. Dultz, B. Hils, T. Weyrauch, S. A. Pikin, W. Haase,
“Polarization non-sensitive optical phase modulators using the deformed helix ferroelectric liquid crystals”
(material of sections 2.1.2 and 4.1 in this Final Report).
Abstract of report presented to SPIE Conf. , 19-24 July, 1999, Denver CO, USA. Article will be submitted
to Proceedings of SPIE.

6. P. P. Banerjee, L. A. Beresnev, and M. A. Vorontsov.
“Cancellation of effects of large phase distortion on images by dynamical holography using ferroelectric
liquid crystal spatial light modulators”
Abstract of report presented to SPIE Conf. , 19-24 July, 1999, Denver CO, USA:
Article will be submitted to Proceedings of SPIE.



Abstract Submission Form

Abstract Due Date:
21 December 1998

Abstract Due Date for On-site Proceedings:
7 December 1998

Presentation title:

Polarization non-sensitive optical phase modulator based on two DHF (deformed helix ferroelectric) liquid crystal layers.

Author list (principal author first):

Full names and affiliations as they will appear in the program.

Leonid Beresnev, #Wolfgang Dultz, *Bernd Hils, @Thomas Weyrauch,
@Wolfgang Haase

Correspondence for each author:

Mailing address, telephone, telefax, and e-mail address.

Army Research Laboratory, 2800 Powder Mill Road, Adelphi MD 20783
USA, tel (301) 394-0213, fax (301) 394-0225, beresnev@iol.arl.mil;
#Deutsche Telekom AG Research Center Darmstadt, Am Kavalleriesand
3, 64276 Darmstadt, Germany, tel 49(6151)832560, fax 49(6151)834323;
*Goethe University of Frankfurt/Main, Germany:
@Darmstadt University of Technology, Petersenstr. 20, 64287
Darmstadt, Germany, tel. 49(6151)163698, fax 49(6151)164924.

Presentation type:

Indicate your preference: ▾

Brief biography (principal author only):

50 to 100 words.

Leonid Beresnev, permanent address: Institute of Crystallography
Russian Academy of Sciences, Moscow; 1971-1982 - Organic Intermediates
& Dyes Institute, Moscow; 1992-1998 - Darmstadt University of
Technology, Darmstadt, Germany. About 100 article and more than 20
Patent Applications in the field of liquid crystals, research and
development of ferroelectric liquid crystal materials, development of
liquid crystal electrooptical devices

Abstract:

250 words describing purpose, methods, results, new or breakthrough work to be presented, and conclusions of the work.

The optical phase modulator is proposed which is non-sensitive to light polarization, consisting of two ferroelectric liquid crystal (FLC) cells mounted in series. FLC layers possess the DHF (deformed helix ferroelectric) effect. The optical axes of both layers remain crossed during the application of electric field. The dependence of effective refractive index of the double DHF modulator is calculated on molecular tilt angle in smectic C* phase, and on value of applied voltage. The strongly twisted helical ferroelectric liquid crystal mixtures are developed with the pitch of helix of the order of 0.2 micron and with large tilt angle 39-40 grad. The effective refractive indices of the materials are measured by standard Abbe refractometer. The double DHF modulator is designed and phase shift was measured by Feazeau interferometer in dependence on light polarization and applied electric field for two crossed DHF cells. The strong nonlinear increase of the phase shift was found in dependence on voltage, without remarkable dependence on light polarization. The maximum phase shift agreed with the calculations and was equal 0.75 wavelength for cell thicknesses 16 microns. The characteristic response time of the modulator is less than 1 ms.

Keywords:

Up to 5 key words noting the nature of the work.

phase modulator, DHF (deformed helix ferroelectric) liquid crystal, crossed DHFLC cells.

Please click the "submit" button **only once**. You will receive confirmation of receipt from SPIE within one working day.

[1999 Annual Meeting Home](#)

[SPIE Web Home](#) | [Publications](#) | [Education](#) | [Meetings](#) | [Employment](#) | [Membership](#) | [Contact SPIE](#)

Telephone: +1 360/676-3290 | Fax +1 360/647-1445 | E-mail: spe@spie.org

© 1998 SPIE - The International Society for Optical Engineering

[SPIE Web Home](#) | [Publications](#) | [Education](#) | [Employment](#)
[Meetings](#) | [Exhibits](#) | [Membership](#) | [Contact SPIE](#)

Telephone: +1 360/676-3290 | Fax +1 360/647-1445 | E-mail: spe@spie.org

© 1999 SPIE - The International Society for Optical Engineering

1. SUBMIT TO: SD112
2. CONFERENCE: High-Resolution Wavefront Control: Methods, Devices, and Applications
3. ABSTRACT TITLE: Cancellation of effects of large phase distortions on images by dynamic holography using ferroelectric liquid crystal spatial light modulators
4. AUTHOR LISTING: P.P. Banerjee*, L. Beresnev and M. A. Vorontsov
Army Research Lab, AMSRL-IS-EE, 2800 Powder Mill Road, Adelphi MD 20723.
Tel: (256) 890 6215 ext 416
Fax: (256) 890 6618
e-mail: banerjee@ece.uah.edu
* on sabbatical leave from Dept. of ECE, U. Alabama in Huntsville, Huntsville AL 35899
5. PRESENTATION: oral
6. ABSTRACT TEXT: The correction of large dynamic aberrations using dynamic holography in optically addressed liquid crystal spatial light modulators (OASLMs) has been demonstrated using a point source at infinity or equivalently a collimated light beam (Gruneisen *et al* 1998, SPIE Proc. 3432 137(1998)). Correction of images received by a telescope using similar aberration compensation technique has been reported by Vasil'ev *et al* (SPIE Proc. 3432 164(1998)). We extend the approach to perform correction of severely aberrated images in general by dynamically writing the hologram of the phase aberration in ferroelectric OASLMs and reading it out with the optical field from the object passing through the same phase aberration at a different wavelength. We find that it is important to *image* the phase distortion on the surface of the OASLM during the recording of the dynamic hologram. We provide examples of severely distorted images and the corresponding corrected images due to phase cancellation in one of the diffracted orders during readout. We show that in the other diffracted orders observed during readout, the phase distortions can be even more severe, due to amplification of the phases during readout. We find that the spatial scale of phase distortion is one more important factor the quality of corrected image depends on. The efficiency of phase distortion correction decreases with decrease of the phase distortion spatial scale.
7. KEYWORDS: dynamic holography, phase aberration correction, optically addressable spatial light modulators.
8. BRIEF BIOGRAPHY: P.P. Banerjee is Professor of Electrical and Computer Engineering at the University of Alabama in Huntsville. His research interests are acoustooptics, photorefractives and nonlinear optics. To date he has over 75 refereed journal papers and numerous conference papers, and he has coauthored a book and working on another. He is a Fellow of the Optical Society of America, Senior Member of IEEE and a member of SPIE.

520

Banerjee

banerjee@ebs330.eb.uah.edu, 1/13/99 1:02 PM +0000, e21701, sd99, sd99 SD11: SD99, GU

1

Date: Wed, 13 Jan 1999 13:02:00 +0000 (GMT)

From: banerjee@ebs330.eb.uah.edu

Subject: SD99, Gonglewski [SD112]

To: abein@spie.org

Reply-to: banerjee@ebs330.eb.uah.edu

Subject: SD99, Gonglewski [SD112]

Output from WWW form to

Received from domain

***** Sender Information *****

Sender name: Partha P. Banerjee

Sender email address: banerjee@ece.uah.edu

***** Author(s) information *****

Author(s):

P.P. Banerjee, L. Berezhov and M. A Vorontsov
Army Research Lab, Adelphi MD

Correspondence Info:

AMS-LIS-IE, 2800 Powder Mill Road, Adelphi MD 20726

Tel: (202) 820 6215 ext 416

Fax: (202) 890 6616

e-mail: banerjee@ece.uah.edu

* on sabbatical leave from Dept. of ECE, U. Alabama in Huntsville, Huntsville AL 35899

Principal author bio

P.P. Banerjee is Professor of Electrical and Computer Engineering at the University of Alabama in Huntsville. His research interests are acoustooptics, photorefractives and nonlinear optics. To date he has over 75 refereed journal papers and numerous conference papers, and he has coauthored a book and working on another. He is a Fellow of the Optical Society of America, Senior Member of IEEE and a member of SPIE.

***** Presentation Information *****

Conference Name:

30 High-Resolution Wavefront Control: Methods, Devices, Applications (SD112)

Conference Chair: Gonglewski [SD112]

Presentation title:

Cancellation of effects of large phase distortions on images by dynamic holography using ferroelectric liquid crystal spatial light modulators

Presentation type: Oral Presentation

Abstract:

The correction of large dynamic aberrations using dynamic holography in optically addressed liquid crystal spatial light modulators (OASLMs) has been demonstrated using a point source at infinity or equivalently a collimated light beam (Gruneisen et al 1998, SPIE Proc. v.3432 p.137(1998)). Correction of images received by a telescope using similar aberration compensation technique has been reported by Vasil'ev et al (SPIE Proc. v.3432 p.164(1998)). We extend the approach to perform correction of severely aberrated images in general by dynamically writing the hologram of the phase aberration in ferroelectric OASLMs and reading it out with the optical field from the object passing through the same phase aberration at a different wavelength. We find that it is important to image the phase distortion on the surface of the OASLM during the recording of the dynamic hologram. We provide examples of severely distorted images and the corresponding corrected images due to phase ca!

Copies of papers, presented for publication

7. W. Dultz, L. A. Beresnev, W. Haase, and A. P. Onokhov.
“Electrooptischer Lichtmodulator (Electrooptical phase modulator”, Deutsches patent 198 52 890.6

Deutsches Patent- und Markenamt

Deutsches Patent- und Markenamt . 80297 München

Deutsche Telekom AG
 Technologiezentrum
 Patenabteilung EK 03
 64307 Darmstadt

München, den - 8. 01. 99
 Ferndurchwahl: (089) 2195-2285

Aktenzeichen: 198 52 890.6
 Ihr Zeichen: P97216
 Anmeldernr.: 5671361
 Deutsche Telekom AG

Deutsche Telekom AG
 Technologiezentrum Darmstadt
 Eing. 15. JAN 1999
 Patentabteilung

EK03-Nagel

- Ad
F 14**Bibliographie-Mitteilung**

IPC Hk1	G02F 1/1347	Akz 198 52 890.6
Ant	17.11.1998	
Bez	Elektrooptischer Lichtmodulator	
Anr	Deutsche Telekom AG, 53113 Bonn, DE	
Erf	Dultz, Wolfgang, Prof. Dr., 65936 Frankfurt, DE; Beresnev, Leonid, Dr., Columbia, Md., US; Haase, Wolfgang, Prof. Dr., 64354 Reinheim, DE; Onokhov, Arkadii, Dr., St. Petersburg, RU	

Die Veröffentlichung der Anmeldung erfolgt voraussichtlich am 18.05.2000.

Die technischen Vorbereitungen gemäß §32 Abs. 4 PatG. sind 8 Wochen vorher abgeschlossen.

Eine Veröffentlichung der Offenlegungsschrift unterbleibt nur dann, wenn früher als 8 Wochen vor dem oben angegebenen Veröffentlichungstag die Anmeldung zurückgenommen oder zurückgewiesen wird oder als zurückgenommen gilt (§32 Abs. 4 PatG.).

Hinweis:

() weitere Anforderungen s. Anlage

(keine weiteren Anforderungen

Prüfungsstelle 11.51

**Bitte Anmelder und Aktenzeichen
 bei allen Eingaben angeben !**



**Bitte beachten Sie die wichtigen
 Hinweise auf der Rückseite !**

HINWEISE

I. Bibliographie

Die umseitige Bibliographie ist - gegebenenfalls mit noch nachzutragenden Ergänzungen - für die Offenlegung der Patentanmeldung vorgesehen. Bitte überprüfen Sie diese Angaben und teilen Sie notwendige Änderungen möglichst bald mit.

Die Angaben in der Bibliographie haben folgende Bedeutung:

Beispiel

IPC HKI: A35H 12-103 AKZ. P 31 09 999.8	= Hauptklasse (Internationale Klassifikation), Aktenzeichen mit Prüfziffer, evtl. ergänzt um die Kennzahl der Patentabteilung, die für das Prüfungsverfahren zuständig ist
IPC NKI: A35H 12-105	= Nebenklassen (Internationale Klassifikation)
Ant 25.02.81	= Anmeldetag
Zus zu 30 09 999.1	= Zusatz zur Patentanmeldung P 30 09 999.1
Aus aus 31 00 999.9	= Ausscheidung aus Patentanmeldung P 31 00 999.9
Pri 07.08.79 CH 8366-79	= Priorität d. früheren Anmeldg. mit Ländercodebuchstaben u. Aktenzeichen
Bez Einrichtung zur Umwandlung eines Einzelbetts in ein Doppelbett	= Bezeichnung der Erfindung
Ann 0958056 Müller, Franz, München	= Anmelder-Code-Nr. für Anmelderangaben: Müller, Franz, München
Vnr 3058 Klappke, H. Dr. Pat.-Anw., 80225 München	= Vertreter-Code-Nr. für Vertreterangaben: Klappke, H. Dr. Pat.-Anw., 80225 München
Erf Deutscher, Michel, 87532 München	= Erfinderangaben

II. Offenlegung

Die Offenlegung erfolgt nach Ablauf des gesetzlich vorgeschriebenen Zeitraums. Über die Offenlegung werden Sie durch Übersendung einer Offenlegungsschrift unterrichtet.

III. Recherchenverfahren

Es kann Recherchenantrag (§ 43 PatG) gestellt werden. Er führt zur Ermittlung der öffentlichen Druckschriften, die für die Beurteilung der Patentfähigkeit der angemeldeten Erfindung in Betracht zu ziehen sind. Die Gebühr beträgt DM 200,-.

IV. Prüfungsverfahren

Eine Prüfung des Gegenstandes einer Patentanmeldung auf Patentfähigkeit wird nur auf besonderen Antrag vorgenommen. Der Antrag kann vom Patentsucher und von jedem Dritten bis zum Ablauf von sieben Jahren nach Einreichung der Anmeldung gestellt werden. Mit dem Antrag ist eine Gebühr nach dem Tarif zu zahlen; wird sie nicht gezahlt, so gilt der Antrag als nicht gestellt. Wird ein Prüfungsantrag nicht innerhalb der gesetzlichen Frist von sieben Jahren nach Einreichung der Anmeldung gestellt, so gilt die Anmeldung als zurückgenommen.

V. Jahresgebühren

Für jede Patentanmeldung ist unaufgefordert bei Beginn des dritten und jedes folgenden Jahres, gerechnet vom Anmeldetag an, eine Jahresgebühr nach folgender Tabelle unter Angabe des Aktenzeichens und des Verwendungszwecks zu entrichten:

Patentjahr:	3.	4.	5.	6.	7.	8.	9.	10.	11.	12.
Betrag in DM:	100.-	100.-	150.-	225.-	300.-	400.-	500.-	600.-	800.-	1050.-
Patentjahr:	13.	14.	15.	16.	17.	18.	19.	20.		
Betrag in DM:	1300.-	1550.-	1800.-	2100.-	2400.-	2700.-	3000.-	3300.-		

Die Gebühr wird jeweils am letzten Tag des Anmeldemonats fällig (Beispiel: Anmeldetag 15.03.92, Fälligkeit der 3. Jahresgebühr 31.03.94). Wird sie danach nicht innerhalb von 2 Monaten entrichtet, ist der Zuschlag von 10 Prozent der vollen Gebühr zu zahlen. Das Patentamt gibt darüber dem Anmelder eine Nachricht mit einer letzten Zahlungsfrist von 4 Monaten. Für Zusatzanmeldungen brauchen keine Jahresgebühren gezahlt zu werden.

VI. Schriftenbestellung

Bestellungen von Offenlegungs- und Patentschriften können vor dem Ausgabetag beim Schriftenvertrieb der Dienststelle Berlin des Deutschen Patentamts, 10958 Berlin nicht entgegengenommen werden. Eine Überwachung vorher eingehender Aufträge kann lediglich erfolgen, wenn mehr als 5 Exemplare einer Schriftennummer bestellt werden. In diesem Falle wird die Bestellung bei der Festlegung der Druckauflage berücksichtigt. Sonstige Bestellungen, die vor dem genannten Zeitpunkt eingehen, können aus verwaltungstechnischen Gründen nicht überwacht und müssen daher zurückgesandt werden. Bitte nehmen Sie daher von solchen Bestellungen Abstand.

VII. Gebrauchsmusterabzweigung

Der Anmelder einer nach dem 1. Januar 1987 mit Wirkung für die Bundesrepublik Deutschland eingereichten Patentanmeldung kann eine Gebrauchsmusteranmeldung, die den gleichen Gegenstand betrifft, einreichen und gleichzeitig den Anmeldetag der früheren Patentanmeldung in Anspruch nehmen. Diese Abzweigung (§ 5 Gebrauchsmustergesetz) ist bis zum Ablauf von 2 Monaten nach dem Ende des Monats möglich, in dem die Patentanmeldung durch rechtskräftige Zurückweisung, freiwillige Rücknahme oder Rücknahmefiktion erledigt, ein Einspruchsverfahren abgeschlossen oder - im Falle der Erteilung des Patents - die Frist für die Beschwerde gegen den Erteilungsbeschuß fruchtlos verstrichen ist. Ausführliche Informationen über die Erfordernisse einer Gebrauchsmusteranmeldung, einschließlich der Abzweigung, enthält das Merkblatt für Gebrauchsmusteranmelder (G 6181), welches kostenlos beim Patentamt und den Patentauslegerstellen erhältlich ist.

Elektrooptischer Lichtmodulator

Die Erfindung betrifft einen elektrisch ansteuerbaren Lichtmodulator mit hintereinander angeordneten Flüssigkristallschichten, die zwischen transparenten Platten mit einer die Moleküle der Flüssigkristalle ausrichtenden Oberflächenanisotropie und mit Elektroden zur Erzeugung eines elektrischen Feldes in den Flüssigkristallen eingeschlossen sind.

Derartige Modulatoren werden zur Phasenkorrektur von Licht in vielerlei optischen Einrichtungen benötigt. Insbesondere im Bereich der adaptiven Optiken werden in zunehmenden Maße Möglichkeiten gesucht, lokale Unschärifen in dem Objektbild eines Fernrohres oder einer Kamera, welche beispielsweise durch atmosphärische Effekte oder Wärmespannungen im Gerät entstehen, korrigieren zu können. Gerade in Verbindung mit schneller digitaler Bildverarbeitungstechnik ergeben sich Möglichkeiten, ein derart verzerrtes Bild noch während des Betrachtens zu korrigieren, indem das Bild von einem elektronisch ansteuerbaren Raster von optisch wirksamen Elementen korrigiert wird, welches in den Strahlengang des Objektbildes eingefügt ist. Damit lassen sich Aufnahme- und Beobachtungsgeräte denken, die auch bei starken Störungen ein scharfes Bild liefern.

...

Flüssigkristalle können aufgrund ihrer elektrooptischen Eigenschaften zur Steuerung der Phase einer durch sie hindurchtretenden Lichtwelle verwendet werden, indem der Brechungsindex einer Schicht aus Flüssigkristallen mittels eines elektrischen Feldes beeinflußt wird. Die wesentlichen elektrooptischen Effekte in Flüssigkristallen ändern sowohl die Doppelbrechung als auch die Orientierung der Indikatrix der Brechungsindizes des Flüssigkristalls. Für die meisten Anwendungen ist dies unerwünscht, denn neben der Phasenverschiebung ergibt sich aufgrund des anisotropen Charakters der Flüssigkristalle beim Durchtritt durch den Flüssigkristall auch eine Änderung der Polarisation. Deswegen kann mit derartigen Flüssigkristallen nur polarisiertes Licht behandelt werden. Wellenfrontänderungen durch Phasenverzögerung sollen aber für die oben genannten Anwendungen polarisationsunabhängig möglich sein.

Bei der Verwendung nematischer Flüssigkristalle ist es möglich, die Phase eines Lichtstrahls zu verändern, ohne daß die Polarisation des Lichts beeinflußt wird. Jedoch ist es auch hier notwendig, daß das Licht parallel zum Direktor der orientierten Flüssigkristallmoleküle linear polarisiert ist. Ferner ist die Reaktionsgeschwindigkeit derartiger Zellen zu gering für die Verwendung in bildverarbeitenden Einrichtungen.

Ferroelektrische Flüssigkristalle (FLC) können in einer hinreichend kurzen Operationszeit angesteuert werden. Die Anwendungsmöglichkeiten gewöhnlicher ferroelektrischer Flüssigkristalle sind aber wegen der geringen erreichbaren Phasenänderungen sehr eingeschränkt. Bei Zellendicken von 10 μm erreicht man gerade eine Phasenverschiebung von etwa 1/10 der Wellenlänge des sichtbaren Lichts. Es ist aber eine Phasenverschiebung von einer ganzen Wellenlänge oder mehr anzustreben, um damit alle notwendigen Phasenkorrekturen durchführen zu können.

...

In EP 0 309 774 wird eine Flüssigkristallzelle beschrieben, die den bei FLC auftretenden DHF-Effekt (Deformation der Helixstruktur im elektrischen Feld) zur kontinuierlichen Phasensteuerung und Graustufendarstellung benutzt. Die optische Phasensteuerung beruht auf einer starken Änderung des mittleren Brechungsindex des Flüssigkristalls durch ein angelegtes elektrisches Feld. Die Änderung der Doppelbrechung der deformierten Helixstruktur kann $d(n) = 5\%$ erreichen, die mittlere Brechungsanisotropie $\langle dn \rangle = 15\%$. Aufgrund der optischen Eigenschaften der helikalen Struktur des dort verwendeten chiralen smektischen Flüssigkristalls im elektrischen Feld ist die Änderung der Doppelbrechung mit starken Orientierungsänderungen der mittleren optischen Indikatrix verknüpft. Das bedeutet, daß sich das Licht nach dem Durchlaufen des Flüssigkristalls in einem Polarisationszustand befindet, der stark vom Polarisationszustand im Eingang abhängt. Diese Abhängigkeit verbietet die Verwendung der beschriebenen Zelle für die geforderten Zwecke.

In Love, Restaino, Carreras, Loos, Morrison, Baur and Kopp: "Polarization Insensitive 127-Segment Liquid Crystal Wavefront Corrector", Adaptive Optics, Vol. 13, pp. 228-290, Optical Society of America, Washington D.C., 1996 wird ein elektrooptisch arbeitender Modulator zur Phasensteuerung von unpolarisiertem Licht vorgestellt, der zwei hintereinanderliegende Flüssigkristallschichten vom nematischen Typ enthält. In der angeführten Arbeit werden zwei nematische Schichten so angeordnet, daß die Direktoren der Flüssigkristalle im feldfreien Zustand senkrecht aufeinander stehen. Die Zelle ist aber, wie oben schon erwähnt wurde, viel zu langsam für den angestrebten Verwendungszweck.

...

Aufgabe der vorliegenden Erfindung ist es, einen elektrisch ansteuerbaren Lichtmodulator anzugeben, der eine Schaltzeit in der Größenordnung von 10^{-4} Sekunden oder darunter bei einer maximalen Phasenverschiebung von über 2π aufweist, der die Phase eines beliebig polarisierten Lichtstrahls stufenlos verändern kann, ohne dessen Polarisationszustand zu ändern, und der zur Erstellung ortsauflösender adaptiver optischer Einrichtungen geeignet, das heißt klein, leicht und verlustarm ist.

Diese Aufgabe wird erfindungsgemäß dadurch gelöst, daß wenigstens zwei Schichten helikaler smektischer ferroelektrischer Flüssigkristalle, deren jeweils schnelle und langsame optische Achse parallel zu der jeweiligen Schicht liegen und deren mittlere optische Anisotropie durch Einwirkung des elektrischen Feldes beeinflußbar ist, hintereinander im Strahlengang eines zu modulierenden Lichtstrahls angeordnet sind und daß die Richtungen der schnellen bzw. langsamen Achsen der einzelnen Schichten gegeneinander derart verdreht sind, daß die Polarisierung des Lichtstrahls vor und hinter dem Modulator gleich ist.

Die "langsame" Achse entspricht dabei derjenigen Richtung, in welcher der Brechungsindex am größten ist. Die "schnelle" Achse ist diejenige Richtung, in welcher der Brechungsindex am kleinsten ist. Das heißt, daß die Phase eines in der langsamen Richtung polarisierten Lichtstrahls stark verzögert wird und die Phase eines in der schnellen Richtung polarisierten Lichtstrahls weniger stark. Durch die Anisotropie der Brechungsindizes kommt es damit bei beliebig polarisiertem Licht zu einer Änderung des Polarisationszustandes beim Durchlaufen der Flüssigkristallschichten. Die Verdrehung der einzelnen Schichten zueinander ist gerade so bemessen, daß die angesprochene Änderung des Polarisationszustandes in den folgenden Schichten wieder rückgängig gemacht wird.

...

Im einfachsten Fall wird der Lichtmodulator so ausgestaltet, daß zwei Flüssigkristallschichten derart hintereinander angeordnet sind, daß die langsame optische Achse der ersten Schicht senkrecht auf der langsamen optischen Achse der zweiten Schicht steht, daß die schnelle optische Achse der ersten Schicht senkrecht auf der schnellen optischen Achse der zweiten Schicht steht und daß die Ausrichtung der langsamen und der schnellen optischen Achsen der beiden Schichten zueinander während des Anlegens und Veränderns der Steuerspannung jederzeit erhalten bleibt.

Durch die Kreuzung der schnellen und langsamen Achsen der beiden Schichten im rechten Winkel werden die Doppelbrechungsänderungen und die Orientierungsänderungen der Indikatrixellipsoide der Brechungsindizes gerade kompensiert.

Es kann zur Reduzierung des Bauvolumens vorgesehen sein, daß die Flüssigkristallschichten zwischen zwei transparenten Platten eingeschlossen sind, an deren Elektroden eine Steuerspannung zur Erzeugung eines elektrischen Feldes anlegbar ist.

Um dagegen den Bauaufwand für den Lichtmodulator zu reduzieren und die Massenfertigung zu erleichtern, kann alternativ vorgesehen sein, daß die Flüssigkristallschichten jeweils zwischen zwei transparenten Platten eingeschlossen sind, an deren Elektroden je eine Steuerspannung zur Erzeugung je eines elektrischen Feldes anlegbar ist.

Zur Herstellung des erfindungsgemäßen Lichtmodulators wird die benötigte Anzahl der so gefertigten Einzelzellen hintereinander angeordnet.

...

Bei der Verwendung gleicher Schichtdicken und Materialien für die Schichten ist vorgesehen, daß die Flüssigkristallschichten die gleichen mittleren Brechungsindizes aufweisen, die gleiche Dicke haben und synchron mit den gleichen Steuerspannungen beaufschlagbar sind.

Bei der Verwendung unterschiedlicher Schichtdicken oder unterschiedlicher Materialien für die einzelnen Schichten ist dagegen vorgesehen, daß das Verhältnis der Steuerspannungen zueinander zur Kompensation der Polarisationsänderungen eines durchtretenden Lichtstrahls einstellbar ist. Dadurch läßt sich eine Überkreuzung der Hauptbrechungsrichtungen auch bei unsymmetrisch aufgebauten Zellen erreichen.

Die Fertigung von Flüssigkristallzellen ist sehr aufwendig; große Stückzahlen entsprechen nicht den Anforderungen an die Genauigkeit und müssen daher aussortiert und dem Produktionsprozeß erneut zugeführt werden. Zur Vereinfachung und Verbilligung der Produktion ist vorgesehen, daß die Steuerspannungen für die einzelnen Flüssigkristallschichten zur Kompensation von Fertigungstoleranzen abgleichbar sind.

Der erfindungsgemäße Lichtmodulator arbeitet mit einer smektischen Flüssigkristallmischung FLC-472/FLC-247 besonders gut im Bereich des sichtbaren Lichts, welche aus 60 gew% Phenyl-Pyridin und 40 gew% einer achiralen smektischen A- oder C-Matrix mit einer chiralen Dotierung auf der Basis von di-substituiertem Ether von Bis-Terphenyl-Di-Carboxilsäure besteht. Diese Dotierung induziert eine spontane Polarisation von etwa 160 nC/cm² in der Matrix mit einer Helixstruktur der Windungsperiode von etwa 0,3 µm in der chiralen smektischen Phase. Bereits eine Arbeitsspannung von 0 V bis 4 V verursacht einen smektischen Ablenkungswinkel von 0° bis ±22,5° bei einer Ansprechzeit

...

von 150 μ s. Die Modulationstiefe zwischen zwei gekreuzten Schichten beträgt damit bis zu 100%. Die Änderung des mittleren Brechungsindex beträgt bei der oben genannten Arbeitsspannung bereits bis zu 5%. Um eine Phasendifferenz von der Größenordnung der Wellenlänge des zu steuernden Lichts zu erhalten, genügt eine summierte Schichtdicke von 10 μ m. Diese Schichtdicke ist die Summe der Dicken der Einzelschichten.

Bei der Verwendung von Kameras oder Fernrohren zur Beobachtung von Objekten innerhalb der Erdatmosphäre oder durch diese hindurch treten lokale Unschärfen in dem Objektbild auf, welche auf atmosphärische Störungen zurückzuführen sind. Zur Korrektur dieser lokalen Unschärfen wird eine adaptive optische Einrichtung vorgeschlagen, welche ein Feld von rasterartig angeordneten Lichtmodulatoren des durch die Erfindung offenbarten Typs enthält. Das Feld ist in dem Strahlengang der Einrichtung angeordnet, wobei jeder einzelne Lichtmodulator zur Kompensation punktuell auftretender Unschärfen eines zu verarbeitenden Bildes ansteuerbar ist.

Dabei kann zur Reduzierung des Bauaufwandes vorgesehen sein, daß die Lichtmodulatoren auf einer gemeinsamen Trägerschicht aufgebracht sind.

Die Einrichtung wird in den Strahlengang des betreffenden Beobachtungsgerätes, beispielsweise einer Kamera oder eines Fernrohres, eingesetzt. Das von dem Beobachtungsgerät aufgenommene Objektbild wird einer Bildauswerteeinrichtung zugeführt, welche die Unschärfen in dem Bild ermittelt und das Modulatorfeld zu deren Kompensation entsprechend ansteuert.

...

Ein Ausführungsbeispiel des erfindungsgemäßen Lichtmodulators ist in der Zeichnung anhand mehrerer Figuren dargestellt. Es zeigt:

Fig. 1 die Anordnung der Flüssigkristallzellen für den Modulator und

Fig. 2 ein schematisches Diagramm der Brechungsindexindikatrixen für verschiedene Betriebszustände.

Gleiche Teile sind in den Figuren mit gleichen Bezugszeichen versehen.

Fig. 1 zeigt die beiden hintereinander im Strahlengang eines zu modulierenden Lichtstrahls 10 angeordneten Flüssigkristallschichten 6 und 8. Die Polarisationsrichtung des einfallenden Lichtstrahls 10 und des ausfallenden Lichtstrahls 11 wird durch jeweils einen Doppelpfeil markiert. Im Beispiel ist die Polarisationsrichtung des einfallenden Lichtstrahls 10 um den Winkel α gegenüber der Senkrechten geneigt.

Die erste Flüssigkristallschicht 6 ist zwischen zwei transparenten Elektroden 1 und 2 angeordnet, die auf zwei transparente Platten 1' und 2' aufgebracht sind. Die smektischen Schichten 12 bilden Versetzungsdomänen, entlang derer sich die Moleküle des Flüssigkristalls anordnen. Die Moleküle des Flüssigkristalls sind von Schicht zu Schicht um einen Winkel verdreht, so daß sich die Struktur einer Helix ergibt, deren Achse 7 in Richtung der Normalen z' zu den smektischen Schichten 12 verläuft. Die zweite Flüssigkristallschicht 8 ist zwischen den transparenten Elektroden 3 und 4 angeordnet, die wiederum auf den transparenten Platten 3' und 4' aufgebracht sind. Die Normalenrichtung z'' der smektischen Schichten 13 der

...

zweiten Flüssigkristallschicht 8 und die Achse der Helix 9 sind um 90° gegenüber der Normalenrichtung z' und der Helixachse 7 der ersten Schicht 6 verdreht.

Zwei in dieser Weise gekreuzte Flüssigkristallschichten 6 und 8 verändern den Polarisationszustand eines durchgehenden Lichtstrahls 10 nicht. Die reine Phasenmodulation der beiden Flüssigkristallschichten wird durch den feldabhängigen mittleren Brechungsindex verursacht. Die Doppelbrechung und Orientierungseffekte der Indikatrix in den durch Anlegen einer Spannung an die Anschlüsse 5 erzeugten elektrischen Feldern werden bei allen Feldstärken kompensiert.

Fig. 2 zeigt die Auswirkungen eines elektrischen Feldes E verschiedener Stärke 0, E' , E'' auf die Brechungsindizes n_s und n_p der Flüssigkristallschichten 6 und 8. Die x- und z-Achse des dargestellten Koordinatensystems liegen parallel zu der Ebene der Flüssigkristallschichten. Die z-Achse liegt zudem parallel zu der Normalenrichtung z' des ersten Flüssigkristalls 6. Die y-Achse zeigt in die Ausbreitungsrichtung des einfallenden Lichtstrahls 10. In Abbildung a) liegt keine Spannung an. Die langsame Achse mit dem Brechungsindex n_p der ersten Flüssigkristallschicht zeigt in Richtung der z-Achse, während die langsame Achse mit dem Brechungsindex n_p der zweiten Flüssigkristallschicht senkrecht zur z-Achse orientiert ist. Der Polarisationszustand des einfallenden Lichts bleibt beim Durchgang durch beide Schichten 6 und 8 erhalten.

In Abbildung b) wird eine kleine Spannung angelegt, die unterhalb derjenigen Spannung liegt, bei der die Helixstruktur verschwindet. Die langsam optischen Achsen mit den Brechungsindizes n_p' sowie die schnellen Achsen mit den Brechungsindizes n_s' der beiden Schichten 6 und 8 reorientieren sich und werden um den Winkel α verdreht. Die rechten Winkel zwischen den Achsen bleiben erhalten. Der

...

Brechungsindex n_p' steigt in den langsamten Achsen mit zunehmender Feldstärke E' an, während der Brechungsindex n_s' in den schnellen Achsen abnimmt. Der optische Weg des durchgehenden Lichts wird mit der Feldstärke E' verändert und folglich verschiebt sich dessen Phase. Die größte optische Wegänderung findet bei einer Spannung statt, die kurz unterhalb derjenigen Spannung liegt, bei der die Helixstruktur des Flüssigkristalls verschwindet. Dieser Zustand ist in Abbildung c) dargestellt. In den nun nicht mehr aufgewundenen Flüssigkristallen ist das Indexellipsoid der Brechungsindizes durch die molekularen Brechungsindizes n_p'' und n_s'' charakterisiert. Die langsamten Achsen mit den Brechungsindizes n_p'' sind in den beiden Schichten 6 und 8 um den molekularen Neigungswinkel T gekippt, was dem Winkel zwischen den smektischen Schichten 12 und 13 und den Helixachsen 7 und 9 entspricht. Auch in diesem Fall bleiben die Achsen unter einem rechten Winkel gekreuzt. Die Phasenverzögerung ist also über den gesamten Betriebsbereich unabhängig von der Polarisierung des Lichts. Somit ist auch die Steuerung unpolarisierten Lichts möglich.

...

Ansprüche

1. Elektrisch ansteuerbarer Lichtmodulator mit hintereinander angeordneten Flüssigkristallschichten, die zwischen transparenten Platten mit einer die Moleküle der Flüssigkristalle ausrichtenden Oberflächenanisotropie und mit Elektroden zur Erzeugung eines elektrischen Feldes in den Flüssigkristallen eingeschlossen sind, dadurch gekennzeichnet, daß wenigstens zwei Schichten (6, 8) helikaler smektischer ferroelektrischer Flüssigkristalle, deren jeweils schnelle und langsame optische Achse parallel zu der jeweiligen Schicht (6, 8) liegen und deren mittlere optische Anisotropie durch Einwirkung des elektrischen Feldes (E) beeinflußbar ist, hintereinander im Strahlengang eines zu modulierenden Lichtstrahles (10) angeordnet sind und daß die Richtungen der schnellen bzw. langsamen Achsen der einzelnen Schichten (6, 8) gegeneinander derart verdreht sind, daß die Polarisation des Lichtstrahls vor (10) und hinter (11) dem Modulator gleich ist.
2. Lichtmodulator nach Anspruch 1, dadurch gekennzeichnet, daß zwei Flüssigkristallschichten (6, 8) derart hintereinander angeordnet sind, daß die langsame optische Achse der ersten Schicht (6) senkrecht auf der langsamen optischen Achse der zweiten Schicht (8) steht, daß die schnelle optische Achse der ersten Schicht (6) senkrecht auf der schnellen optischen Achse der zweiten Schicht (8) steht und daß die Ausrichtung der langsamen und der schnellen optischen Achsen der beiden Schichten (6, 8) zueinander während des Anlegens und Veränderns der Steuerspannung jederzeit erhalten bleibt.

...

3. Lichtmodulator nach einem der vorhergehenden Ansprüche, dadurch gekennzeichnet, daß die Flüssigkristallschichten zwischen zwei transparenten Platten eingeschlossen sind, an deren Elektroden eine Steuerspannung zur Erzeugung eines elektrischen Feldes anlegbar ist.
4. Lichtmodulator nach einem der Ansprüche 1 oder 2, dadurch gekennzeichnet, daß die Flüssigkristallschichten (6, 8) jeweils zwischen zwei transparenten Platten (1' und 2', 3' und 4') eingeschlossen sind, an deren Elektroden (1 und 2, 3 und 4) je eine Steuerspannung zur Erzeugung je eines elektrischen Feldes (E) anlegbar ist.
5. Lichtmodulator nach einem der vorhergehenden Ansprüche, dadurch gekennzeichnet, daß die Flüssigkristallschichten (6, 8) die gleichen mittleren Brechungsindizes aufweisen, die gleiche Dicke haben und synchron mit den gleichen Steuerspannungen beaufschlagbar sind.
6. Lichtmodulator nach Anspruch 4, dadurch gekennzeichnet, daß das Verhältnis der Steuerspannungen zueinander zur Kompensation der Polarisationsänderungen eines durchtretenden Lichtstrahles einstellbar ist.
7. Lichtmodulator nach einem der vorhergehenden Ansprüche, dadurch gekennzeichnet, daß die Steuerspannungen für die einzelnen Flüssigkristallschichten zur Kompensation von Fertigungstoleranzen abgleichbar sind.
8. Lichtmodulator nach einem der vorhergehenden Ansprüche, dadurch gekennzeichnet, daß die Flüssigkristallschichten aus einer smektischen Flüssigkristallmischung FLC-472/FLC-247 bestehen.

...

9. Lichtmodulator nach einem der vorhergehenden Ansprüche, dadurch gekennzeichnet, daß die Flüssigkristallmischung aus 60 gew% Phenyl-Pyrimidin und 40 gew% einer achiralen smektischen A-Matrix mit einer chiralen Dotierung auf der Basis von di-substituiertem Ether von Bis-Terphenyl-Di-Carboxilsäure besteht.

10. Lichtmodulator nach einem der Ansprüche 1 bis 8, dadurch gekennzeichnet, daß die Flüssigkristallmischung aus 60 gew% Phenyl-Pyrimidin und 40 gew% einer achiralen smektischen C-Matrix mit einer chiralen Dotierung auf der Basis von di-substituiertem Ether von Bis-Terphenyl-Di-Carboxilsäure besteht.

11. Adaptive optische Einrichtung, gekennzeichnet durch ein Feld von rasterartig angeordneten Lichtmodulatoren nach einem der vorhergehenden Ansprüche, welches in dem Strahlengang der Einrichtung angeordnet ist, wobei jeder einzelne Lichtmodulator zur Kompensation punktuell auftretender Unschärfen eines zu verarbeitenden Bildes ansteuerbar ist.

12. Adaptive optische Einrichtung nach Anspruch 11, dadurch gekennzeichnet, daß die Lichtmodulatoren auf einer gemeinsamen Trägerschicht aufgebracht sind.

13. Adaptive optische Einrichtung nach einem der Ansprüche 11 oder 12, gekennzeichnet durch die Anordnung vor dem Bildsensor einer Digitalkamera, wobei das von der Kamera aufgenommene Bild einer Bildauswerteeinrichtung zur Ermittlung punktueller Unschärfen des Bildes zuführbar ist und wobei die adaptive optische Einrichtung von der Bildauswerteeinrichtung zum Ausgleich der Unschärfen ansteuerbar ist.

...

14. Adaptive optische Einrichtung nach einem der Ansprüche 11 oder 12, gekennzeichnet durch die Anordnung in einer optischen Beobachtungseinrichtung, wobei das zu beobachtende Bild parallel einer Bildauswerteeinrichtung zur Ermittlung punktueller Unschärfen des Bildes zuführbar ist und wobei die adaptive optische Einrichtung von der Bildauswerteeinrichtung zum Ausgleich der Unschärfen ansteuerbar ist.

15. Adaptive optische Einrichtung nach einem der Ansprüche 11 oder 12, gekennzeichnet durch die Anordnung in einer Kamera, wobei das zu beobachtende Bild einer Bildauswerteeinrichtung zur Ermittlung punktueller Unschärfen des Bildes zuführbar ist und wobei die adaptive optische Einrichtung von der Bildauswerteeinrichtung zum Ausgleich der Unschärfen ansteuerbar ist.

Zusammenfassung

Bei einem elektrisch ansteuerbaren Lichtmodulator mit hintereinander angeordneten Flüssigkristallschichten, die zwischen transparenten Platten mit einer die Moleküle der Flüssigkristalle ausrichtenden Oberflächenanisotropie und mit Elektroden zur Erzeugung eines elektrischen Feldes in den Flüssigkristallen eingeschlossen sind, sind wenigstens zwei Schichten helikaler smektischer ferroelektrischer Flüssigkristalle hintereinander im Strahlengang eines zu modulierenden Lichtstrahles angeordnet. Die Richtungen der schnellen bzw. langsamen Achsen der einzelnen Schichten sind gegeneinander derart verdreht, daß die Polarisation des Lichtstrahls vor und hinter dem Modulator gleich ist. Es wird eine adaptive optische Einrichtung angegeben, welche ein Feld von rasterartig angeordneten Lichtmodulatoren aufweist. Die Modulatoren sind in dem Strahlengang der Einrichtung angeordnet, wobei jeder einzelne Lichtmodulator zur Kompensation punktuell auftretender Unschärfen eines zu verarbeitenden Bildes ansteuerbar ist.

1/1

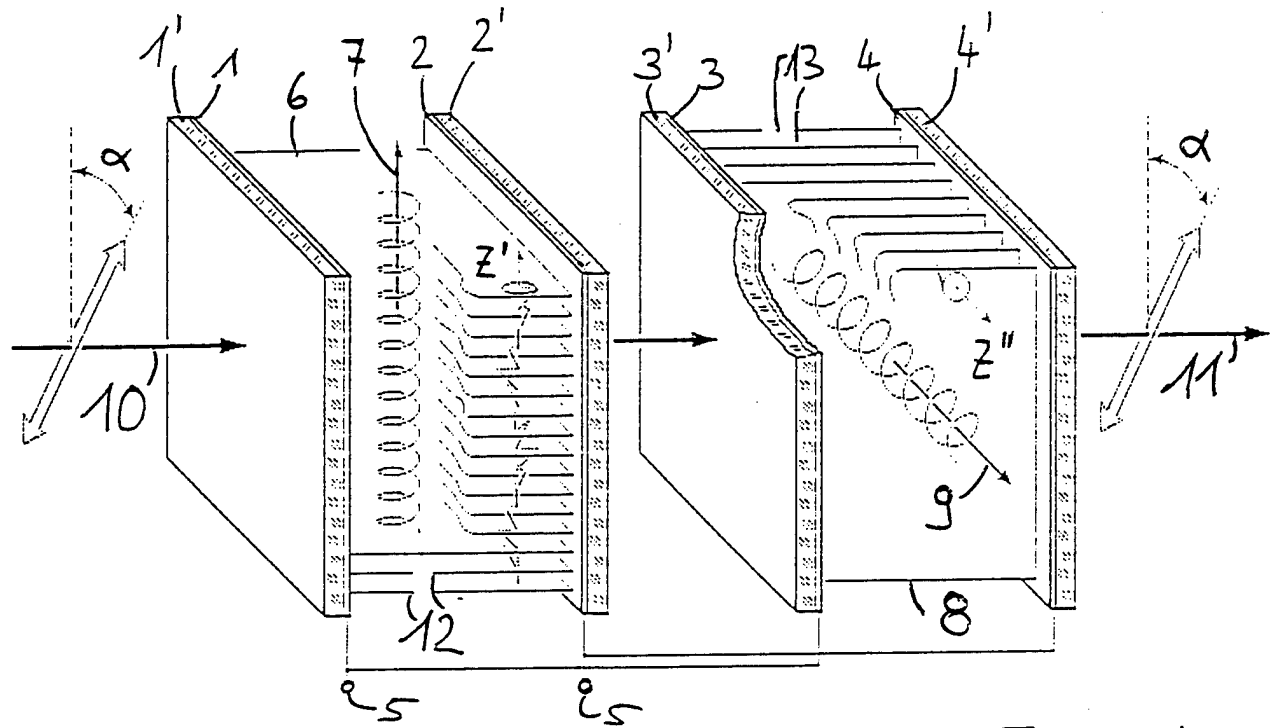


Fig. 1

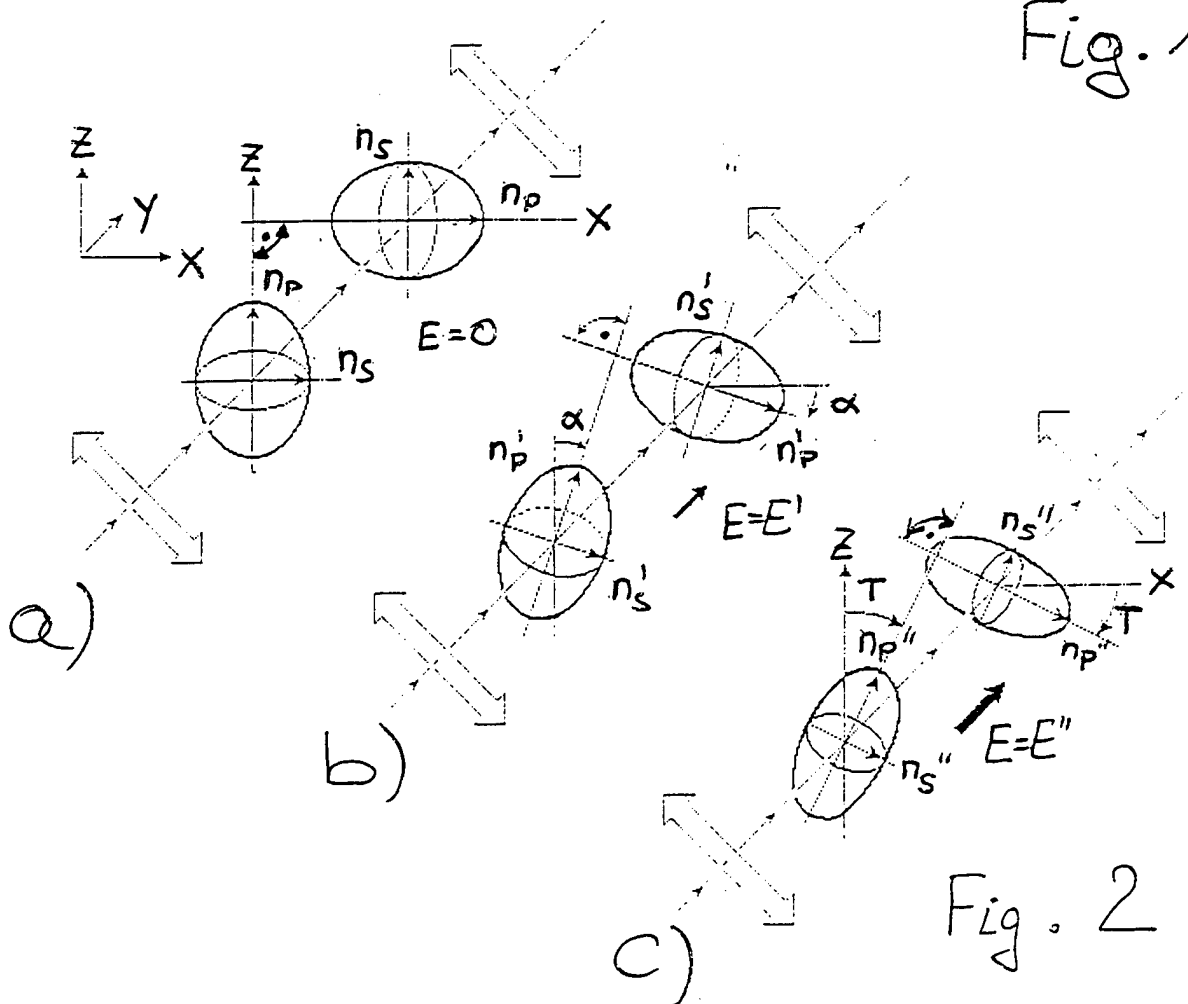


Fig. 2

Copies of papers, presented for publication

8. David V. Wick, Ty Martinez, Michael V. Wood, James M. Wilkes, Mark T. Gruneisen, Vladimir A. Berenberg, Michael V. Vasil'ev, Arkady P. Onokhov, and Leonid A. Beresnev,
“Deformed-helix ferroelectric liquid-crystal spatial light modulator demonstrating high diffraction efficiency and 370 line pairs per millimeter resolution”, submitted to Applied Optics, 1999.

Deformed-helix ferroelectric liquid-crystal spatial light modulator demonstrating high diffraction efficiency and 370 line pairs per millimeter resolution

D. V. Wick, T. Martinez, M. V. Wood, J. M. Wilkes and M. T. Gruneisen

*United States Air Force Research Laboratory
AFRL/DEBS, Kirtland AFB, New Mexico 87117*

V. A. Berenberg, M. V. Vasil'ev, A. P. Onokhov

*Institute for Laser Physics, SC "Vavilov State Optical Institute"
St. Petersburg 199034, Russia*

Leonid A. Beresnev

*Army Research Laboratory, Intelligent Optics Laboratory
2800 Powder Mill Road, Adelphi, Maryland 20783*

ABSTRACT

New liquid-crystal media and photoconductor materials are being utilized in spatial light modulators to increase their resolution, diffraction efficiency, speed, and sensitivity. A prototype device developed for real-time holography applications has shown 8% diffraction efficiency from a holographic grating with a spatial frequency of 370 lp/mm. At 18 lp/mm the device has demonstrated 31% diffraction efficiency with a 600 μ sec holographic write time using 400 nJ/cm² write beams.

Keywords: spatial light modulator, ferroelectrics, liquid crystals, aberration compensation

1. INTRODUCTION

Dynamic compensation of severe aberrations by holographic phase subtraction requires real-time holographic (RTH) recording media that are simultaneously capable of high diffraction efficiency, fast response times, high resolution, and high sensitivity. Optically-addressed spatial light modulators (OASLM) have previously been used to compensate hundreds of waves of aberration caused by poor quality primary mirrors in telescopic systems with write beam intensities as low as 50 μ W/cm² but with limited efficiency, speed, and resolution.¹⁻³

A schematic of a typical OASLM being used for RTH phase subtraction is shown in Figure 1. The device consists of a photoconductor (PC) and a thin liquid-crystal (LC) layer situated between a pair of transparent electrodes. If the device is used in a reflective geometry, there may also be a high reflectivity mirror between the PC and LC. A diffraction hologram is written in the device by interfering two mutually coherent wavefronts on the PC. The resulting interference pattern modifies the local conductivity of the PC, creating a spatially varying electric field across the LC layer. The local field then induces a reorientation of the LC molecules, creating a spatial pattern in the LC layer which directly corresponds to the interference pattern on the PC.⁴ This distribution of molecules creates a phase or polarization grating which diffracts the read beam. In the case of aberration compensation, an aberrated image-bearing beam is diffracted from a grating containing the aberration information, thus subtracting out the aberrations and yielding a corrected image.⁵

Historically the performance of OASLMs has been limited by both the PC and the LC media. In order to achieve DEs greater than 1%, devices which used an amorphous hydrogenated silicon (a-S:H) PC were limited to spatial frequencies of less than 110 lp/mm^{6,7,8}. Organic polymer PCs have been used to increase the resolution, but the response time of the device suffers due to the low carrier mobility.⁹ Among LC media there has historically been a trade-off between the rate at which the grating can be repeatedly written, read, and erased (refresh rate) and high diffraction efficiency (DE). Nematic LC devices were developed with DEs in excess of 30%, approaching the theoretical limits for an analog device¹⁰. Unfortunately, typical refresh rates for these devices are limited to around 30 Hz due to the slow recovery times of the LC media, and diffraction occurs for only one linear polarization state. On the other hand, surface-stabilized ferroelectric LC devices can operate with refresh rates greater than a kHz, but the low-tilt-angle LC media that have previously been available restrict the DE to less than ten percent¹¹.

Recently, OASLMs which use a deformed-helix ferroelectric liquid crystal (DHFLC) have received considerable attention due to the potential for grey-scale response.¹² While such devices have been described in the literature,^{7,8} the relatively small tilt angles (27° and 23°, respectively) of these DHFLC devices are far from the ideal case of 45°, thus restricting the attainable DE.

OASLMs which utilize a high-tilt-angle DHFLC and a carbon-doped amorphous hydrogenated silicon (a-Si_{1-x}:C_x:H) PC are currently being developed to simultaneously achieve high DE and fast response time with minimal write light irradiance at high resolution. DHFLC media with molecular tilt-angles that approach 45° can be used to generate DEs that approach theoretical limits.² a-Si:H can be doped with carbon to reduce the dark conductivity, allowing higher resolution, while still maintaining relatively fast response times.^{9,13} Here we describe characterization measurements performed on a prototype DHFLC device that utilizes an a-Si_{1-x}:C_x:H PC. This OASLM was built for the US Air Force by the Institute for Laser Physics in St. Petersburg, Russia.

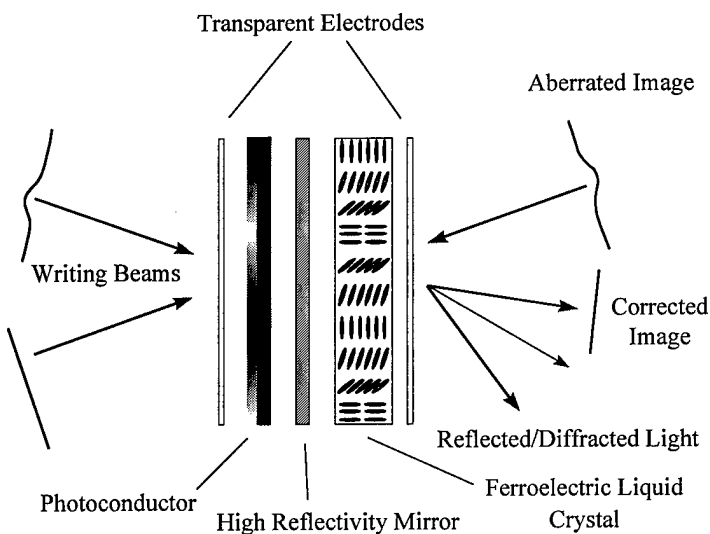


Figure 1. Optically addressed spatial light modulator showing write, aberrated read, and reflected/diffracted beams. Note that the deformed-helix ferroelectric liquid-crystal molecules actually rotate within the plane that is parallel with the liquid-crystal layer (normal to the page).

2. EXPERIMENTAL

High resolution was obtained in this OASLM by experimentally varying the amount of carbon in the PC layer. The a-Si_{1-x}:C_x:H layer was deposited using radio-frequency dissociation (also known as plasma enhanced chemical vapor deposition) in a multichamber setup.¹⁴ During this procedure, the carbon concentration was varied by adjusting the flows of the CH₄ and SiH₄ gaseous mixtures. The thickness of the PC is approximately 1.2 μm, and carbon content is given by x = 0.33.

The response time and efficiency of this OASLM is primarily determined by the reorientation of the ferroelectric molecules with changing electric fields. The LC used in this device was specifically developed for RTH applications and resulted from further improvements to previous mixtures.⁹ In this device, the LC molecules are aligned in the planar or homogenous orientation through a technique that is described in detail elsewhere.¹⁵ The LC exhibits a smectic C* phase between 0 °C and 61 °C. At 23 °C, the strongly twisted helical structure has a pitch of 0.18 μm, a molecular tilt angle of 39.5°, and a spontaneous polarization of 115 nC/cm². The nominal thickness of the LC layer is 12 μm.

The response time and efficiency of this OASLM is primarily determined by the reorientation of the ferroelectric molecules with changing electric fields.

The LC used in this device was specifically developed for RTH applications and resulted from further improvements to previous mixtures.⁹ In this device, the LC molecules are aligned in the planar or homogenous orientation through a technique that is described in detail elsewhere.¹⁵ The LC exhibits a smectic C* phase between 0 °C and 61 °C. At 23 °C, the strongly twisted helical structure has a pitch of 0.18 μm, a molecular tilt angle of 39.5°, and a spontaneous polarization of 115 nC/cm². The nominal thickness of the LC layer is 12 μm.

In contrast to more conventional surface-stabilized ferroelectric liquid crystals, the DHFLC molecules maintain their normal helical arrangement in an unbiased state. The pitch of this helix is small compared to the optical wavelength, and incident light will experience an index of refraction that is spatially averaged over the helical arrangement of molecules. This averaging can be described by an average index ellipsoid whose spatial characteristics and temporal dynamics determine the efficiency and speed of the OASLM.^{12, 16} A small applied voltage, on the order of several volts, will distort the helix and cause a transverse rotation of the spatially averaged index ellipsoid. If the electric field across the LC layer is large enough, the helix is believed to completely untwist, leading to maximum index ellipsoid rotation.

The temporal response of this average index ellipsoid to varying fields was investigated using the experimental setup shown in Figure 2a. A cw linearly-polarized collimated beam at 810 nm is incident normal to the surface of the OASLM. An alternating positive/negative polarity square-wave voltage is applied across the device to rotate the index ellipsoid. The OASLM is rotated about its surface normal until either the major or minor axis of the index ellipsoid is aligned with the input polarization wave when the device is negatively biased. The transmitted wave passes through an orthogonal analyzer before being measured by a fast photodiode. Figure 2b shows the transmission through the analyzer (solid line) as the voltage across the OASLM (dashed line) is switched from +42 V to -42 V. When the voltage is switched, the index ellipsoid rotates through twice the molecular tilt angle, or approximately 80°. The thickness of the DHFLC layer is approximately 13 μm, and the net optical retardance at 810 nm is about $\lambda/2$, leading to a 160° polarization rotation in the input wave. Thus the transmission through the analyzer is nonzero initially, when the device is positively biased, and eventually goes to zero after the voltage is switched. As the molecules reorient themselves after the voltage is switched, a peak occurs in the transmission when the average index ellipsoid passes through 45°. The oscillatory behavior during this reorientation is currently being investigated, but we believe that it is primarily due to scattering that occurs in the LC when the polarity of the voltage across the OASLM is switched. Figure 2b shows that it takes about 5 ms for the index ellipsoid to reach steady state for the given voltage.

The molecular switching time can be dramatically reduced by illuminating the PC with a spatially uniform write beam. Photo-induced carriers increase the conductance of the PC layer. As a result, the internal field across the LC layer is enhanced, which can significantly increase the speed at which the index ellipsoid rotates. In Figure 2c, a single write pulse with energy 275 nJ/cm² at 532 nm illuminates the PC layer while the voltage is switched from +42 V to -42 V. The rotation time for the index ellipsoid under these conditions is reduced to slightly more than 1 ms. This switching time can be further reduced by increasing either the write pulse energy or the bias voltage.

The difference in molecular switching times with and without PC illumination may be utilized to write a transient diffraction hologram in the OASLM. Figure 3 shows schematically how the writing of the transient holographic grating takes place. Initially, the molecules are all aligned by putting a large negative voltage across the OASLM. All of the molecules within the DHFLC layer are oriented at -40°, and there is no diffraction. The voltage is switched to a smaller positive voltage, and then the write pulses are introduced, creating a nearly straight-lined interference pattern on the PC. Photo-excited carriers are only created within the “bright” areas of this fringe pattern. The applied voltage causes these carriers to migrate across the PC layer, increasing the local electric field across the LC layer. Thus, the interference pattern on the PC induces a spatially varying field across the LC layer. Ferroelectric molecules within the bright regions experience a significantly larger electric field and therefore rotate quickly compared to those in the “dark” regions, creating a polarization grating within the LC layer with a period equal to that of the interference fringe spacing. Ideally, those molecules in the bright areas would rotate very quickly while those in dark regions would maintain their orientation for an extended period, creating a persistent grating. Eventually, however, the dark-region molecules will rotate, and the grating will fade.

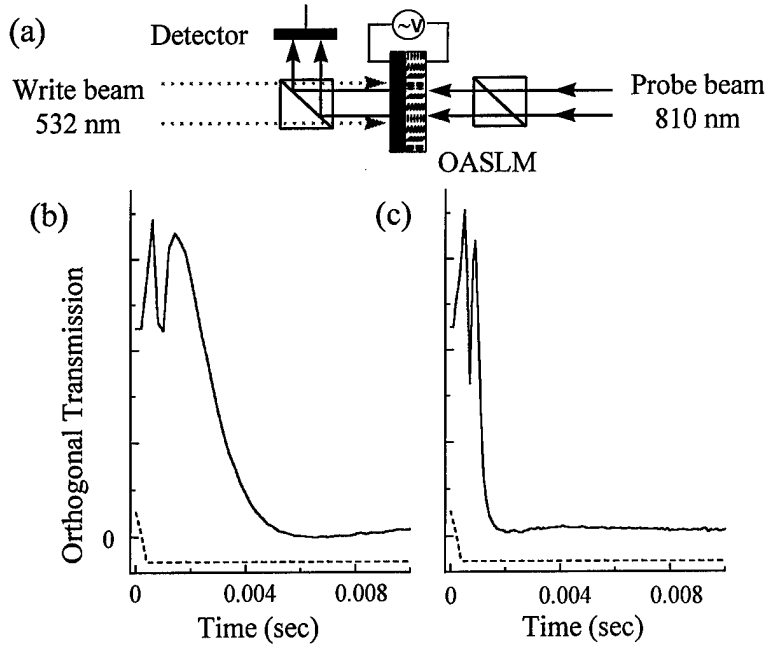


Figure 2. (a) Experimental configuration for measuring molecular switching dynamics. The measured switching dynamics (b) without and (c) with photoconductor illumination. The dashed line shows the bias voltage.

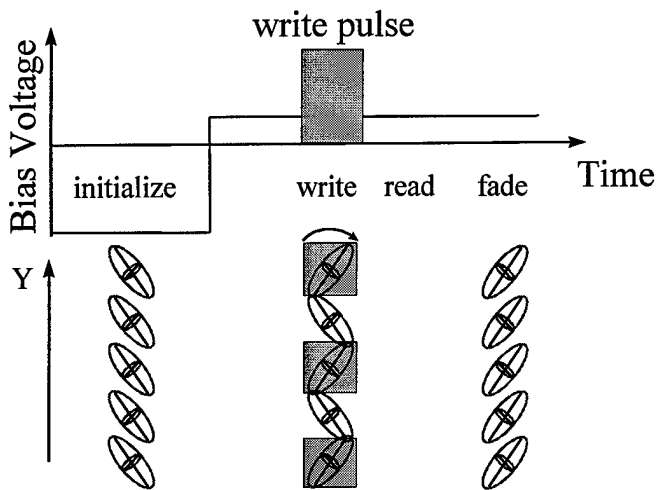


Figure 3. Timing diagram for transient hologram formation and decay showing OASLM bias voltage, spatially and temporally modulated write-pulse, and orientation of index ellipsoid.

The experimental setup to characterize this process is shown in Figure 4. A 532 nm write beam is passed through an electronic LC shutter in order to control the temporal profile of the write pulse on the OASLM. The beam is then defocused and sent through a Mach-Zehnder type interferometer such that the two write pulses interfere on the PC. This interference pattern creates the diffraction grating within the LC layer. The 810 nm read beam is diffracted by this grating, and the temporal dynamics of the first diffracted order are measured by a fast photodiode. Resolution measurements are made by

varying the angle between the two write beams. Because this prototype device was not AR coated for 810 nm, and there is some residual absorption in the PC at this wavelength, the DE is defined here as the power in the first diffracted order divided by the power of the transmitted beam when no grating is present. We define the holographic write time of the device to be the time interval from the onset of the write pulse until the DE reaches 90% of its maximum value.

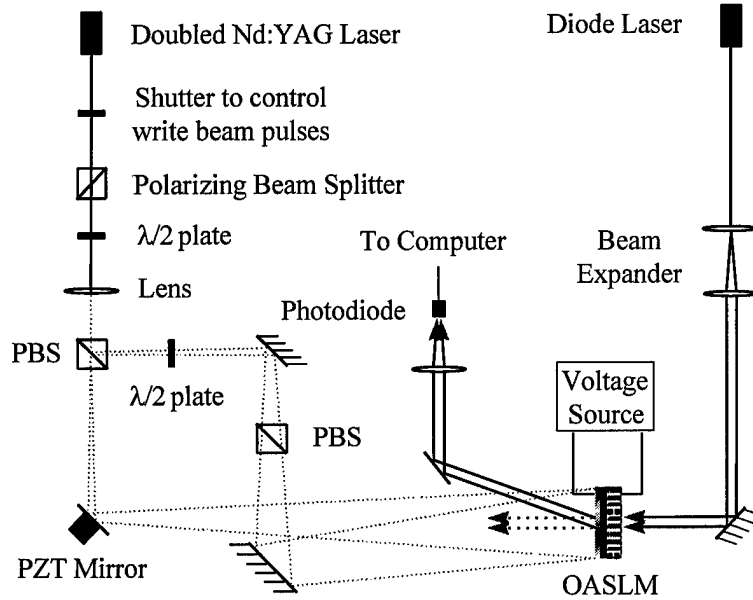


Figure 4. Experimental setup for measuring diffraction.

In Figure 5, the write pulse (dotted line) and voltage (dashed line) are adjusted to minimize the holographic write time while still maintaining relatively high DE.

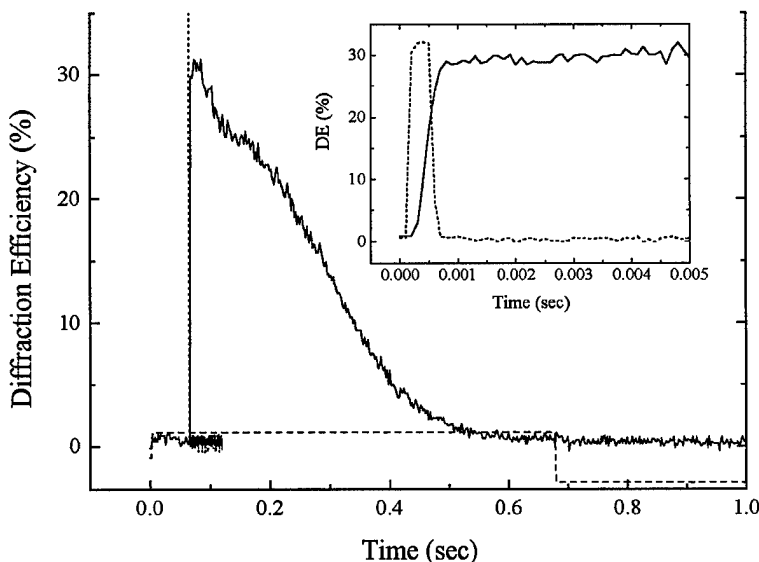


Figure 5. Transient diffraction hologram dynamics showing 600 μ sec holographic write time with 30% diffraction efficiency. The inset shows similar data taken with higher temporal resolution.

In this case, the spatial frequency of the interference pattern is measured to be 18 lp/mm, resulting from the $\sim 0.5^\circ$ angle between the write beams. Using a 0.4 ms (FWHM) write pulse with an energy of 400 nJ/cm^2 and setting the voltage pulse from -42.5 V to 16 V with a 1 second period, the peak DE is 31% and the holographic write time is about 600 μ s, as shown in the inset. Experimentally there is

a trade-off between fast response and high DE. While the rate of rotation of the index ellipsoid can be increased, eventually the DE declines with increasing applied voltages because the dark-region molecules are also rotating quickly. With slight adjustments to the write pulse and voltage, 34% DE can be achieved, but the holographic write time is about 5 ms.

Experimentally, the highest DE occurs when the OASLM is rotated such that the LC layers are perpendicular to the grating vector. Also, the DE is moderately improved by aligning the polarization of the read beam with the grating vector, an observation that is currently being investigated.

Figure 6 shows how the peak in the DE curve varies with spatial frequency, which is adjusted by changing the angle between the writing beams. For each spatial frequency, the DE is maximized with small adjustments to both the voltage and write pulses. At 370 lp/mm, 8% DE is still achieved. Note that when the spatial frequency is less than 50 lp/mm, the grating spacing is measured directly by imaging the interference pattern onto a camera. Larger frequencies are inferred by measuring the angle separating the zeroth and first diffracted orders.

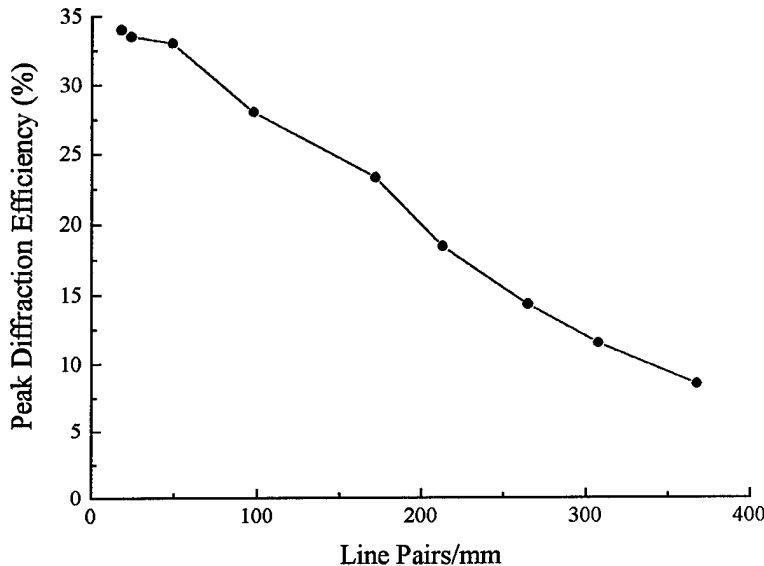


Figure 6. Peak diffraction efficiency for several grating spatial frequencies.

Because the DE goes completely to zero in Figure 5, we believe that all of the molecules have been given enough time to rotate and that all remnants of the grating have been eliminated, as illustrated by the “fade” portion of Figure 3. Therefore, grating memory in the LC should not be an issue despite the fact that an identical grating is being rewritten every cycle. To verify this, the setup was adjusted so that a spatially shifted diffraction grating was written on the PC every period. By affixing one of the mirrors in the interferometer to a piezo-electric transducer (PZT), as shown in Figure 4, the interference pattern translates in time as the mirror oscillates. The dithering mirror is driven by a triangle wave voltage whose amplitude is set such that the optical path length changes exactly one wave (2π phase shift) at the peak voltage. This causes the fringe pattern on the OASLM to spatially shift one complete fringe before returning back to its original position. With the PZT dithering at 1.0 kHz and with the same voltage and write pulses used to generate the data taken with a stationary mirror in Figure 5, the measured DE and holographic write time of the device are very similar. There is, however, about a 5% reduction in DE that is most likely due to the fact that the mirror is moving during the 0.1 ms pulse width of the write light, and therefore the grating becomes slightly washed out. We believe that this reduction would be eliminated by using shorter write pulses with the same pulse energy, but unfortunately our equipment was not able to deliver such pulses. It should be noted that care was taken to assure that the write pulse and the mirror were not synchronous in such a way that the write pulse happened to strike the mirror when the mirror was in the same position every cycle.

Depending on the application, the data acquisition rate could be an important consideration for RTH. This refresh or “frame” rate is the time it takes to write, read, and then erase the grating. In Figure 5, a 1 Hz refresh rate is used so that the dark-region molecules have time to completely rotate and the DE goes to zero. If faster acquisition rates are required, the voltage could be switched and an erase pulse could be introduced immediately after the grating is read to reinitialize all of the molecules. Thus the refresh rate is only limited by the holographic write time of the device and the time needed to read the signal, which is determined by the application.

By significantly altering the amplitude and period of the applied voltage, high DE can be made to last for an extended period of time. In Figure 7, 34% DE is maintained for nearly 40 ms of the 48 ms period before the grating is erased.

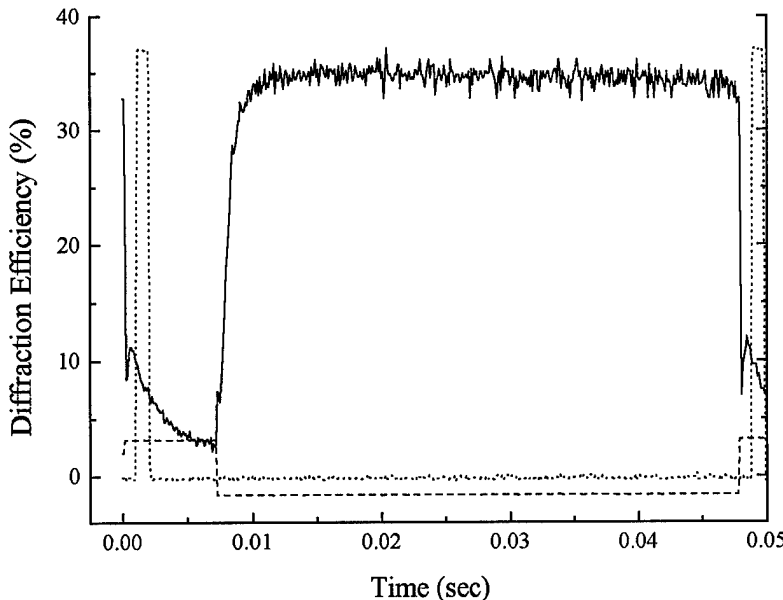


Figure 7. Time resolved diffraction efficiency showing high-duty cycle operation.

In this case a grating is established when the voltage switches from +39 V to -21 V, even though write light is not present, because the carrier lifetime in the PC layer is much longer than the 48 ms period. Because the write pulse occurs during the “initialize” portion of the cycle, see Figure 3, the enhanced electric field across the LC in the bright regions simply increases the speed at which those molecules rotate back to the initial orientation. The molecules in the dark regions never completely rotate, and +39 V

is high enough that they quickly reset to the initial orientation. After the voltage switches to -21 V, the carriers quickly migrate across the PC layer, increasing the local field across the LC layer. This creates the spatially varying field across the LC layer which forms the grating. In Figure 7, the energy of each 1.0 ms long write pulse is only 36 nJ/cm² and the spatial frequency of the grating is 18 lp/mm. These results are promising for applications which require a high average signal, since the DE can be maintained for 83% of the duty cycle. Here, however, the DE never reaches zero during the erase portion of the cycle indicating that the grating never totally disappears. Such a scenario might only be useful if the interference pattern and hence the diffraction grating do not change significantly from period to period.

3. CONCLUSION

In order to apply real-time holographic phase subtraction to dynamic aberration compensation systems, spatial light modulators must simultaneously fulfill demanding resolution, speed, efficiency, and sensitivity requirements. A novel optically-addressed spatial light modulator which utilizes a deformed-helix ferroelectric liquid-crystal and a carbon-doped amorphous silicon photoconductor appears to be the first such device that is capable of simultaneously meeting all of these requirements. Specifically, this device has demonstrated 31% diffraction efficiency with a 600 μ s holographic write time at a spatial frequency of 18 lp/mm using write beam intensities of 400 nJ/cm². It is also capable of producing 8% diffraction efficiency at a spatial frequency of 370 lp/mm. Such a device could be used to compensate severe aberrations that change on a millisecond time scale.

4. ACKNOWLEDGEMENTS

We gratefully acknowledge the contributions of Vladimir Venediktov, Alexey Leshchev, Leonid Soms, Donald Lubin, and Roger Ramsey. The contribution of LAB was supported in part by European Research Office, Contract N68171-97-M-5781.

5. REFERENCES

1. N. L. Ivanova, A. P. Onokhov, A. N. Chaika, V. V. Resnichenko, D. N. Yeskov, A. L. Gromadin, N. A. Feoktistov, L. A. Beresnev, “Liquid crystal spatial light modulators for adaptive optics and image processing,” Proc. of SPIE, **2754**, p. 180-185 (1996).

2. M. T. Gruneisen, K. W. Peters and J. M. Wilkes, "Compensated Imaging by Real-Time Holography with Optically Addressed Liquid-Crystal Spatial Light Modulators," Proc. of SPIE, **3143**, p. 171-181 (1997).
3. M. V. Vasil'ev, V. A. Berenberg, A. A. Leshchev, P. M. Semenov, and V. Yu. Venedikov, "Large numerical aperture imaging bypass system with dynamic holographic correction for primary mirror distortions," SPIE's International Symposium on Astronomical Telescopes and Instrumentation, paper **3353-146** (20-28 March 1998).
4. An in-depth description of the liquid-crystal molecular behavior can be found in *Spatial Light Modulator Technology : Materials, Devices, and Applications*, U. Efron, ed., (Marcel Dekker, Inc., New York, 1995).
5. J. W. Goodman, D. W. Jackson, M. Lehmann, and J. Knotts, "Experiments in long-distance holographic imagery," Appl. Opt. **8**, p. 1581-1586 (1969).
6. S. Fukushima and T. Kurokawa, "Real-time hologram construction and reconstruction using a high-resolution spatial light modulator," Appl. Phys. Lett. **58**, p. 787-789 (1991).
7. B. Landreth, C. C. Mao, and G. Moddel, "Operating Characteristics of Optically Addressed Spatial Light Modulators Incorporating Distorted Helix Ferroelectric Liquid Crystals," Jap. J. Appl. Phys. **30**, p. 1400-1404 (1991).
8. G. B. Cohen, R. Pogreb, K. Vinokur, and D. Davidov, "Spatial light modulator based on a deformed-helix ferroelectric liquid crystal and a thin a-Si:H amorphous photoconductor," Appl. Opt. **36**, p. 455-459 (1997).
9. A. P. Onokhov, V. A. Berenberg, A. N. Chaika, N. L. Ivanova, M. V. Isaev, N. A. Feoktistov, L. A. Beresnev, and W. Haase, "Novel liquid-crystal spatial light modulators for adaptive optics and image processing," Proc. of SPIE, **3388**, p. 139-148 (1998).
10. Hamamatsu technical data sheets for model X5641 PAL-SLM parallel aligned nematic liquid-crystal spatial light modulator and model X4601 FLC-SLM ferroelectric liquid-crystal spatial light modulator, Hamamatsu Corporation, 360 Foothill Rd., Bridgewater, NJ 08807 (1997).
11. C. C. Mao, K. M. Johnson, and G. Moddel, "Optical phase conjugation using optically addressed chiral smectic liquid crystal spatial light modulators," Ferroelectrics **114**, p. 45-53 (1991).
12. I. Abdulhalim and G. Moddel, "Electrically and optically controlled light modulation and color switching using helix distortion of ferroelectric liquid crystals," Mol. Cryst. Liq. Cryst. **200**, p. 79-101 (1991).
13. K. Akiyama, A. Takimoto, and H. Ogawa, "Photoaddressed spatial light modulator using transmissive and highly photosensitive amorphous-silicon carbide film," Appl. Opt. **32**, p. 6493-6500 (1993).
14. *Amorphous Semiconductor Technologies & Devices*, Y. Hamakawa, ed., (Ohmsha Ltd., Tokyo, 1981).
15. L. A. Beresnev, W. Dultz, A. Onokhov, and W. Haase, "Local optical limiting devices based on photoaddressed spatial light modulators, using ferroelectric liquid crystals," Mol. Cryst. Liq. Cryst. **304**, p. 285-293 (1997).
16. L. A. Beresnev, L. M. Blinov, and D. I. Dergachev, "Electro-optical response of a thin layer of a ferroelectric liquid crystal with a small pitch and high spontaneous polarization," Ferroelectrics, **85**, p. 173-186 (1988).